Evaluating Conceptual Numerical Models of Boreal Plains Hydrology

by

Sarah Grass

A thesis
presented to the University of Waterloo
in fulfillment of the
thesis requirement for the degree of
Master of Applied Science
in
Civil Engineering (Water)

Waterloo, Ontario, Canada, 2018

AUTHOR'S DECLARATION

I hereby declare that I am the sole author of this thesis. This is a true copy of the thesis, including any required final revisions, as accepted by my examiners.

I understand that my thesis may be made electronically available to the public.

Abstract

The Boreal Plains (BPs) ecoregion spans the northern potions of Alberta, Saskatchewan, and Manitoba and is an area of high ecological sensitivity. With large industrial developments in the region, including the Athabasca Oil Sands extraction projects, informed decision making and reclamation is critical. Hydrologic models are tools which are often used to inform such tasks. The BPs are characterized by their deep soils, their mosaic of forests and wetlands and their corresponding complicated hydrology. This complicated hydrology, including variable hydrologic connectivity, fill and spill mechanisms, and variable annual moisture deficit make selecting or developing appropriate hydrologic models a challenge. Current fixed model approaches have thus far been unable to demonstrate good representation of the hydrology of the BPs.

To address this gap in the literature for BPs hydrologic representation, three model structures were developed which attempt to capture the complicated physical nature of the BPs. This was achieved by utilizing an iterative, step-wise, and flexible model development approach within the Raven Hydrologic Modelling Framework (Raven). Additionally, physical realism was checked throughout the development process using multiple model diagnostic criteria and hydrologic signatures. Three study basins in the Athabasca River Basin were used to calibrate and validate the model structures. The results were compared to a baseline model which employed standard fixed modelling approaches.

The model development process faced numerous challenges including limited data availability, limited understanding of the physical environment at large scales, accurately representing wetland functional groups, representing the variable contributing area, equifinality of calibrated data sets, and limiting available winter algorithms in Raven. For the three data-limited basins examined here, it was found that lack of sufficient data made it difficult to properly constrain model structure and parameterization. Due to the complexity of BPs hydrology, it was found that while inclusion of additional BPs-specific hydrologic structures generally improved model performance in calibration, similar performance was unattainable in validation. This indicates that basins in the BPs will likely required additional data sources, beyond hydrographs, to properly inform and constrain local models.

Acknowledgements

I would like to sincerely thank my supervisor, Dr. James R. Craig, for his help, guidance, and support throughout this entire process. Without him I would have gone on so many tangents unchecked that this thesis probably wouldn't be possible. I also appreciate him dealing with my pragmatism especially when discussing fractals.

This journey would not have been happened without the amazing group of individuals in Dr. Craig's and Dr. Tolson's research groups. It was a wonderful experience laughing and learning with each and every one of you. In particular I need to thank Robert Chlumsky, Élise Devoie, Genevieve Brown, and Konhee Lee who all helped me progress in my research and without whom I would have most likely have lost my sanity along the way. Also, without them I would not have consumed as much ice cream, a true tragedy. I also need to thank the numerous other friends who made me feel welcome in a new province and made my time here truly memorable.

Finally, I need to thank my family, especially Bill Dad and Bio Dad, and my partner Jared, I don't think I could have done this without you.

Table of Contents

List of Figures

List of Tables

Chapter 1
Introduction

Water resources management decisions often rely on hydrologic models. These models are tools that can help to predict the impact of decisions and thus can aid in informing them. These numerical models can be used to model different hydrologic process, at a variety of scales, and for various reasons. However, to ensure that good decisions are being made, the models must get the right answers for the right reasons (Kirchner 2006). A major hydrologic challenge is developing scientifically meaningful and operationally reliable models (Fenicia et al. 2011) which be further complicated in certain regions which have atypical hydrology such as the Boreal Plains in western Canada. Numerical models tend to perform poorly in this region, due to deep soil storage and complex wetland connections which challenge standard modelling assumptions, making properly informing decisions difficult. Thus, there is a need for improved model configurations capable of simulating the complex hydrologic processes in this region.

The Boreal Plains are the home of major industry developments such as the Athabasca Oil Sands (AOS) extraction projects. The AOS projects result in large disturbed areas that must be reclaimed, as regulated by the Government of Alberta. However, due to the unique hydrology of the region, proper reclamation is a challenge (Johnson and Miyanishi 2008). Additionally, the BPs are an area of high ecological sensitivity that is expected to be greatly impacted by climate change (Michaelian et al. 2011). The presence of industry will only exacerbate this, resulting in the need for strong and well-informed water management decisions. How can we trust that the right management decisions are being made if the hydrologic models used to inform these decisions do not accurately capture the physical hydrology of the region? This lack of adequate models forms the main motivation of this thesis. The goal being to explore different model conceptualizations to generate a more capable model in the Boreal Plains that can be used to better inform important management decisions.

1.1 Thesis Goals and Objectives

There are two primary goals of this thesis: 1) To demonstrate the need for improved modelling methods in the Boreal Plains through a literature review and evaluation of existing models which have applied standard modelling methodologies to the region; and 2) To propose and rigorously evaluate improved modelling methods for hydrologic models developed in the Boreal Plains ecoregion. The second goal necessitated a unique modelling approach of stepwise iterative conceptual model development.

To achieve these goals the following objectives were set:

1) To conduct a thorough literature review to identify existing practices and any gaps in knowledge that exist;
2) To iteratively develop a semi-physical, process-based model which is more fundamentally suitable to the Boreal Plains ecoregion by manipulating both model structure and parameterization; and
3) To determine the level of complexity necessary to achieve "good" model performance in the Boreal Plains given limited data.

1.2 Thesis Organization

This thesis consists of 6 chapters with the first chapter providing the introduction to this thesis.

Chapter 2 is the background information relevant to the goals of this thesis. It discusses the hydrology of the Boreal Plains, existing field sites and research which has been done, modelling challenges, and an exploration of existing models of the Boreal Plains. It also discusses modelling practices which may be applicable in a Boreal Plains model.

Chapter 3 describes model development, including introducing the Raven hydrologic modelling framework and baseline models. It describes the required data processing and the selected model evaluation criteria. The chapter also discusses the methodology employed to develop the final model structures.

Chapter 4 discusses the results of the model development process including the final set of structures, descriptions of the selected algorithms, and the reasoning behind the selected algorithms. It also describes how the model structures were calibrated and validated.

Chapter 5 presents the model performance results and compares them to previous BPs models and baseline models. The chapter discusses how the models performed, where they did well and areas where they underperformed. It then discusses potential reasons for areas of poor performance or where the model performance could be improved.

Chapter 6 presents the summary and conclusions of this thesis, including the major contributions from the work of this thesis which include utilizing a flexible modelling approach to develop a model structure for a specific region at the catchment scale and providing recommendations on BPs model structures. It also discusses potential for future research areas.

Chapter 2
Background

This chapter will provide the necessary background knowledge to understand the purpose and motivation for this research. It describes the geographic extent of the Boreal Plains (BPs) and the characteristics of the region, which will aid in model conceptualization. It then goes on to detail the hydrology of the Boreal Plains, modelling approaches and challenges in the BPs, and explores existing model approaches applied to the BPs.

2.1 The Boreal Plains

This section will examine how the characteristics of the BPs combine to form a unique and complicated hydrologic regime which creates challenges for hydrologic modelling.

2.1.1 Overview

The BPs are a sub-region of the Boreal Forest ecozone (ESWG 1995). Approximately 10% of global forest cover is in Canada, spanning 417.6 million hectares, and the Boreal Forest (**Figure 2.1**) accounts for most of this (Granger and Pomeroy 1997, Watson et al. 2008). The western portion of the Boreal Forest that contains the BPs is sensitive ecologically to natural and man-made disturbances (Granger and Pomeroy 1997, Ireson et al. 2015). As such, the western Boreal Forest is expected to be greatly impacted by climate change (ex. Hogg and Hurdle 1995, Pomeroy and Granger 1997, Balland et al. 2006, Zhang et al. 2009, Michaelian et al. 2011, Price et al. 2013, Chasmer et al. 2016). Predicted impacts of climate change include irreversible permafrost damage, increased number of forest pests (Price et al. 2013), and droughts (Hogg and Hurdle 1995, Michaelian et al. 2011, Chasmer et al. 2016). The BPs are one of the most threatened regions of the Boreal Forest (Petrone et al. 2007) due to accelerated industry, agricultural, and recreational developments (Ferone and Devito 2004); climate change will only exasperate this.

Figure 2.1: Map of the Boreal Forest extent in Canada (from BSBI, 2015).

The Athabasca Oil Sands (AOS) projects are located within the BPs, primarily in northwest Alberta, and have contributed to large areas of land disturbance. Subsequently, the entire disturbed area must be rebuilt during reclamation as mandated by Alberta Environment and Parks. However, the complex hydrologic processes of the BPs are not fully understood, which makes designing these reclaimed ecosystems difficult (Johnson and Miyanishi 2008). Hydrologic models can be powerful tools to inform the policy decisions related to the impacts of AOS extraction. However, when the hydrologic processes are not well understood, effective and useful modelling becomes a challenge. Furthermore, upscaling critical BPs processes to a catchment scale, which is the scale at which most water resource management problems occur, provides additional challenges (Spence 2010). Before these challenges can be discussed there must be a basic understanding of where the BPs are located and how this shapes the hydrology of the region.

2.1.2 Location of the Boreal Plains

The BPs are a mosaic of forests and wetlands that covers approximately 65 million hectares, stretching from the eastern border of British Columbia to the southwest corner of Manitoba and covering large areas of Alberta and Saskatchewan (Watson et al. 2008). Within Canada there are different definitions of the Boreal Forest and BPs regions based on climate, vegetation, and soil type. Hydrology depends greatly on these factors, therefore, knowing what ecozone one is studying can provide useful insight into expected hydrologic patterns. This thesis uses the Federal definition as presented in **Figure 2.2**.

The terms Boreal and Taiga indicate climatic definitions, with the Taiga being colder than the BPs and supporting extensive zones of continuous and discontinuous permafrost (Ireson et al. 2015). The mountains and Canadian Shield present geologically defined boundaries, while the southern boundary of the BPs is defined by the vegetation transition (Ireson et al. 2015). The BPs is a transition zone where many forest species meet their southern climate limits (Ireson et al. 2015).

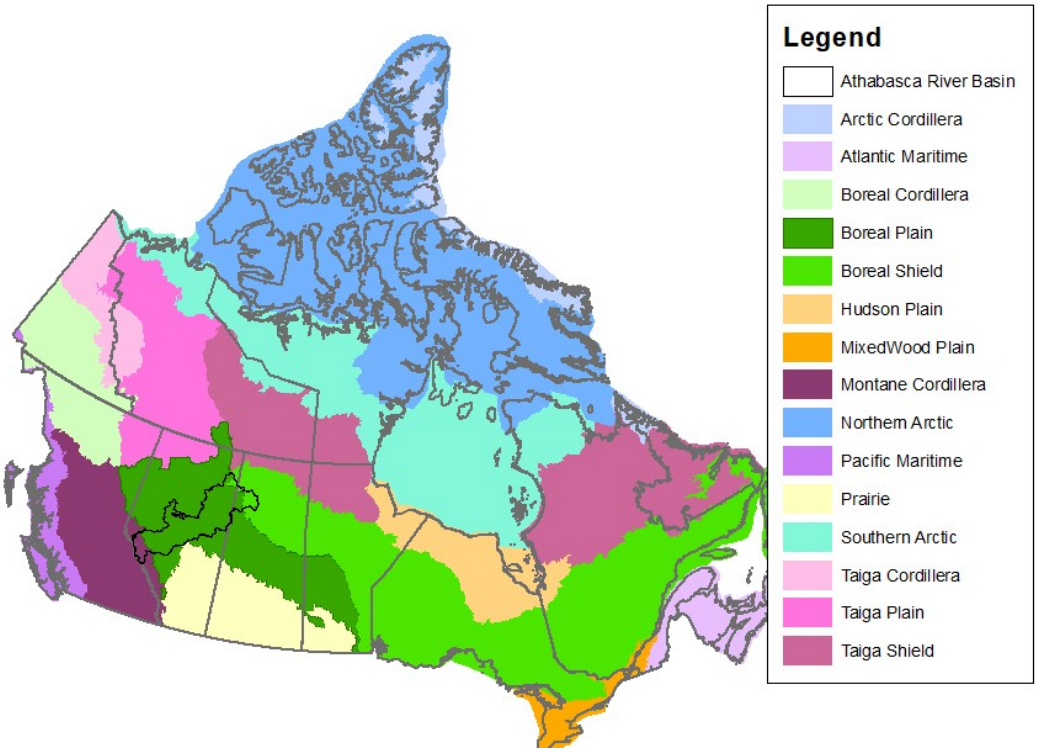

Figure 2.2: Map of the federally defined ecoregions in Canada; the Athabasca River Basin is outlined in black.

Note that the federal definition is non-unique; the province of Alberta defines their own natural regions. **Table 2.1** presents a comparison of the Alberta provincial and federal definitions, note the inclusion of the foothills and parkland in the federal definition.

Table 2.1: Comparison of Provincial and Federal definitions (recreated from Table 1-3, NRSC 2006).

Provincial Definition (2006)		Federal Ecological Framework (1995)	
Natural Region	**Natural Sub-Region**	**Ecozone**	**Ecoregion**
Grassland	Dry Mixed Grass	Prairie	Mixed Grassland
	Mixed Grass		Moist Mixed Grassland
	Foothills		Fescue Grassland
	Northern Fescue		Cypress Upland
Parkland	Central Parkland		Aspen Parkland
	Foothills Parkland		
Boreal Forest	Peace River Parkland	Boreal Plain	Boreal Transition
	Dry Mixedwood		Peace Lowland
	Central Mixedwood		Slave River, Wabasca
	Peace-Athabasca Delta		Lowlands
	Lower Boreal Highlands		Mid-Boreal Uplands
	Upper Boreal Highlands		
	Northern Mixedwood	Taiga Plain	Hay River Lowland
	Boreal Subarctic		Northern Alberta Uplands
	Athabasca Plain	Boreal Shield	Athabasca Plain
Canadian Shield	Kazan Upland	Taiga Shield	Tazin Lake Upland
Foothills	Lower Foothills	Boreal Plain	Western Alberta Upland
	Upper Foothills		
Rocky Mountains	Montane	Montane Cordillera	Eastern Continental Ranges
	Subalpine		Northern Continental Divide

2.1.3 Boreal Plains Characteristics

BPs hydrology is shaped by its climate, vegetation distribution, geology, and relief. This section will discuss each in detail.

Climate

Climate is a primary control of hydrology and may be characterized in part by the relationship between precipitation (P) and potential evapotranspiration (PET) (Devito et al. 2012). The BPs has a sub-humid climate which means that the climate can vary from water deficit to surplus conditions on monthly, annual, or decadal timescales (Smerdon et al. 2008). In most years the annual P is less than the annual PET, with "wet" years occurring infrequently (conservative estimates as a 15 year return period) (Ferone and Devito 2004). The BPs experience extreme temperature variations, with January averages ranging between -10°C and -22°C and July averages between 15°C and 20°C (Ireson et al. 2015).

While total annual P volumes vary (Johnson and Miyanishi 2008), the majority of P falls as rain in the summer months (Devito et al. 2012, Ireson et al. 2015). The reported annual P in the BPs ranges

from 300 mm to 640 mm (Johnson and Miyanishi 2008, Ireson et al. 2015). Most P occurs in the uplands of northwest Alberta and in the eastern BPs in central Manitoba, with the lowest amounts occurring in the central BPs. The fraction of P which falls as snow ranges from 21-31% at the southern edge to as much as 40% in the north. The snow cover period ranges from 3 months in the south to 6 months in the north (Ireson et al. 2015).

The diverse landscape of the BPs results in different rates of evapotranspiration (ET) which can be related to differences in leaf area index and available soil water. Similar to P, ET peaks during the summer months (Devito et al. 2012, Ireson et al. 2015). Despite variation between vegetation types, the annual PET is relatively constant when compared to P values (Johnson and Miyanishi 2008). Actual evapotranspiration (AET), which can represent the largest export of water in a catchment (Devito et al. 2005b) has high inter-site variability. One source reported AET ranges of 250 mm/yr for harvested Jack Pine, 433 mm/year for Aspen, and 441 mm/year for a fen (Ireson et al. 2015). This is a fairly unique feature that must be addressed in modelling efforts.

Vegetation and Landcover

Upland vegetation distribution at the regional scale is a function of climate, altitude, and latitude gradients. At the local scale, geomorphology, such as soil texture, slope, and aspect, are the key distribution factors. In the central BPs, up to 60% of the forests may occur on level terrain, giving soil texture and type a major influence on vegetation distribution (Ireson et al. 2015). The variability in vegetation is partially responsible for the variability in snow accumulation, melt rates, and runoff as canopy and root distribution effect the accumulation, soil infiltration, and solar radiation exposure of snow (Redding and Devito 2011).

Common upland tree species include Aspen, White Spruce, Jack Pine, Balsam Poplar, Balsam Fir, Easter Larch, and Black Spruce. The different tree types prefer different soil moisture conditions (Rowe and Coupland 1984, Redding and Devito 2011, Ireson et al. 2015). One would expect to see a mixture of Aspen and White Spruce on the poorly-drained glacial till hillslopes with White Spruce on top, Balsam Fir on the midslope, and Black Spruce at the wetter base. On the better drained glacial fluvial hillslopes one would expect Jack Pine to dominate the top with Black Spruce along the base (Johnson and Miyanishi 2008).

Lowlands are usually covered with peat. Peatlands cover approximately 16.3% of Alberta, with the most extensive peatlands in the northern two-thirds. Shrub fens have willows and sedges, while

forest fens have Tamarack and Black Spruce. Bogs tend to have periphery Black Spruce and moss (Johnson and Miyanishi 2008).

Aspen Trees

Aspen trees are of particular interest, not only have they been reported as the most prevalent tree species in North America, but they are also reported as the most abundant broadleaf tree in the Boreal Forest (Michaelian et al. 2011). Once established from a seed, a single Aspen will reproduce and spread its roots to form dense clones that can be one hectare or greater in size (Rowe and Coupland 1984). Their clonal nature and spatial distribution allows Aspens to strongly control ET, with the ability to greatly influence the water balance at both local and regional scales. Aspen tree canopies can intercept as much as 25% of the incoming P for large events (> 5 mm) and as much as 15% on an annual basis. Aspens also have more undergrowth than conifer trees, which adds additional under-canopy ET (Brown et al. 2014).

Aspen dominated catchments typically have P-ET deficits which are greater than the soil water storage capacity (Devito et al. 2005b). Aspen trees can laterally redistribute water with their deep and extensive root systems by moving water during the low ET period of the night and "bleeding" into surrounding soils. This process is proposed to be the reason why Aspen trees can survive in a climate with relatively low P (Brown et al. 2014).

Geology and Relief

The area that is now the BPs was covered by ice 10,000 to 12,000 years ago (Johnson and Miyanishi 2008), as a result there are deep surficial glacial deposits up to 300 m thick. Bedrock consists of sandstones and shales (Ireson et al. 2015) overlain with deposits of loamy till, gravel-sand glaciofluvial deposits, and lacustrine deposits. (Johnson and Miyanishi 2008). The high spatial variability of soil texture is a function of the spatial distribution of the glacial landforms (Redding and Devito 2011). Glacial till deposits have low saturated hydraulic conductivity (K_s) with decreasing K_s with increasing depth (Redding and Devito 2010). The soils near the surface have typically been weathered and their permeability is increased (Ireson et al. 2015). Low topographic relief dominates the Boreal Plain landscape (Prepas et al. 2006) with low rolling moraines, low lying clay plains and coarse textured outwash areas (Ferone and Devito 2004).

Typical Landforms

The dominant water balance processes are all dictated by landform type (Devito et al. 2016). The BPs can be broken down into two distinct landforms: wetlands, also called lowlands; and forestlands, which are also called uplands. On a broad scale, approximately 47% of the BPs are classified as forested and 20% are classified as wetlands(Ireson et al. 2015), however, due to high variability in the BPs one research site observed that wetlands composed 25% to 50% of the study areas (Devito et al. 2005a).

Wetlands

Wetlands are defined as shallow, dynamic, aquatic systems where water levels and surface areas show short-term and long-term variations (Dadaser-Celik et al. 2006). They are areas where the soil layering, landform shape, and climate, enable a long-term moisture surplus (Devito et al. 2012). The first type of wetlands is referred to as mineral soil wetlands and produce little to no peat. The second type is peatlands, which are wetlands with peat accumulation greater than 40 cm. The distribution of wetlands and wetland types are a function of latitude and meridian as peat accumulation is a function of moisture availability and temperature (Price et al. 2005). In northern areas decomposition is not as efficient resulting in thicker developments of peat (Rowe and Coupland 1984), making peatlands the dominant wetland type in the BPs (Ireson et al. 2015).

One process that can allow wetlands to form is a surface depression providing water storage, while the second process is soil layering that impedes flow and promotes ponding. In peatlands, these fine-textured layers can develop as organics are decomposed with lower layers being compacted by additional layers, further lowering infiltration and soil storage capacity in a continuous cycle. In the BPs, many wetland systems are perched above low conductivity layers and are consequently isolated from the regional groundwater system (Devito et al. 2012). Wetlands maintain greater antecedent moisture conditions than forestlands due to their different vadose zone storage capacity, thermal properties, and vegetation cover (Devito et al. 2005a) which typically have shallow root zones and subsequently low ET (Devito et al. 2012).

It has been suggested that wetlands should be defined by function, and not by size or other criteria (Devito et al. 2012). There are two functional groups of wetlands: riparian and geographically isolated wetlands (GIWs) (Fossey et al. 2015). Riparian wetlands are defined as wetlands which are periodically flooded by the bordering stream network (Zhang et al. 2011, Fossey et al. 2015) and are primarily dependent on river network and groundwater contributions (Freeze 1972, Fossey et al.

2015). GIWs are defined as areas with semi-permanent water and limited hydrologic connections with surface waters (Golden et al. 2016, Neff and Rosenberry 2018). The primary inputs to GIWs are spring snowmelt from upstream areas and direct precipitation, while the primary output is evapotranspiration. However, other minor outputs do exist, such as overland spillage and seepage. The seepage that does occur typically enters perimeter soils, with a small portion reaching the regional aquifers (Evenson et al. 2016). While surface connectivity can be limited, it has been suggested that GIWs can impact streamflow (Park et al. 2014, Golden et al. 2016) through groundwater connections, or more likely, through overland fill and spill. **Figure 2.3** shows the difference between typical riparian and GIW hydrologic connections with a river network.

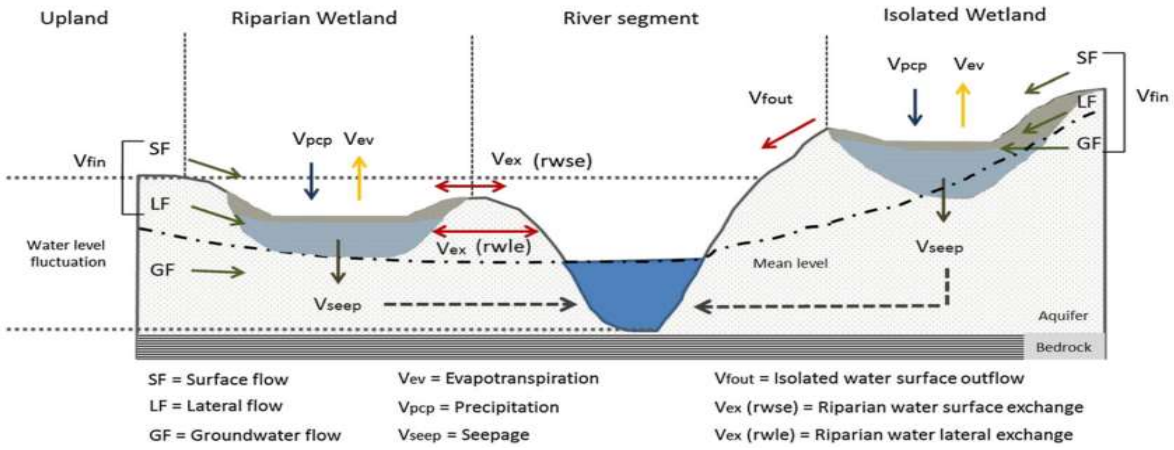

Figure 2.3: The difference between riparian and geographically isolated wetlands (from Fossey et al. 2015).

Forestlands

A defining characteristic of the forestlands in the BPs are the deep soil deposits with large storage capacities and corresponding deep root zones and high ET rates (Devito et al. 2012) leading to infrequent runoff events (Devito et al. 2016). The deep soils and large ET of the forestlands results in deep water tables that often decline from surrounding wetlands (Thompson et al. 2015) with field measurements of root distribution and hydraulic lift indicating that wetlands can be sources of water to adjacent forestlands. This phenomena has been observed at research sites in Alberta and Saskatchewan (Barr et al. 2012, Petrone et al. 2016).

2.1.3 Field Research Locations

This section provides a brief overview of the various sites which have researched BPs hydrology. Long-term study sites in Alberta (**Figure 2.4)** have mostly focused on the impacts of forest harvesting and water quality, with a small number focusing on runoff generation. **Figure 2.5** presents a map of the Prince Albert Model Forest (PAMF) in central Saskatchewan.

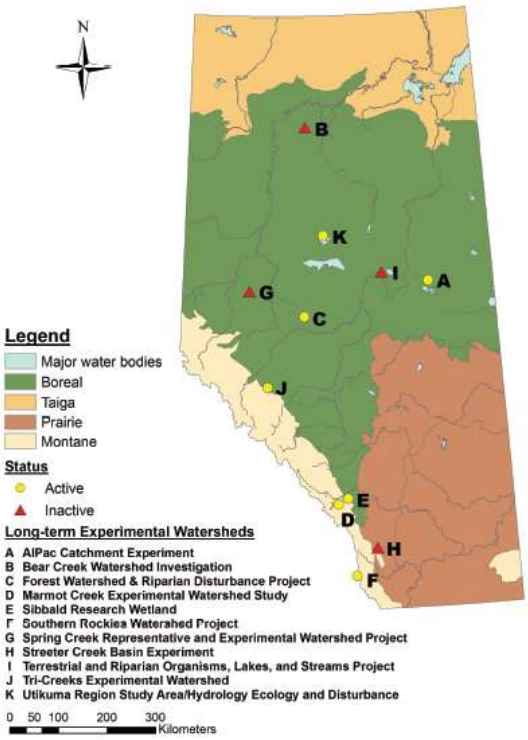

Figure 2.4: Long-term watershed research locations in Alberta (from Spencer et al. 2016).

Figure 2.5: Location of the PARMF research area (from Hyenegaard et al. 2016).

Table 2.2 summarizes the BPs research sites, two of the most important sites will be discussed further.

Table 2.2: Summary of research projects in the BPs.

Site Name	Location	Purpose	Site Characteristics/Project Description
Utikuma Region Study Area (URSA)[1]	Peace River Basin, AB; Point K (Figure 6)	To develop modelling tools to predict the cumulative impacts of land use changes and natural disturbances	- mean annual temperature of 1.2 °C - mean annual P of 483 mm; 137 mm falling as snow - annual PET is 518 mm - Soil depths range from 80 to 240 m of heterogeneous glacial sediments - low topographic relief. - 150 km south of the discontinuous permafrost zone - winter season typically occurring between November and April
Prince Albert Model Forest (PAMF)[2]	Central Saskatchewan; (Figure 7)	early research: - economic value of the forests more recent: - disturbance hydrology - climate change impacts - bird studies, - caribou management - hydrology of harvested, recovering, and clear-cut areas	- subarctic climate - mean annual P is 452 mm - waterbodies cover 15% of the PAMF - approximately 48% of the PAMF is forested
Boreal Ecosystem – Atmosphere Study (BOREAS)/ Boreal Ecosystem and Monitoring Sites (BERMS)[3]	White Gull Creek in PAMF	To characterize controls of the carbon, water, and energy balances in the southern boreal forest	- mature Aspen, Black Spruce and Jack Pine forest stands - annual P ranged from 391 mm to 537 mm, mean annual P is 467 mm; P peaks in summer - mean annual air temperature of 0.4°C
Terrestrial and Riparian Organisms, Lakes, and Streams (TROLS)[4]	12 fish bearing lakes in Lac La Biche, South Pelican Hills, and South Calling Lake; Point I (Figure 6)	Primary focus was on water quality; some research was done on runoff generation	- Aspen dominated mixedwood forest - Operated from 1994 to 200 - Summer dominated P

Site Name	Location	Purpose	Site Characteristics/Project Description
Al-Pac Catchment Experiment (ACE)[5]	Athabasca River Basin; Point A (Figure 6)	Examine the impacts of Aspen harvesting	- Began in 2005 - Studied pre- and post-harvest catchments - Low relief - Variable surficial geology - Closely associated with URSA HEAD projects - Mean annual P 462 mm - Mean annual PET 538 mm - Mean annual temperature of 1.5°C
Forest Watershed & Riparian Disturbance (FORWARD) Project[6]	Swan Hills; Point C (Figure 6)	To develop numerical models to predict hydrologic and water quality impacts following watershed disturbance in forested watershed in the BPs	- Looking at impacts of forest fire and oil sands reclamation - Focused on runoff and water quality - Mean annual P 580 mm - Mean annual temperature 2.6 °C - Watersheds between 2.6 km^2 and 247 km^2

1. (Smerdon et al. 2007, Redding and Devito 2011, Devito et al. 2016)
2. (Zha et al. 2010, Hvenegaard et al. 2015)
3. (Nijssen and Lettenmaier 2002, Balland et al. 2006, Barr et al. 2007, 2012)
4. (Gibson et al. 2002, Whitson et al. 2004)
5. (Donnelly et al. 2016)
6. (Prepas et al. 2006, McEachern 2016)

Utikuma Region Study Area (URSA)

Located in the Peace River Basin in Alberta, research at URSA comprises several multi-year projects, including the Hydrology Ecology and Disturbance research projects (HEAD1 and HEAD2) (Devito et al. 2016). Kevin Devito is the primary researcher and most of the research done on landscape hydrology in the BPs has been done at URSA, consequently, his research program is also the most cited BPs field research (Johnson and Miyanishi 2008). In 2012 Devito et al. published a guide to conceptualizing water movement in the BPs which represented the culmination of over 75 scientific papers published on research done at URSA since 1998 (Devito et al. 2012). Since this research is focused on a small area within the BPs the field observations may not be representative of the entire BPs.

Several hypotheses have been presented from Devito's research group, with the most important being that there is a regional or net moisture deficit with decadal wet and dry cycles (Devito et al. 2016). This may not be the most accurate phrasing as a net moisture deficit implies that water is continually lost from the system and should therefore eventually be completely consumed. A more appropriate phrasing would be that there is an annual average net moisture deficit, with intermittent wet years replenishing water storage. Another important hypothesis is that wetlands provide water to adjacent forestlands and Aspen trees play a major role in water transmission (Devito et al. 2012).

Prince Albert Model Forest (PAMF)

Model forests are partnerships of multiple stakeholders, including industry, Aboriginal groups, and local communities, that make shared decisions on social, environmental, and economic sustainability issues within the model forest. The PAMF was one of the founding model forests in Canada. It was created in 1992 and is located in central Saskatchewan with a current area of approximately 4,400,000 ha (Hvenegaard et al. 2015). It is the second most prolific research site after URSA and has observations there can conflict with observations from URSA. These contradictions are discussed at length in subsequent sections but highlight the importance of not overlying on URSA observations since there are limited sites that can corroborate their observations.

2.2 Hydrology in the Boreal Plains

This section will discuss the complicated way water moves in the Boreal Plains and why these processes are difficult to capture in conventional hydrologic models.

2.2.1 Fill and Spill

In areas with humid climates (P>PET) and shallow soils, water runs off into channel networks and leaves the catchment with relatively low retention times (Spence and Woo 2003). In the BPs, where P-ET deficits can be equal to or greater than soil storage capacity, annual runoff is controlled more by the distribution and timing of P than annual P volume (Devito et al. 2005b).

Thresholds are defined as the critical point, either in time or space, where runoff behaviour rapidly changes (Ali et al. 2013). Different types of hydrologic thresholds exist, likely caused by the interaction between primary controls such as climate, soil, and vegetation (Ali et al. 2013). Threshold mechanisms exist at a variety of scales ranging from the soil matrix to the catchment scale (Spence 2010). In a process known as fill and spill the threshold would be the point at which the soil or wetland switches from storing water (filling) to generating runoff (spilling). Threshold behaviour has been observed in a variety of landscapes including humid landscapes (Lehmann et al. 2006), the Canadian Shield (Spence and Woo 2003), the prairie potholes (Leibowitz et al. 2016) and the BPs (Devito et al. 2012). These thresholds can be a key factor in the partitioning of P into storage or runoff and are typically not well represented in conventional hydrologic models.

Storage

In the BPs, fine grained glacial deposits slow infiltration past the weathered surface layer, where the stored water is then utilized by vegetation (Devito et al. 2005a). Soil storage is typically variable within a catchment and the satisfaction of this storage occurs as a series of discontinuous thresholds instead of as one continuous succession (Spence 2010). At URSA, lakes can act as “evaporation windows” and be sources of water loss in the system instead of locations of water storage. Comparatively, once the water table is below the shallow root zone, wetlands can store water with limited ET losses (Smerdon et al. 2005).

Despite the fine grained soils, infiltration in the BPs forests is dominated by vertical flow, minimizing runoff (Gibson et al. 2002, Nijssen and Lettenmaier 2002, Redding and Devito 2010) and depending on the soil structure, can recharge local, intermediate, and/or regional groundwater systems (Devito et al. 2005a). In the western boreal forest observed regional groundwater discharge is low (Redding and Devito 2011), making recharge to local and intermediate systems more likely. The majority of groundwater recharge occurs when ET is limited, which in the BPs means during the fall or in early spring before the forest canopy has been established. This often results in snowmelt being the primary source of groundwater recharge (Smerdon et al. 2008).

Surface water and groundwater sheds do not necessarily coincide, although a standard hydrologic modelling assumption is that they do (Winter et al. 2003). This belief also assumes that groundwater follows a similar gradient to the surface water gradient. This assumption would then conclude that groundwater from the upland forests should reach the shallow groundwater connections of the lowland wetlands. However, this is not what has been observed at URSA. As illustrated in **Figure 2.6** the groundwater table declines away from the wetlands or is completely beneath them. The high ET in the forestlands and deep roots of Aspen trees result in the water table being drawn down more than in traditional landscapes (Devito et al. 2012).

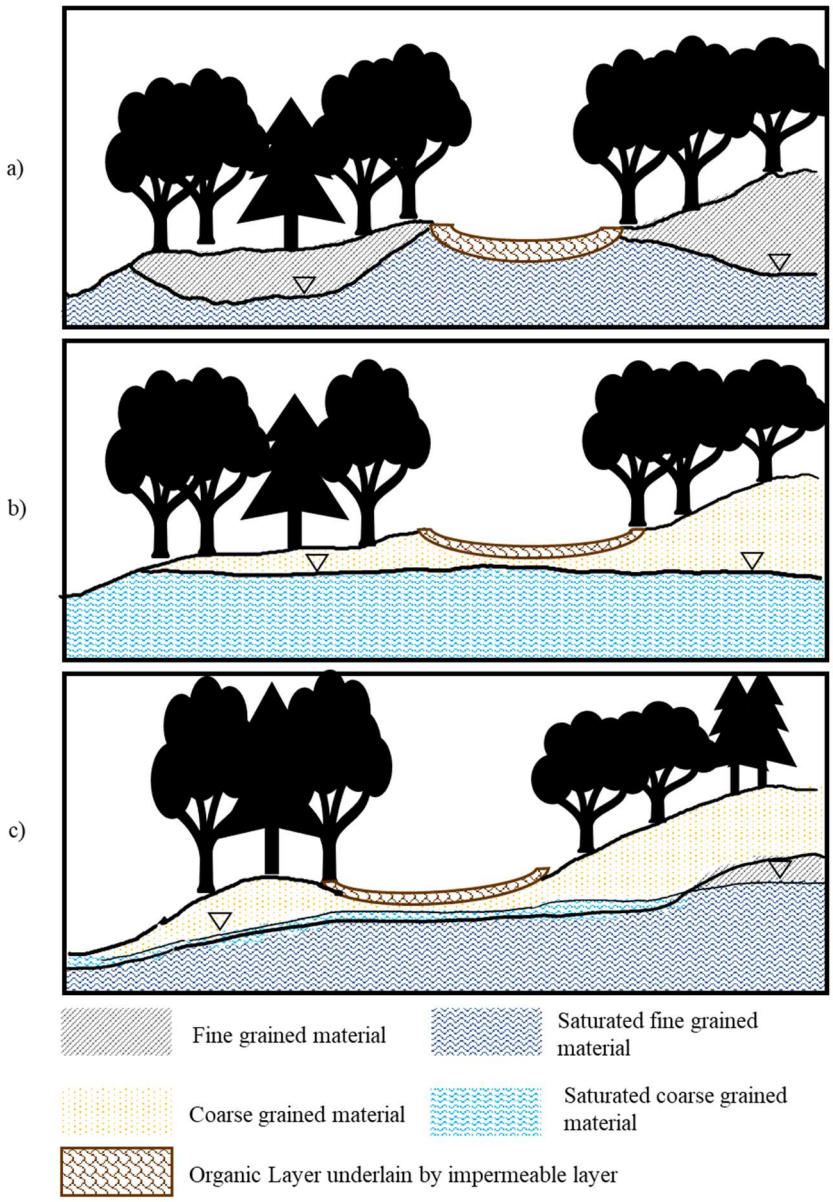

Figure 2.6: Depiction of observed groundwater tables in a) fine grained soils, b) coarse grained soils, and c) fine grained overlain with coarse grained soils. Adapted from Devito et al. (2012)

Runoff

The partitioning between runoff and infiltration is a dynamic and complex process (Ireson et al. 2015). Traditional runoff generation involves water reaching the ground surface and then partitioning into either surface runoff or infiltration. This partitioning is controlled by shallow surface soil moisture which can become saturated from above (Hortonian runoff or infiltration-excess runoff) when the rainfall intensity exceeds the soil infiltration capacity or from below when the water table

rises to the surface (saturation-excess runoff) (Dingman 2015). Both processes assume that partitioning is a function of the magnitude and intensity of the precipitation.

Traditional interpretations of runoff generation may not be entirely appropriate in the BPs as it appears that existing storage capacity exerts more control on runoff response than precipitation magnitude. The cumulative moisture deficit (CMD) is the result of consecutive years where ET exceeds precipitation (Devito et al. 2012) and it has been considered as the primary factor for determining water availability in the BPs (Devito et al. 2016). At URSA, the annual runoff has a poor correlation with the magnitude of precipitation, but instead exhibits a strong threshold relationship with the CMD (Devito et al. 2016). This is similar to observations by Spence and Woo (2003) in the Canadian Shield where spill thresholds were variable and were a function of antecedent moisture conditions and ET (Spence 2010).

It is likely that how runoff progresses towards the catchment outlet is also a function of existing storage capacity. Spence and Woo (2003) observed in the Canadian Shield that the upstream segments were first filled via lateral inflow before saturated overland flow could contribute to downstream runoff, meaning that the upstream flow needed to satisfy the downstream storage deficit. The further downstream the spill, the greater the impact on runoff response was as there was less distance the water had to travel to reach the outlet. Implying if there was less ground to cover over which runoff could potentially be taken into storage more runoff would be observed (Spence and Woo 2002). The deeper glacial deposits and root zones of the BPs, combined with the fact that peak precipitation and ET are in phase, result in a more pronounced decrease in runoff than observed in the Canadian Shield (Devito et al. 2005b, Redding and Devito 2008).

In addition to surface runoff, shallow subsurface flow, also called quickflow, can play an important role in streamflow generation. Quickflow is usually dictated by a layer which restricts infiltration and redirects flow laterally. In areas without shallow bedrock, such as the BPs, the mechanisms for lateral flow are unclear, however, it is hypothesized that the interface where coarser textured soils meet finer textured soils could be this boundary (Redding and Devito 2010). When lateral subsurface flow does occur in forested uplands it is primarily ascribed to Aspen tree macropores (Redding and Devito 2010). Wetlands by definition have limited vertical infiltration (Section 2.1.2) and more lateral flow has been observed in the BPs wetlands than in the forested uplands (Ferone and Devito 2004, Smerdon et al. 2007, Thompson et al. 2015). It was also observed that the primary non-atmospheric wetland connections were short, shallow groundwater connections

(Ferone and Devito 2004). One study at FORWARD observed that only peatlands generated runoff, while a second study proposed that the proportion of wetland coverage in a catchment dictated runoff generation (Prepas et al. 2006, McEachern 2016). The research then seems to indicate that forestlands should have low runoff, higher vertical infiltration rates, and high ET, while wetlands should have limited deep groundwater connections, low ET, and higher runoff and quickflow connections.

Both URSA and BOREAS sites have observed low annual streamflow volumes with high intensity precipitation events producing the few larger flows (Nijssen and Lettenmaier 2002, Redding and Devito 2011). A study at the PAMF observed that three adjacent forest types experienced similar meteorological events, but exhibited different runoff responses, indicating the importance of vegetation type on runoff response (Zha et al. 2010). It can therefore be concluded that runoff in the BPs is primarily controlled by precipitation intensity, antecedent storage conditions, and vegetation distribution. Hydrologic models which use traditional runoff approaches that don't consider storage deficits will likely perform poorly.

Snow Sourced Runoff

Snow can cover the BPs for as much as half of the year (Ireson et al. 2015), meaning snowmelt can represent a large amount of accumulated water. Additionally, with low spring ET, snowmelt presents the possibility of creating a moisture surplus (Redding and Devito 2011). Frozen soils have lower K_s than unfrozen soils due to ice occupying the larger pores (Harms and Chanasyk 1998) which influences meltwater partitioning.

There is some disagreement in the literature about snowmelt partitioning in the BPs. Ireson et al. (2015) claim that there is large runoff in spring due to the frozen soils limiting infiltration capacity. Conversely, studies conducted at URSA have concluded that most snowmelt infiltrates with minimal runoff. These studies also concluded that when snowmelt runoff does occur aspect is critical, observing the most runoff on south-facing slopes (Devito et al. 2005b, Redding and Devito 2011). The importance of slope and aspect on snowmelt was also observed at a BPs research site at Highvale Mine in central Alberta. However, this study observed the most runoff on the north-facing slope (Harms and Chanasyk 1998). The dominance of infiltration of snowmelt was also observed at one of the 12 study lakes of the TROLS project. Despite soil temperatures near 0°C, water percolated through the soils with no observed generation of runoff (Whitson et al. 2004). Forested runoff can be further reduced by canopy interception. A study at PAMF observed conifer canopies intercepted as much as 40% of the snow which was subsequently sublimated (Pomeroy and Granger 1997).

Wetland ice storage can play an important role in runoff generation. Storage of the previous year's moisture as ice results in decreased soil storage capacity and increased probability of water transmission during spring melt. Additionally, ice lenses prevent groundwater recharge and ET losses, further protecting stored water (Devito et al. 2012). From these observations it appears that most meltwater should infiltrate in the forestlands and runoff in the wetlands.

2.2.2 Hydraulic Connectivity

While hydraulic connectivity has not been clearly defined in literature (Bracken and Croke 2007, Bracken et al. 2013, Golden et al. 2017), for the purpose of this thesis it will be defined as the ability to transfer water from one part of the landscape to another (Spence and Phillips 2015). Hydraulic connectivity is a useful concept as it combines multiple processes such as runoff, infiltration, and quickflow, into a pattern which describes the overall movement of water. Macropores, preferential flow paths, and hysteresis plays an important role in hydraulic connectivity. However, accurately measuring hydraulic connectivity is challenging since there is no single soil property that can fully capture the complicated hydraulic connections (Bracken and Croke 2007, Bracken et al. 2013).

Wetland Connectivity

Wetland hydraulic connectivity is a function of the wetland type. For example, bogs tend to be hydraulically isolated while fens are hydraulically connected, even in dry periods. Increased fen cover has been associated with increased runoff because of these connections (Gibson et al. 2002, Prepas et al. 2006).

Wetlands can have fill and spill connections as well as fill and merge connections. Fill and spill are shorter, pulsed connections, while fill and merge is a longer, continuous connection where the combined wetlands act as one hydrologic unit. In a study of North Dakota prairie potholes, it was observed that fill and spill connections dominated on steep landscapes while fill and merge dominated on flatter landscapes (Leibowitz et al. 2016). It could then be concluded that fill and merge connections should dominant the flat topography of the BPs. **Figure 2.7** shows the different type of connections, note the elevation difference in the fill and spill (a) when compared with the fill and merge (b) scenario.

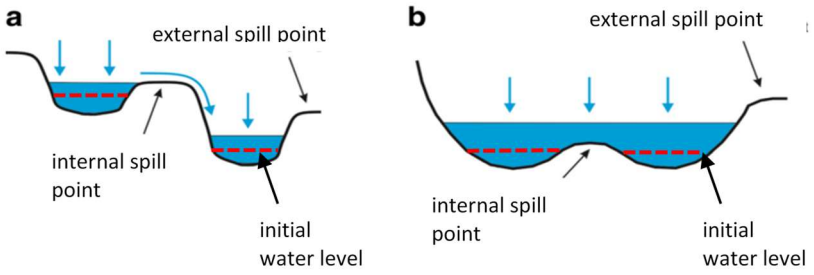

Figure 2.7: Depiction of fill and spill (a) and fill and merge (b) connection types; adapted from Leibowitz et al. 2016.

In the case of GIWs, surface connectivity occurs when the available volume of depression storage in the individual depressions is satisfied, allowing runoff to cascade downgradient into adjacent wetlands. Whether this water reaches the outlet is a function of the topography and antecedent conditions in the basin, making the contributing area and outlet runoff volume dynamic (Shaw et al. 2012).

2.2.3 Miscellaneous Processes

There are unique hydrologic processes which impact Boreal Plains hydrology including beaver dams and ice jams. Beavers can greatly impact peat formation, wetland hydrologic function, and control downstream connectivity (Donnelly et al. 2016, Spencer et al. 2016). Depending on the conditions, beaver dam breaches can result in discharges significantly greater than naturally occurring flood events (Hillman and Rothwell 2016).

Ice jams can occur during spring breakup resulting in flooding of the surrounding areas. In low areas, especially the Peace-Athabasca Delta, ice jam flooding functions to refill and replenish riparian wetlands in the area and in some areas ice jam floods can produce higher water levels than open water floods (NHRI 1990, Jepsen et al. 2016). While these are important processes, they will not be explicitly addressed in this thesis.

2.3 Hydrologic Modelling of the Boreal Plains

The following section will explore general modelling techniques, how BPs models have been conceptualized, specific model development challenges, and different modelling approaches. Particular attention is paid to representations of wetlands and degree of model complexity.

2.3.1 Hydrologic Model Types

Simulation models are defined as systems which are simpler than the real system they represent and which can produce some, but not all, characteristics of reality. A hydrologic simulation model therefore is a system, either physical or mathematical, who's purpose it to reproduce the essential aspects of a portion of the hydrologic cycle (Dingman 2015). This thesis will detail mathematical hydrologic simulation models, henceforth referred to as hydrologic models. One of the primary goals of hydrologic science is to understand the hydrologic cycle. However, due to the complexity of hydrologic processes, tools, such as hydrologic models, are required to test hypotheses and increase understanding. Outside of academia, hydrologic models are used to inform decisions through prediction and simulation (Dingman 2015).

Each hydrologic model is developed with a different purpose and thus there are wide variations between them. Hydrologic models can be defined by process complexity, which is the extent the model explicitly represents hydrologic processes (Clark et al. 2017). It can also be defined by spatial complexity, which is the extent a model represents the details of the landscape and the flow connections across the different model elements (Clark et al. 2017). Current hydrologic models include bucket models, conceptual models, physically distributed models, transfer function models, and automated neural networks (Fenicia et al. 2011). What the "best" model approach is has been heavily debated in literature (ex. Beven 2006, Kirchner 2006, McDonnell et al. 2007, Clark et al. 2017) and is often a function of data availability and the natural complexity of the area to be modelled.

How a model represents water movement has been described in many ways such as: physical, analytical, empirical, stochastic, deterministic, and conceptual (Kampf and Burges 2007). For the purposes of this thesis there will be two spectrums discussed: physical vs empirical and lumped vs distributed.

Process Complexity - Physical vs Empirical

Early hydrology was based on empirical relationships, these have been incorporated into many aspects of hydrologic modelling such as the Penman ET algorithm (Singh and Woolhiser 2002). With the advancements of computers, more complex and advanced numerical hydrologic models are possible (Singh and Woolhiser 2002) which include more physical representations. Physical models approximate the physical processes which occur in the environment using conservation equations and appropriate constitutive laws to track water movement between different domains (Kampf and Burges

2007). The theoretical advantage of physical models is their ability to be deployed in ungauged basins, areas without observation data, or areas subject to future changes for which data is not available. Physical models are useful for concept development, hypothesis testing, and field experiment design. When properly executed, they can be used to test hypotheses and support further understanding of processes or regions, such as the BPs. A major disadvantage of physical models is overparameterization, which is when there are more model parameters than can be identified from the data (Kampf and Burges 2007). Issues with overparameterization are discussed further in Section 2.4. Additionally, a physical model will often still require empirical generalizations to parameterize the represented processes (Zheng et al. 2018).

Where a model falls on the physical-empirical spectrum depends on how it represents hydrologic processes. For example, conceptual models are often semi-physical as they seek to represent the dominant hydrologic process in a physically meaningful way but are frugal in their parameterization (Fenicia et al. 2011). An example of a fully physically based approach would be the three-dimensional Richard's Equation (eq. 1) which describes unsaturated flow.

$$\frac{\partial}{\partial x}\left[K_h(\theta)\cdot\frac{d\psi(\theta)}{dx}\right]+\frac{\partial}{\partial y}\left[K_h(\theta)\cdot\frac{\partial\psi(\theta)}{\partial y}\right]+\frac{\partial}{\partial z}\left[K_h(\theta)\cdot\left(\frac{\partial\psi(\theta)}{\partial z}+1\right)\right]=\frac{\partial\theta}{\partial t} \quad \text{(eq.1)}$$

Here θ is the volumetric water content, K_h is the saturated hydraulic conductivity, and ψ is the pressure head. This approach is based on conservation of mass in a portion of an unsaturated soil column (Dingman 2015).

Conversely, an example of a fully empirical method would be the Soil Conservation Service Curve Number (SCS) method. This approach uses soil information and a design rainfall volume to calculate a peak discharge (eq. 2).

$$q_{peak}=\frac{0.208\cdot P^{*}\cdot A_D}{T_r} \quad \text{(eq. 2)}$$

Here A_D is the area of the basin and T_r is the time to peak and assumes the runoff hydrograph is triangular, P^* is the effective rainfall and is a function of the gross precipitation and the maximum retention capacity of the catchment which is in turn a function of a curve number. The curve number describes the amount of runoff that is expected on a certain landcover with a certain soil type and is based entirely on empirical observations and is usually presented in various empirical tables or figures (Dingman 2015).

Spatial Heterogeneity - Lumped vs Distributed

Lumped models do not account for the spatial distribution of input variables making them effectively one-dimensional as they average processes over the modelled domain. In contrast, distributed models account for spatial variability by representing the water pathways in two- or three-dimensional space (Kampf and Burges 2007). Lumped or distributed can refer to the spatial or parameter representation in the model. Distributed models have the advantage of being able to explicitly represent key linkages between model elements but require more data and computational power than lumped models (Singh and Woolhiser 2002, Paniconi and Putti 2015) . Additionally, distributed models need better sub-grid parameterization schemes to account for topology and storage at appropriate time scales (Spence 2010), as representation of sub-grid topographic variability can have significant impacts on the simulated responses (Paniconi and Putti 2015). To be completely distributed, every aspect of the model, such as parameters and boundary conditions, must be distributed (Singh and Woolhiser 2002, Kampf and Burges 2007). However, the practical limitation of data availability often prevents models from being fully distributed (Singh and Woolhiser 2002).

2.3.2 Conceptualizations

This section discusses the different ways modellers can conceptualize the physical landscape and processes of the natural environment.

Bucket Theory

Devito et al. (2012) proposed conceptualizing wetlands and forestlands in the BPs as different sized buckets. The wetlands would be shallow buckets with minimal storage and would spill readily while the forestlands would be deeper buckets with large storage capacity that rarely spill. One could then extrapolate this theory so that an entire catchment could be represented by a series of different sized buckets. The simplicity of this conceptualization allows for various scales and combinations of buckets to be used to understand water movement within the landscape.

This theory explains thresholds as a function of water storage capacity, however, thresholds don't depend on a mean storage value but rather on the heterogeneity of the hillslope and the spatial arrangement of the different properties (Lehmann et al. 2006). It can be argued that the main aspect of fill and spill hydrology is the spatially variable storage, since key storages must be satisfied before water can be transmitted (Spence 2010). In other words, how the buckets are connected is more important than the buckets themselves.

A slightly more evolved form of the bucket conceptualization is used in this thesis; referred to as the compartment method. Instead of buckets, which can only fill and then spill, model elements are conceptualized as different storage compartments with different fluxes moving water into and out of the compartments.

Hydrologic Response Units (HRUs)

An HRU can be defined based on land-surface form, geology, and climate where HRUs can either store, transmit, or contribute runoff (Spence and Woo 2006). The streamflow in the catchment can then be envisioned as the outflow response from a series of these elements which are hydraulically connected to the catchment outlet (Spence et al. 2009).

In a well cited paper, Devito et al. (2005a) express the need for broad-scale classification of HRUs. When delineating HRUs it is common practice to rely on topography, however, in many environments, including the BPs, special considerations for hydrologic aspect, such as for groundwater inputs, are required. Modelling in low relief wetland covered areas, challenges the typical overreliance of models on topography, which is not particularly relevant in such landscapes (Gibson et al. 2002). An alternative to topographic drainage networks could be the CMD since it alters hydrologic connectivity between different HRUs (Devito et al. 2016). However, this requires measured soil moisture and/or AET data to calculate the CMD which can be difficult to obtain and therefore limits its applicability.

2.3.3 Explicitly Modeling Wetlands

Wetland modelling in and of itself is a challenge. The theory of fill and spill is physically-based and therefore appealing to include in models, however, fill and spill is difficult to implement at large scales where threshold characteristics are unknown. How to best incorporate processes like coalescence and disaggregation during fluctuating moisture conditions and the influence of surface and groundwater connections on wetlands has not been thoroughly demonstrated in existing literature (Mekonnen et al. 2015, Liu et al. 2016).

Nevertheless, there have been some strategies used to model wetlands such as the Hydrologically Equivalent Wetland (HEW) approach first proposed by Wang et al. (2008). A HEW is a lumped representation of all wetlands in an area with the area of the HEW equivalent to the sum of all individual wetlands in the subbasin. It has identical function to its component wetlands and therefore is presumed to represent the hydrology of the individual wetlands, including the nonlinear

relationship between runoff and wetlands (Wang et al. 2008). **Figure 2.8** illustrates the HEW approach.

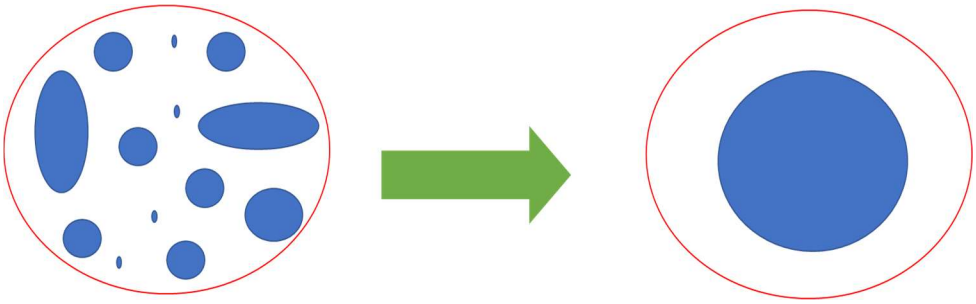

Figure 2.8: Demonstration of the HEW concept, all individual wetlands in a subbasin (left) can be combined into one hydrologically equivalent wetland (right).

The HEW approach has been applied in various models and landscapes including the prairie pothole region (Wang et al. 2008), GIWs in North Carolina (Golden et al. 2014), and riparian and GIWs in Quebec (Fossey et al. 2015). Fossey et al. (2015) had one HEW representation for GIWs and one HEW representation for riparian wetlands in their subbasins, allowing their model to explicitly acknowledge the different functionality of the two wetland groups.

The arguments for the HEW approach is that it is simple to use and it upscales well (Wang et al. 2008, Golden et al. 2014, Fossey et al. 2015). However, it is a simplification and is therefore less physically based than a more explicit representation. Additionally, how the HEWs are parameterized presents an issue, as there is only one representation for each process in every wetland. For example, the threshold of the HEW needs to represent how the thresholds of all of the individual wetlands act together in the subbasin. This raises the question of how to select these values and if these values are truly physically representative.

Another suggested approach is to explicitly model each wetland and the order of the fill and spill cascades. Evenson et al. (2016) represented each individual wetland physically and spatially in a GIW dominated basin in North Dakota. They identified the fill and spill relationships between each GIW to determine the cascade order and the overlapping and nested wetland catchment areas using the United States National Wetland Inventory. **Figure 2.9** provides an example of how the model was modified to include the GIW catchment areas.

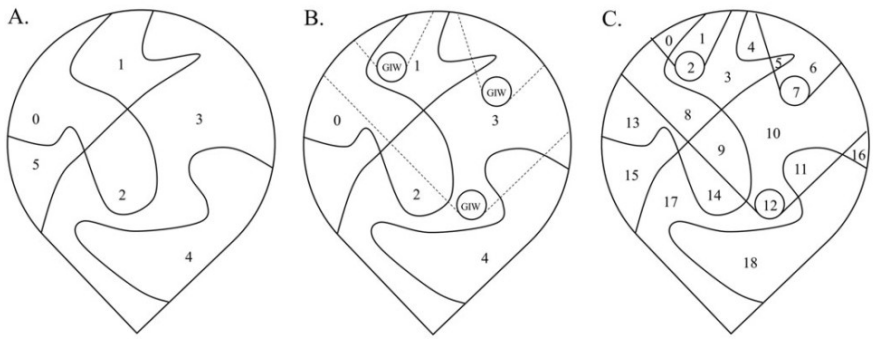

Figure 2.9: Progression of HRU boundaries from the standard (a) to delineating upgradient catchments for GIWs (b) to separating HRUs based on these boundaries (c) (from Evenson et al. 2016)

The argument for this approach is that it explicitly considers the fill and spill cascade order and is therefore a more physical representation of the basin. However, the model was deployed in a modestly sized basin (1,672km^2), and applying this approach in larger basins would present huge computational challenges. Additionally, detailed spatial data, including a wetland inventory and detailed topographic data, was required. Thus, making this approach difficult to deploy in data limited basins.

This thesis uses the HEW approach even though this is somewhat contradictory to the argument that the spatial distribution of storage matters more than the magnitude of storage. This simplification was applied due to data limitations and scale issues related to implementing the explicit representation approach, which is discussed in Section 2.3.4 and Chapter 5.

2.3.4 Modelling Challenges

There are challenges that face any modeller trying to represent the complex hydrology of the BPs. These can range from data limitations to limited understanding of the physical environment and others.

Current Understanding of the Natural Environment

Many aspect of BPs hydrology is still up for debate and there are limited field observations outside of URSA. URSA has a more wetland dominated landscape than the average BPs region (Devito et al. 2005a, Ireson et al. 2015), so do observations of how the wetlands interact with the environment translate to other, less wetland intensive basins? How snowmelt partitions in the landscape, the impact of vegetation type on water losses, and the importance in distinguishing between GIW and riparian wetlands are all areas which have contradictory or limited observations and still require

further research. Additionally, all observations of the BPs have been at the field scale, so how the landscape behaves at the catchment scale is unknown. These existing research gaps make developing a representative hydrologic model of the BPs even more challenging.

Scale Issues

The definition of scaling is using information at one scale to derive data or processes which occur at a different scale. Scaling issues can arise both spatially and temporally (Singh and Woolhiser 2002, Paniconi and Putti 2015). Upscaling refers to using data or physical descriptions at one scale and applying it to a coarser or larger scale (Blöschl and Sivapalan 1995, El Maayar and Chen 2006) and is a major research challenge in hydrologic modelling (Blöschl and Sivapalan 1995, Clark et al. 2017).

Often, upscaling requires some form of simplification of landscape heterogeneity, which may present a challenge for properly representing the system (El Maayar and Chen 2006, Spence et al. 2009) as it has been demonstrated that ignoring heterogeneities can lead to decreased prediction performance (Hartmann 2016). It is also unclear whether the element-scale equations correspond with reality at larger scales (Clark et al. 2017). While it is a common assumption that as catchment size increases, local complexities are attenuated (Singh and Woolhiser 2002), this is not always the case (Spence 2010). In the BPs upscaling presents a particularly difficult challenge since there is no definitive study which shows how thresholds at a small scale influence the catchment runoff response (Spence 2010).

Another challenge of upscaling is distributing the data; what is the best way to represent the impact of small-scale heterogeneities on the large-scale fluxes? On approach is to use macroscale parameters called effective parameters. Effective parameters are defined as a single parameter applied to the model domain which will produce the same model performance as if the model was based on a heterogenous parameter field (Blöschl and Sivapalan 1995, Lehmann et al. 2006, Bracken et al. 2013). This thesis will use effective parameters to upscale the local BPs processes.

HRU Delineation - Wetlands

Catchment delineation in the BPs is complicated by flat topography and watershed boundaries that are indeterminate from Digital Elevation Maps (DEMs). Usually, DEMs are used in combination with GIS software to automatically delineate watersheds, subbasins, and HRUs. However, most DEMs have errors and are not hydrologically continuous. Standard DEM processing involves artificially filling erroneous depressions, however, in wetland dominated landscapes this results in the loss of

wetlands in the DEM and is therefore not appropriate (Chu 2017). Furthermore, differentiating between the two functional wetland groups (riparian and GIW) also presents a challenge. There is no set way to delineate the two and oftentimes an arbitrary buffer region around the stream network or some threshold of adjacency is used (Fossey et al. 2015, Evenson et al. 2016).

Variable Contributing Area

A standard hydrologic modelling assumption is that contributing area is constant, however, in wetland dominated landscapes, the contributing area evolves based upon whether portions of the landscape are spilling (Chu 2017). Therefore, conventional hydrologic models with fixed contributing area are prone to be incorrect (Shook et al. 2013). In the BPs it has been suggested that the effective watershed area should be defined as the total area of connected wetlands, since they contribute to runoff most frequently (Devito et al. 2012). Bracken and Croke (2007) propose using the term active area instead of contributing area since this better illustrates what occurs in these landscapes. They observed that during an event where 50% of the basin was active and generating runoff the contributing area was 0% as none of this water reached the outlet. There do not appear to be any models which incorporate this concept into its structure.

Data Availability and Limitations

One of the main modelling challenges is the availability and quality of information to inform model parameterization (Fenicia et al. 2008). For some parameters, spatial information is not available, while for others, available information may have limited spatial representativeness (e.g. limited point measurements are not representative at large spatial scales) (Clark et al. 2017). If the required data exists there are still issues with completeness and inaccuracy (Singh and Woolhiser 2002). Data limitation often requires that catchment behaviour be inferred (Fenicia et al. 2008), or it leads to hard-coded parameters which underestimate the natural spatial heterogeneity of the landscape (Clark et al. 2017).

Data limitations can be particularly difficult in the BPs, where the low topographic relief ideally requires precise and detailed elevation data in order to properly map the connectivity of the wetland dominated landscape (Huang et al. 2013). There is limited freely available high-quality data in Canada. While 50k DEMs are available for all regions of Canada, they are not hydrologically corrected and do not provide the necessary elevation precision for the BPs.

A majority conclusion in the literature is the need for better metrics and measurements of field parameters (ex. Kirchner 2006, Ali et al. 2013, Spence and Phillips 2014) as there is a lack of measuring techniques capable of identifying the underlying hydrologic mechanisms (Fenicia et al. 2008). Ali et al. (2013) supposed that a catchment may respond to a precipitation event in such a subtle way that existing monitoring techniques may not be able to read it, further emphasizing the importance of improved field techniques.

2.3.5 Standard Modelling Approaches

How a model structure is developed is a function of the model objective (Singh and Woolhiser 2002) as different models utilize different approaches (i.e. lumped vs distributed, physical vs empirical) and solve the underlying mathematical equations differently. All hydrologic models were created for different reasons so there are differences between all of them (Paniconi and Putti 2015).

When developing models there are two general approaches: top-down and bottom-up. The top-down approach is based on deductive reasoning, trying to determine the causes of the overall effects observed in the system. This approach starts with a simple structure that increases in complexity as needed until it can represent the overall catchment behaviour with the available data (Fenicia et al. 2008). The bottom-up approach uses a detailed physical representation of all the catchment processes and tries to represent all the known physics in the model in as comprehensive a manner as possible, regardless of data availability. This thesis uses the top-down approach.

Hydrologic models can have a predictive purpose (are used to obtain a specific answer to a specific problem) or an investigative purpose (seeking to further the understanding of hydrological processes) (Blöschl and Sivapalan 1995). Engineering models are often predictive, they seek to answer a single question such as what are the flood extents of a specific return period, or what is the volume of water available for hydropower. Researchers can seek to answer predictive questions such as identifying reasons for a particular water balance characteristic (Hwang et al. 2018), or how to better represent wetlands (e.g. Watson et al. 2008, Fossey et al. 2015), or they can use investigative models to try to answer specific questions such as how a specific climate controls the root zone capacity development in catchments (Gao et al. 2014).

Usually modellers start with some basic fixed structure or a model with limited algorithm options, such as SWAT, HBV-EC, or GR4J/GR4H. However, in literature there are a number of arguments for

using flexible models as opposed to this standard fixed model approach (ex. Fenicia et al. 2008, 2011, Clark et al. 2011, van Esse et al. 2013).

The appeal of fixed models is the simplicity of using them, since repeatedly using the same model structure allows for easier model improvement, training of personnel, and interpretation of large-scale model applications (Fenicia et al. 2011). However, this approach assumes that a single model structure is capable of representing multiple catchments and climate conditions (van Esse et al. 2013). The main disadvantage of fixed models is their inherent assumptions and representations may not represent the actual dominant processes of a particular basin (van Esse et al. 2013). For example, TOPMODEL assumes that the baseflow-storage relationship is a power law function (Fenicia et al. 2011) which may not be appropriate in all basins. Flexible model structures allow modellers to build different model structures and test them in a specific environment which is useful at the catchment scale where challenges such as data limitations and limited physical understanding are prominent (Fenicia et al. 2011).

The advantage of the flexible modelling approach over the fixed approach was demonstrated in a study by van Esse et al. (2013) where twelve different flexible model structures were compared against a fixed GR4H structure in 237 catchments. The models were calibrated to two different periods and if the difference in parameter values between the average of the two periods was less than 50% the models were considered consistent. Additionally, the flexible model was considered consistent when the same model structure was selected as the "best" between the two periods. The results indicated that the flexible model approach outperformed the fixed model, although the flexible approach had a higher chance of being inconsistent. The study only used one diagnostic in calibration and model performance evaluation. By including additional metrics, it is possible that the flexible models could have had both better performance and consistency (see Section 2.4 for discussion). Another study utilized a top-down, stepwise model improvement approach to incorporate new hypotheses of catchment behaviour coupled with a multi-objective model evaluation (discussed in section 2.4.3) in order to evaluate single and competing model performance. The stepwise approach allowed for the identification of the dominant processes in the study catchment that would not have been possible with a fixed model structure (Fenicia et al. 2008). This stepwise approach is incorporated into the model development of this thesis.

In the above discussion of over 50 research papers, most model advancements involved the implementation of a new model algorithm or approach (ex. HEW) in an existing model structure or

the coupling of two existing models. Researchers often choose to improve "legacy" models instead of beginning the model development process from scratch (Quinn et al. 2012). A portion of the research community is utilizing flexible model structures, although they appear more focused on the idea of flexible models than utilizing flexible models for a specific modelling purpose. There are few studies on application of flexible model building in support of specific modelling objectives aside from hydrograph fitting. Therefore, this thesis provides a somewhat unique approach of developing a flexible model structure from scratch for the specific purpose of modelling the hydrology of the BPs. To the author's knowledge this is the first documented case of the stepwise model improvement application for simulating a specific landform driven hydrology.

2.3.6 Model Complexity and Parametrization

Models will always be a simplification of the natural environment, regardless of their complexity. To create a robust model, a balance must be struck between the complexity necessary to capture the functioning of the system and being prudent with the number of parameters in the context of architectural uncertainty (Hrachowitz et al. 2014). It is therefore the job of the modeller to properly limit the model by constraining model structure, model parameterization, model objectives, and *a priori* assumptions (Hrachowitz et al. 2014).

Parameters are inputs to the model that are not calculated directly by the model and can be constant or time-varying. If a parameter can be measured in the field it is classified as a physical parameter, hydraulic conductivity, for example, (Kampf and Burges 2007) while an empirical parameter can not be directly measured and does not necessarily have physical meaning. However, physical parameters can be set to values that are outside of a physically meaningful range and therefore become an empirical parameter in practice (Kampf and Burges 2007).

In general, the more physical processes that are included in a model the more parameters are required, which creates a trade-off between compressive representation and overparameterization (Kampf and Burges 2007). Overparameterization can lead to equifinality, where multiple model parameter sets can result in the same model output. Equifinality makes finding the "true" or "best" model a challenge and limits the likelihood that a model can be successfully used outside of a specific basin. This is one advantage of the top-down approach, as only the necessary complexity that captures dominant hydrologic processes is included. In an ideal world, models would only include parameters which can be estimated from available data, are at a known scale, have minimal interactions with

other parameters, are adaptable, and transferable (Kampf and Burges 2007). However, in practice this becomes difficult to achieve.

2.4 Model Evaluation

It is the modellers task to sufficiently constrain the model to a subset of all possible models that are representative of the system. This is usually achieved by comparing model outputs, typically hydrographs, to observation values (Hrachowitz et al. 2014). The degree of similarity between model and observation is characterized using some form of evaluation criteria. What model evaluation criteria is used varies depending on the purpose of the study and how rigorously the model was tested.

2.4.1 Model Diagnostic Metrics

The most common form of model evaluation are model diagnostics which compare model outputs to observed values. While there are numerous model diagnostics, **Table 2.3** summarizes the ones used to evaluate the performance of the models of this thesis. Note that Φ_i is an observation value (e.g., discharge in a stream), $\widehat{\Phi}_i$ is the corresponding modelled value, $\overline{\Phi}$ is the weighted mean of the observations and $\overline{\widehat{\Phi}}$ is the weighted mean of the modelled values.

Table 2.3: Summary of model diagnostics used in model evaluation.

Diagnostic	Equation	Description	Range
Nash Sutcliffe Efficiency (NSE)[1]	$NSE = 1 - \frac{\sum_{i=1}^{N}(\widehat{\Phi}_i - \Phi_i)^2}{\sum_{i=1}^{N}(\overline{\Phi} - \Phi_i)^2}$	Describes how closely the modelled data matches the observed data. A value of 0 means the modelled results are as accurate as the mean of the observations.	-∞ to 1
Percent Bias [2]	$PBias = \frac{\sum_{i=1}^{N}(\widehat{\Phi}_i - \Phi_i)}{\sum_{i=1}^{N}\Phi_i}$	Measures whether the average modelled result is larger or smaller than the observations. Negative numbers are an underestimation and vice versa.	-∞ to ∞
Root-Mean-Squared Error (RMSE)[3]	$RMSE = \sqrt{(\widehat{\Phi}_i - \Phi_i)^2}$	A measure of the standard of deviation of the differences between the observation and modelled values.	*function of the variable being optimized

Diagnostic	Equation	Description	Range
Kling-Gupta Efficiency (KGE)[4]	$KGE = 1 - \sqrt{(r-1)^2 + (\alpha-1)^2 + (\beta-1)^2}$	A derivative of the NSE. It addresses the underestimation of the NSE when there is minimal variability in flows. Where r is the correlation, α is the relative variability, and β is the bias.	-∞ to 1
R-squared (R2)	$R^2 = \frac{\sum_{i=1}^{n}(\Phi_i - \bar{\Phi})(\hat{\Phi}_i - \overline{\hat{\Phi}})}{\sqrt{\sum_{i=1}^{n}(\Phi_i - \bar{\Phi})^2} - \sqrt{\sum_{i=1}^{n}(\hat{\Phi}_i - \overline{\hat{\Phi}})^2}}$	A regression statistic. Describes how close the modelled data matches the observation data.	0 to 1

1. (Gupta et al. 2009)
2. (Craig et al 2018)
3. (Dingman 2015)
4.(Gupta et al. 2009)

2.4.2 Hydrologic Signatures

Hydrologic signatures are spatial and temporal patterns observed in a basin, such as the standard hydrograph. Another example of a hydrologic signature would be a regime curve, which is a description of the long-term monthly averages of various components of the water cycle such as discharge depth, rain, and PET. A realistic model is one that captures the relevant runoff processes, and thus the hydrologic signatures. Model performance is the ability for the model to represent a specific hydrologic behaviour. Model consistency is the ability to represent multiple hydrologic signatures while using the same parameter set. To determine if a model structure is realistic it must have both good performance (often good hydrograph fit as determined through metrics, e.g. NSE) and hydrologic consistency (Euser et al. 2013).

In the literature it has been acknowledged that evaluating models with a single metric is insufficient (Fenicia et al. 2008, Euser et al. 2013, Westerberg and McMillan 2015). Using different hydrologic signatures to analyse different catchment responses and understand different hydrologic processes is one solution (McMillan et al. 2014). Individual hydrologic signatures often represent a specific aspect of the hydrologic response of a basin. This allows for easier interpretation of the underlying processes when compared to single metrics such as the NSE. However, this can be a disadvantage as only small aspects of catchment response are represented by each signature, making it necessary to use multiple hydrologic signatures when evaluating model performance (Euser et al. 2013).

A study by Hrachowitz et al. (2014) examined models with varying complexity and demonstrated the need for hydrologic signatures in model evaluation. All of the models had similar calibration performance, however, the more complex model had higher model consistency. Without using hydrologic signatures determination of the best representation would not have been possible as they would have all been deemed adequate.

2.4.3 Calibration and Validation

Model calibration is the process of selecting a representative parameter set for a model by comparing model output to a specific data set. Validation is the use of an independent data source from model calibration to evaluate model performance, and is considered good practice (Zheng et al. 2018). An inherent problem of calibration is equifinality (Singh and Woolhiser 2002), thus the need for other evaluation criteria such as hydrologic signatures and validation.

There have been many different techniques developed in the past five decades (Paniconi and Putti 2015) with large advancements in automated calibration in the past two decades (Singh and Woolhiser 2002). A standard calibration approach involves manual calibration followed by automatic parameter estimation which generally has four elements: 1) an objective function, such as the NSE; 2) an optimization algorithm; 3) termination criteria; and 4) calibration data. The choice of each element influences parameter estimation and the resulting quality of the model (Singh and Woolhiser 2002).

Multi-objective calibration involves simultaneous evaluation of an objective function for objectives which describe different aspects of the systems behaviour. This generates a Pareto-optimal front that identifies the best performance that can be achieved within a given model structure as demonstrated by Fenecia et al. (2008).

A common method for calibration and validation is the split sampling approach, where the entire period of observed data is split into a calibration period and a validation period (KlemeŠ 1986). However, how the data set should be split has not been well reported in literature, despite results indicating that the selection of this split can significantly impact model performance (Zheng et al. 2018). If extreme events are not included in the calibration period the model will be unable to capture extreme events in the validation period (Watson et al. 2008, Zheng et al. 2018). It has been suggested that a minimum of 5 years is required for calibration and there should be at least one “wet” year and one “dry” year in the calibration data set (Watson et al. 2008).

2.5 Existing Models of the Boreal Plains

To the authors knowledge there are two papers which discuss the creation of a model specifically for the Boreal Plains. The first is by Watson et al. (2008) where they modified the Soil Water Assessment Tool (SWAT) as part of the FORWARD project. The second is by Hwang et al. (2018) where they used HydroGeosphere (HGS) to model the entire Athabasca River Basin (ARB). There is also a discussion on some other models of the ARB that were not developed specifically for the BPs.

2.5.1 SWATBF

SWAT is a semi-physical model originally developed for agricultural applications (Watson et al. 2008) that operates at the basin scale and on a daily time step (Gassman et al. 2007). There have been over 200 peer-reviewed articles published about SWAT (Gassman et al. 2007) with several papers discussing various modifications that were made to SWAT. Watson et al. (2008) made modifications to SWAT to better represent the processes which occur in forested watersheds in the BPs called SWATBF.

The study occurred at the primarily forested and undisturbed Willow Creek basin (15.1 km^2) which was part of the FORWARD project. To create SWATBF several modifications were made, including algorithms to account for the effects of cloud cover, slope, and aspect on solar radiation, and the addition of a litter layer as a storage compartment. The study claims that in the Boreal Forest the litter layer is thick and plays an important role in water storage. This claim is based primarily on an ecological carbon modelling paper of the Boreal Forest by Peltoniemi et al. (2007). None of the other papers reviewed for this thesis mentioned the significance of the litter layer. Modifications also allowed water transfer between HRUs, so runoff from the upland forests can be routed through the lowland wetlands. The traditional SWAT wetland model only allows one wetland per subbasin and treats wetlands as open water sources, ignoring vegetation cover. This representation was updated so wetlands were represented with two organic soil layers (Watson et al. 2008) and had the water balance shown in **Figure 2.10**.

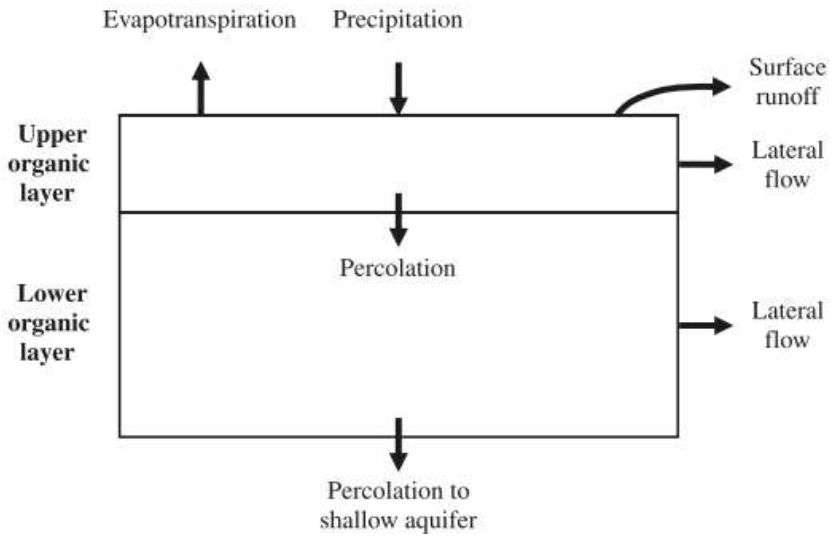

Figure 2.10: Wetland representation in the SWATBF model (Watson et al. 2008)

The model only considered shallow groundwater connections, since, due to the size of the basin, they assumed regional aquifer connections would contribute to streamflow outside of the study area. The SWATBF model accounted for frozen soils by transferring any shallow baseflow to the snowpack if the average air temperature was less than 0°C. While the objective of the study was to create a practical model that could be deployed by industry engineers, data not readily available outside of research basins, such as solar radiation, relative humidity, and wind speed, were required by the model.

The study used a split sample calibration approach with a calibration period from 2001-2003 and a validation period from 2004-2006, with a warm up period from 1997 to 2000. While the study acknowledges that this is a short period of time for calibration, the calibration period did incorporate a dry and a wet year. The model had 15 calibrated parameters with some of the calibrated values reaching their specified upper and lower bounds (Watson et al. 2008). This could indicate that a better model value exists outside of this range or that the calibration was trying to turn off a specific process. The study uses the NSE to evaluate model performance. In calibration there was good model performance with the NSE for monthly runoff values at 0.89 and 0.81 for daily runoff values; the percent bias was less than 15%. However, in validation the NSE dropped to 0.44 and 0.27 for monthly and daily runoff, respectively and the percent bias exceeded 40% (Watson et al. 2008). The drop in model performance in validation indicates that the model does not successfully represent the BPs. The study claims the limited availability of streamflow data and spatial variability of

precipitation likely impacted the models performance (Watson et al. 2008). While not mentioned in the article, it is possible that the limited representation of wetlands also impacted model performance.

2.5.2 HydroGeoSphere

HGS is a three-dimensional physically-based hydrologic model designed to simulate fully-integrated surface-subsurface water flow and solute transport using the control-volume finite element method. The purpose of the study was to determine why downstream mean annual streamflow in the ARB is higher than upstream even though there are water deficit conditions in the downstream (BPs) reaches (Hwang et al. 2018). While this is a model of the entire ARB, since the focus is on the water balance in the BPs it is being considered a BPs model.

The study generated a high resolution, three-dimensional, 22-layer, model of the entire ARB based on bedrock, surficial geology, and spatial generation of peatlands for long-term steady state conditions. The landcover was split into five classes: Boreal Uplands, Boreal Foothills, Boreal Mixedwood, peatlands, and water bodies. The two-dimensional surface domain was generated from 1 km resolution DEMs and discretized into 44,592 nodes and 87,568 elements with an average horizontal resolution of 3 km in the upland, and 0.5 km along major surface drainage features. The HGS subsurface model had a 13 geological unit discretization with 1 million nodes and 1.9 million elements. The subsurface model considered peatland connections and macropores in the shallow subsurface. AET in the model is a function of partitioning coefficients, root distribution functions, and PET (Hwang et al. 2018).

The streamflow rate at different gauges was used to estimate net precipitation for each of the six model subbasins. There were three types of boundary conditions in the HGS model: critical depth, rainfall, and ET. Critical depth conditions were applied along the outer boundary of the surface domain while the other two were applied at the top of the integrated surface-subsurface domain (Hwang et al. 2018).

The model was not a continuous simulation, but rather output single long-term steady state values for each of the six subbasins. Calibration included 55 parameters and two calibration steps. The first step estimated a spatially averaged AET for each subbasin through an iterative method, while the second step calibrated the model based on measured surface flow and groundwater table elevations. This was done by manually fitting the model parameters with 83 observations and the AET estimates from the previous time-step (Hwang et al. 2018).

The HGS model was used to simulate steady-state long-term surface water and groundwater conditions between 1971 and 2010. The model outputs a single mean flow rate for the entire 40-year period and reported a R^2 value of 0.96; the model does not report monthly or daily streamflow values (Hwang et al. 2018).

There are some questions raised by this study that are not answered. For example, at a resolution of 0.5 km, can the model accurately capture wetland processes? At this large of a scale does root distribution have any physical meaning? Is one spatially averaged AET value appropriate for $1/6^{th}$ of the entire ARB? However, for the purposes of their study, a single 40-year averaged long-term discharge value is appropriate, however, for the purposes of decision making, daily values are often required, and therefore, it is doubtful that this model will be appropriate for such a purpose.

2.5.3 Other Models in the ARB

While not focused on the BPs, Faramarzi et al. (2015) used SWAT to develop models of the 17 major river basins in Alberta, including the ARB. The focus of the paper was to examine the impact different input data sets had on model performance. The study also stressed the importance of correct model structure, stating that correct model structure can reduce parameter uncertainty. The study also claims that poor model structure and/or inappropriate input data can be compensated for with unrealistic model parameters acquired during calibration (Faramarzi et al. 2015) and thus get the right answers for the wrong reasons.

To achieve their objective, 13 SWAT models were constructed with different gridded climate and topographic data; mostly global or country-wide products. The different models also included different hydrological processes such as pothole, regulated dams, and glacier representations. Despite the emphasis on the importance of proper model structure there was limited discussion on the structure of the models used in the analysis. The models produced monthly runoff values which were compared to 40 WSC stations. The average NSE for the 13 different SWAT model structures for the entire province ranged from -6000 to 0.12. In the ARB the pre- and post-calibration monthly NSE values ranged from -8.7 to -0.024, and -5.8 to 0.112, respectively (Faramarzi et al. 2015). This would be considered poor performance; while other diagnostics were used in the paper they were similarly poor. However, if the monthly values have poor diagnostics the daily values would likely be worse. The primary relevance from this paper to this thesis is that while input data does matter, perhaps model structure matters more, and careful consideration of model structure is required.

A study by Shaw et al. (2005) focused on improving the derivation of physiographic parameters and flow direction for input into a WATFLOOD distributed model for routing purposes. The study focused on a variety of scales including the local scale at Wolf Creek (a subbasin of the ARB), the regional scale at the ARB, and the continental scale in the Mackenzie River Basin. The study concluded that improved upscaling of physiographic parameters and flow direction could improve model performance but did not focus on model structure improvements (Shaw et al. 2005). There was no discussion on use of model structure specific to the BPs.

Kerkhoven and Gan (2006) also looked at global circulation model routing techniques in the ARB. The objective of the paper was to improve streamflow simulation by developing a new statistical approach for the treatment of moisture variability and its role in producing runoff such that this moisture variability could be easily incorporated in a hydrologic model. The study compared two large scale climate data sets and produced monthly, mean annual, and minimum annual flows. The method focused mainly on developing an empirical relationship between soil texture, soil moisture, and runoff and statistical representations of landcover and precipitation variability (Kerkhoven and Gan 2006).

There was also a large-scale study of climate change impacts on the Peace-Athabasca Delta using the WATFLOOD distributed model. The study added a new wetland module which considered wetland storage impacts on dampening runoff. The model provided daily flows but evaluation metrics were calculated at a monthly scale. The model achieved an NSE of 0.76 in the Peace River Basin and 0.72 in the ARB with both river models overestimating flow by 19% and 29%, respectively (Toth et al. 2006). At the river basin scale the local influence of the Boreal Plains on the outlet hydrograph should be overwhelmed by the upstream water contribution so proper BPs representation is less critical at this scale.

Gibson et al. (2015) focused on the small individual lake catchment scale. The study developed steady-state isotope mass balances in 50 lakes across northeastern Alberta, including several in the south portion of the study area which are in the vicinity of the three study basins discussed in Chapter 3. The study calculated water yields, runoff ratios, and lake residence times (Gibson et al. 2015). However, at this small scale the study does not describe how to determine catchment scale model representation in the BPs.

Table 2.4 summarizes these additional studies.

Table 2.4: Summary of other Athabasca River Basin studies

Model Used	Model Scale	Model Focus
SWAT[1]	Regional river basin	Testing 13 model structures in 17 major river basins in AB
WATFLOOD[2]	Multiple: small local scale, regional river basin, and continental scale	Representation of physiographic features in models
SVAT[3]	Regional river basin	Compare two large scale climate data sets
WATFLOOD[4]	Regional river basin	Testing wetland module change of model of the Peace and Athabasca river basins
N/A[5]	Local lake scale	Used isotopes to create mass balances at individual lakes

1. Faramarzi et al. 2015
2. Shaw et al. 2005
3. Kerkhoven and Gan 2006
4. Toth et al. 2006
5. Gibson et al. 2015

Other modelling focuses in the ARB have included constructed wetlands (Nicholls et al. 2016, Ketcheson et al. 2016), nitrous oxide emissions (Shrestha and Wang 2018b), predicting sediment yield (Shrestha and Wang 2018a) and ecological models. From the literature it appears that no current models have the skill to adequately capture the hydrology of the Boreal Plains at the individual catchment scale. Additionally, they are more focused on either large scale models with large time steps or small local catchment scales as opposed to individual river catchments at daily time steps as this thesis is.

Chapter 3
Baseline Models & Data Preparation

The purpose of this chapter is to explain the model development process including the reasoning behind development decisions. One of the purposes of this thesis is to generate a practical model of the BPs. This means that it needs to only use data that is freely available and not specific to a particular research basin. The other purpose of the model is to balance physical realism with a complexity that is appropriate for the available data. As such, the model development process is informed with soft constraints on physical plausibility. Throughout the model development process, attempts were made to balance representing the complex physical hydrology of the BPs with the constraints enforced by limited data. This is discussed in detail in Chapter 4.

3.1 Baseline Model

An initial model of the region studied in this thesis was developed by the consulting company MacHydro on behalf of Alberta WaterSMART (AWS). AWS is a company based in Alberta who are currently undertaking the task of building a coupled hydrologic and hydraulic model of the entire Athabasca River Basin (ARB). The ARB is shown in the context of the federal ecologic definition in **Figure 3.1**. MacHydro used a fixed modelling approach by utilizing a variant of the HBV-EC model emulation in the Raven Hydrologic modelling framework (Raven) to simulate the ARB in the AWS model. The model performed well upstream of the Boreal Plains, but inadequately in the BPs. This thesis will use 3 subbasins (**Figure 3.2**) upstream of Fort McMurray, AB, from the AWS model of the ARB as a testbed for developing a sound model configuration within the Raven framework. **Table 3.1** summarizes the original AWS model diagnostics for each of the study basins taken from the AWS model files; note the run period was from 2003-09-01 to 2014-11-22. All of the models in the AWS baseline case were not calibrated. Instead the calibrated data set from a different basin in the ARB was used to generate the study basin models. Note that all of the models are underestimating flow volumes and have fairly poor NSE and R2 values, which is expected since the HBV-EC model is missing critical BPs processes such as wetland function. Subsequent sections will briefly discuss basin locations and characteristics.

Table 3.1: Summary of original AWS model results

Study Basin	NSE	%Bias	R2
House River	0.324	-15.40	0.346
Hangingstone River	0.293	-11.89	0.298
Christina River	0.259	-22.18	0.323

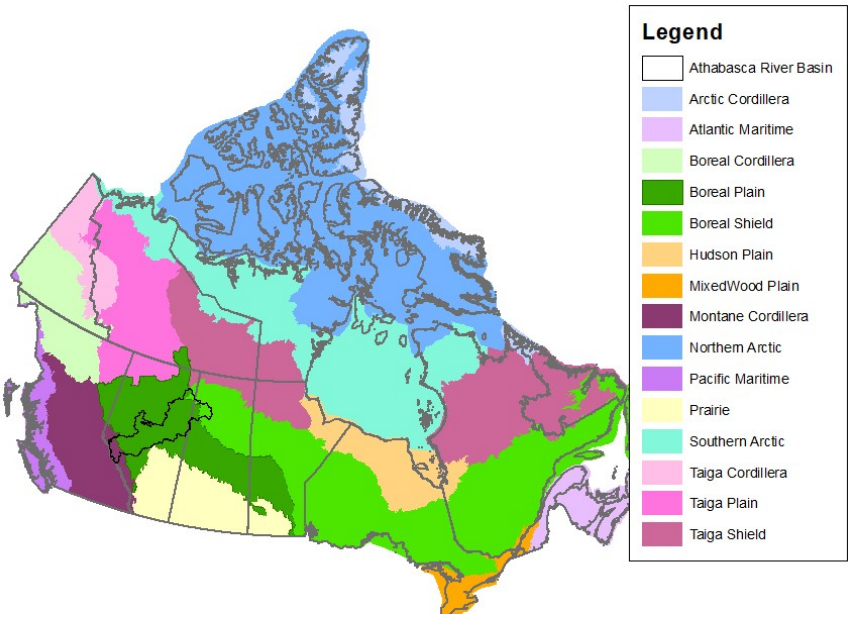

Figure 3.1: The ABR within the Federal Ecological Framework

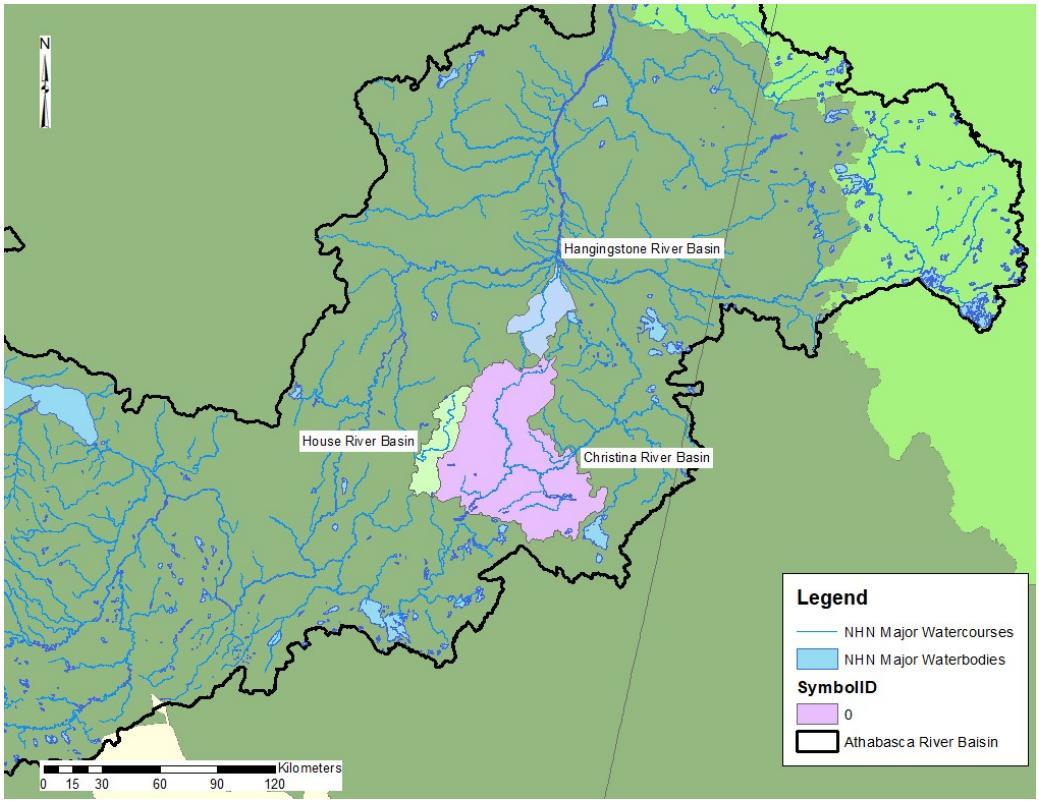

Figure 3.2: Map of the three subbasins used in this study: The House River (green), the Christina River (pink), and the Hangingstone River (blue). The basins are shown in the context of the Federal Ecological

Framework, the dark green is the Boreal Plains, light green is the Boreal Shield, and light yellow is the Prairies.

3.1.1 Basin 1 – House River Basin

The House River gauge (**Figure 3.3**) has an approximate gross drainage area of 773 km^2 and is the basin where the primary model structure of this thesis was developed. The single Water Survey of Canada (WSC) hydrometric gauge (07CB002) is near the headwaters of the basin and is approximately 65 km upstream of the confluence of the House River with the Athabasca River. The basin is mostly undisturbed and is covered primarily with forest and riparian wetlands. It has the least relief of the three study basins with elevation ranging from approximately 675 m to 750 m. This basin was selected as the primary test basin for the BP model development due to its low relief, undisturbed landscape, and lack of complicated features such as large lakes.

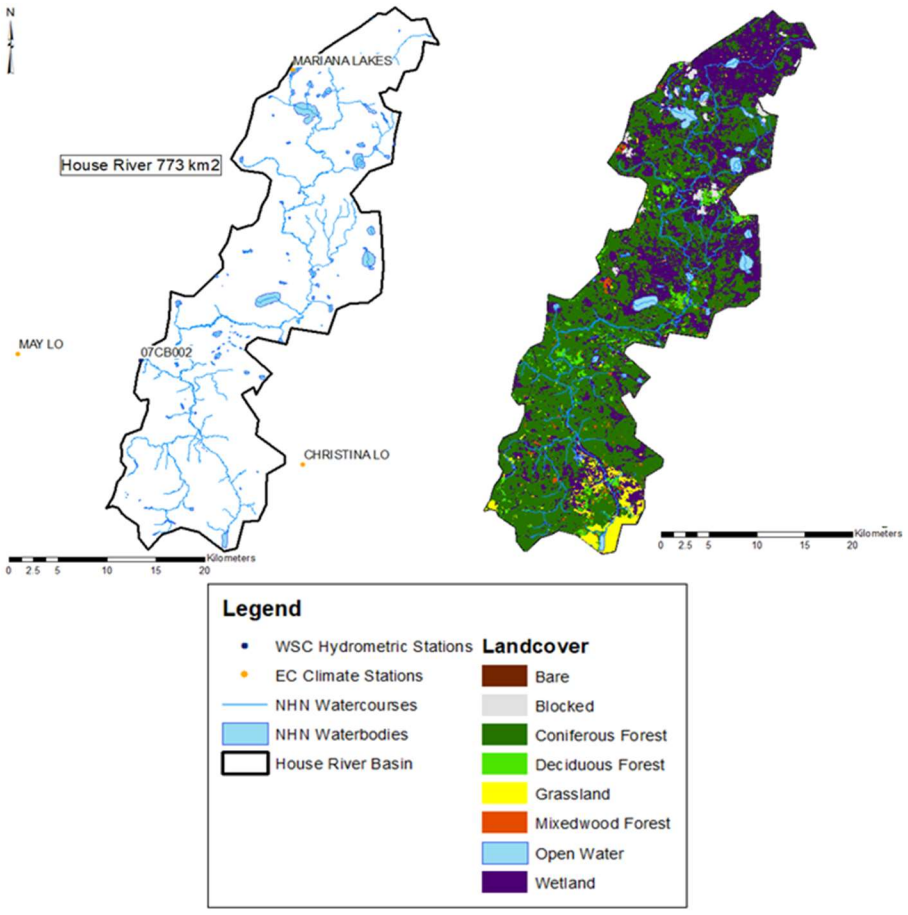

Figure 3.3: Maps of the House River Basin including available WSC and EC gauges (left) and landuse classification (right)

3.1.2 Basin 2 – Hangingstone River Basin

The Hangingstone River basin and available stations are shown in **Figure 3.4**. At 760 km^2 in size, it is a comparable size to the House River Basin. The lone WSC gauge (07CD004) is very close to the confluence with the Clearwater River. The primary landuses are forest and riparian wetlands; however, there is a larger portion of deciduous forest and disturbed areas than in the House River Basin, such as the visible linear right-of-way (classified as Bare). The basin has the most vertical relief of the three study basins, with the headwaters at approximately 733 m and the outlet at approximately 254 m.

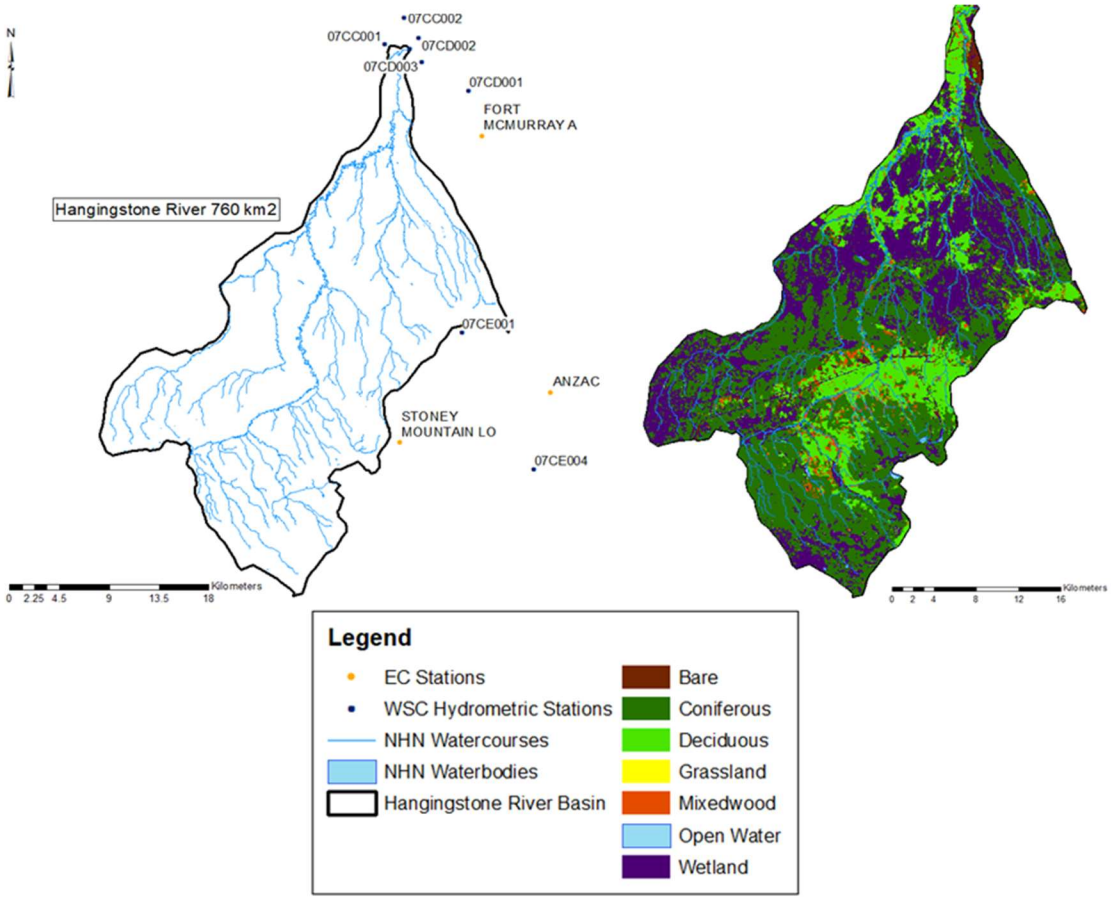

Figure 3.4: Maps of the Hangingstone River Basin. Left shows basin extents, river network, and available WSC and EC gauges. Bottom Shows the land use classification.

3.1.3 Basin 3 – Christina River Basin

At 4,865 km^2, the Christina River Basin (**Figure 3.5**) is larger than either of the other study basins, it is also the only study basin with a large lake (Christina Lake, 21.3 km^2 surface area). The WSC gauge (07CE002) at the outlet of the basin is located approximately 120 km upstream from Christina River's confluence with the Clearwater River. As with the other basins, the primary landuses are forest and riparian wetlands, however, there are large portions of the basin covered by deciduous trees, grasslands, and disturbed areas. The elevation varies by approximately 300 m from the edges of the basin to the outlet. This basin also has some active industry processes including water extraction and release, however, these were not included in the model (Hatfield Consultants et. al 2016).

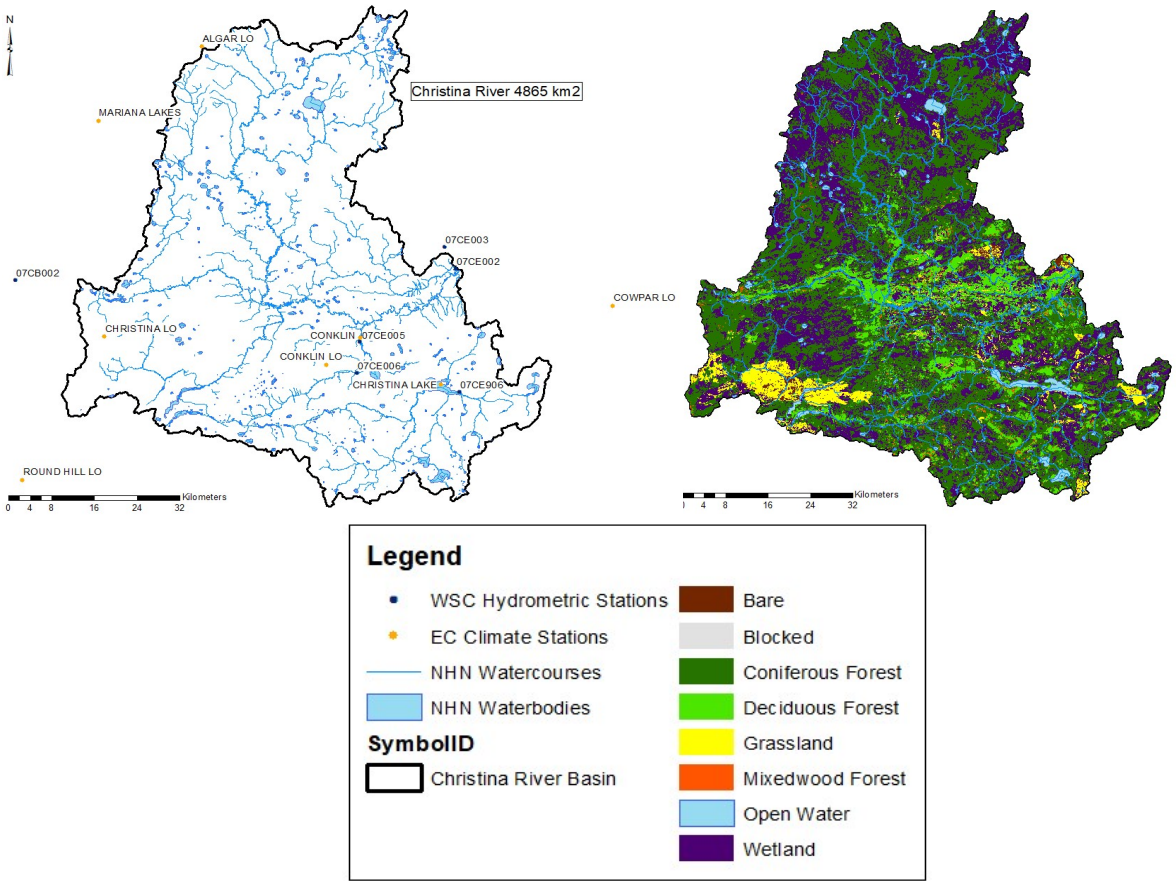

Figure 3.5: Christina River Basin with available EC and WSC gauges and river network (left) and landuse classification (right).

3.2 Raven Hydrologic Modelling Framework

Raven (Craig et al. 2018) is an open source flexible modelling framework with modelling capacity ranging from individual storm events to long term mass balances. What makes Raven unique is its numerical robustness and flexibility. Raven includes a large variety of algorithms and hydrologic processes and allows the user to choose which processes to include and how to represent those processes. Raven requires various input text files which are briefly described in **Table 3.2**. Raven is the sole software system used for model development in this thesis.

Table 3.2: Summary of Raven input files

File Extension	Purpose
.rvi	Model specification file. Main inputs including time period for model to run, which algorithms and processes are to be used, routing options, number of soil layers, forcing function options, transport options, and output options
.rvh	Model discretization file. Subbasin definitions, HRU definitions, HRU group definitions.
.rvc	Initial model conditions. Initial flow in each subbasin.
.rvp	Model parameter file. Define all model parameters including global parameters, soil parameters, vegetation parameters, landuse parameters, and channel profiles.
.rvt	Model time series files. All time series inputs including climate observations, hydrometric gauge observations, transient parameters, and inflow histories.

3.3 Model Inputs

This section briefly describes the data and subsequent data processing that was required to produce the necessary model input files (**Table 3.2**). Data include GIS data, Environment Canada (EC) climate data and hydrometric gauge stations.

ArcMap was used to process the GIS data used to generate the subbasins and HRUs for the .rvh (basin discretization) file. The GIS data sets that were used are summarized in **Table 3.3**.

Table 3.3: Summary of GIS data used.

Data Type	Source	Purpose & Specifications
Digital Elevation Map (DEM)[1]	Canadian Digital Elevation Dataset	50k resolution DEM; for elevation and topographic data
Hydrologic Network[2]	National Hydrologic Network (NHN)	Shapefiles of watercourses and waterbodies, completion level 1 so errors are possible
Landcover[3]	Land Cover, circa 2000-Vector (LCC2000-V)	Shapefile of landcover by NTS grid, used for landuse types

1. (NRCan 2007)
2. (NRCan 2016)
3. (NRCan 2002)

The 43 default landuse classes of the LCC2000-V data set were merged into 9 landuse categories for modelling purposes: NoData, Blocked, Open Water, Bare, Grasslands, Wetlands, Coniferous Forest, Deciduous Forest, and Mixedwood Forest. Blocked refers to areas that were covered with clouds or shadows and Bare refers to areas that are barren, exposed, or developed. Subbasins (**Figure 3.6**) were first delineated for each study basin manually using contours since no hydrologically corrected DEM was freely available and current GIS tools could not satisfactorily condition the 50k resolution DEM. The landuse classes were then aggregated such that each subbasin only had one of the 9 categories as an HRU. Average elevation, aspect, and slope were calculated for each HRU while the latitude and longitude for each HRU was set to the coordinates of the center of the subbasin. Areas classified as NoData or Blocked were added to the dominant landuse of the subbasin which in all cases was Coniferous Forest. The Mixedwood forests were added to the Deciduous Forest HRUs. The percentage of area classified as NoData or Blocked was less than 1% so aggregating it into the dominant land class should not impact the overall distribution of HRU types. Additionally, while Mixedwood Forest was originally left as its own HRU class, in all three basins the total Mixedwood Forest area was less than 2% of the entire basin, therefore, it was aggregated into the Deciduous Forest HRU group. It was aggregated into the Deciduous Forest HRU as opposed to the Coniferous Forest HRU since when the average elevation, aspect, and slope were calculated the Mixedwood and Deciduous values were almost identical while there were differences from the Coniferous Forest class. The final HRU class for each study basin is summarized in **Table 3.4**.

Table 3.4: Summary of each proportion of HRU type in the three study basins.

Study Basin	%Lake	%Bare	%Grassland	%Wetland	%Deciduous Forest	%Coniferous Forest
House River	2.71	0.34	2.35	32.18	2.78	59.64
Hangingstone River	0.53	1.13	0.01	31.65	18.65	48.04
Christina River	3.17	1.01	4.03	32.41	9.57	49.81

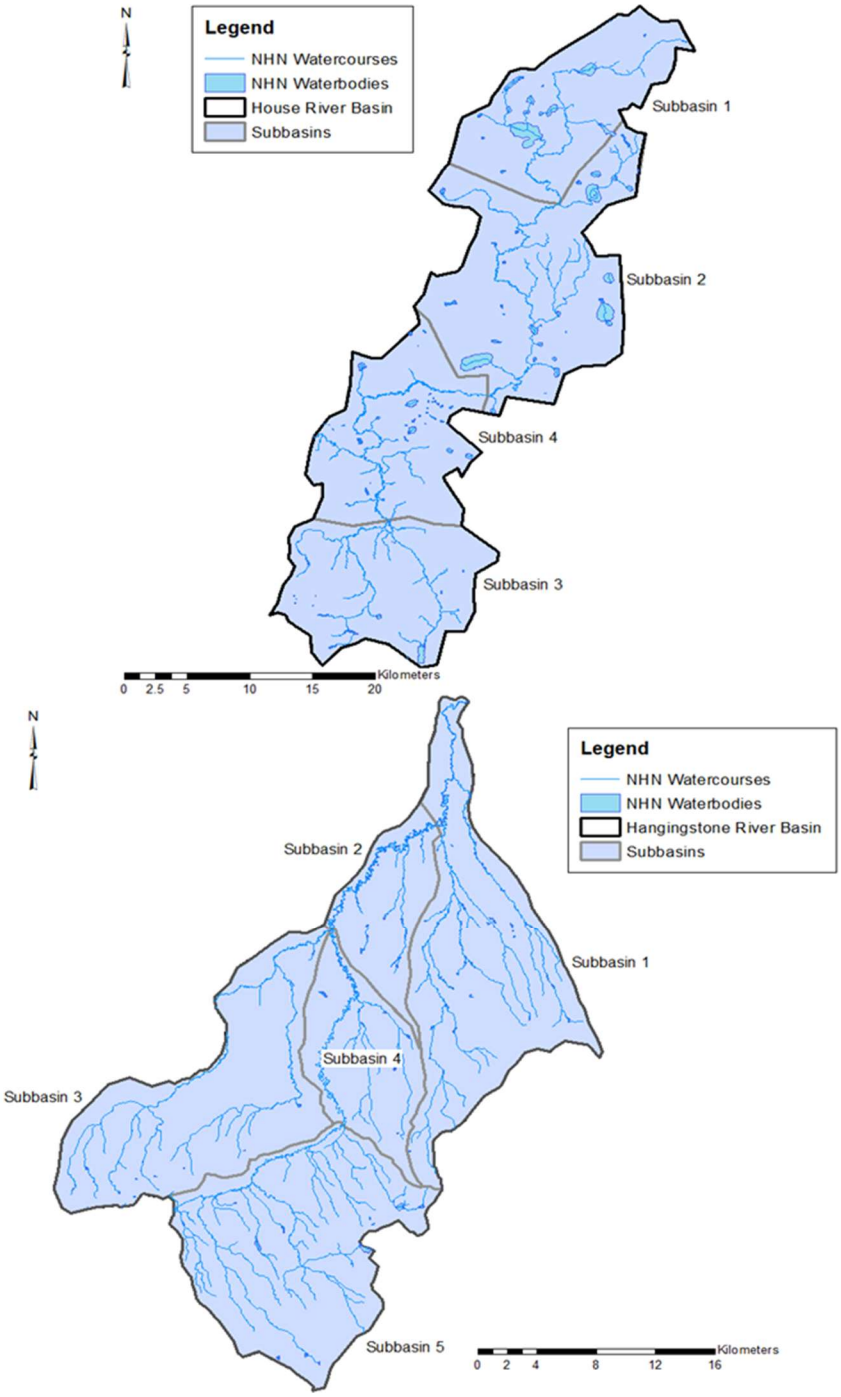
N
Legend
NHN Watercourses
NHN Waterbodies
House River Basin
Subbasins
Subbasin 1
Subbasin 2
Subbasin 4
Subbasin 3
0 2.5 5 10 15 20
Kilometers
N
Legend
NHN Watercourses
NHN Waterbodies
Hangingstone River Basin
Subbasins
Subbasin 2
Subbasin 1
Subbasin 4
Subbasin 3
Subbasin 5
0 2 4 8 12 16
Kilometers

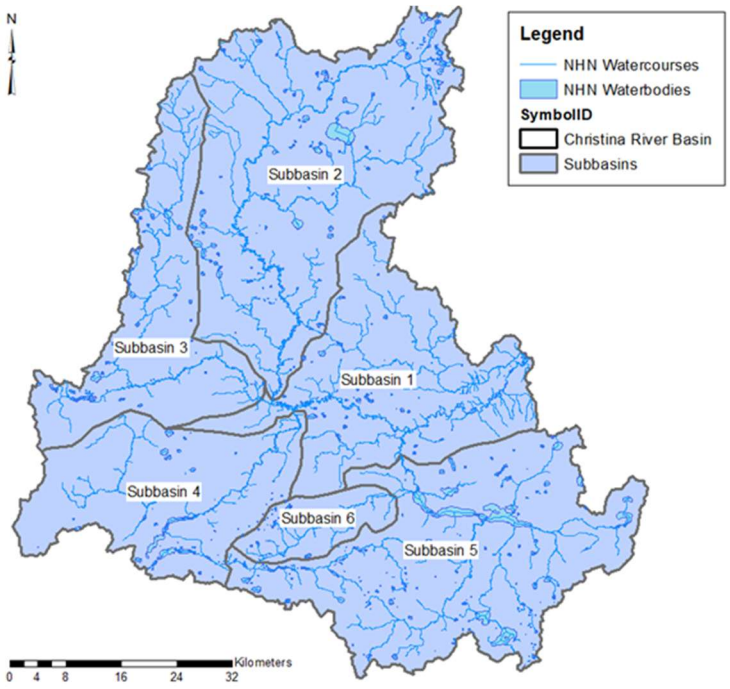

Figure 3.6: Subbasin discretization for House River (top), Hangingstone River (middle) and Christina River (bottom).

Available EC climate stations are shown in **Figures 3.3**, **3.4** and **3.5** for each study basin, note that there are limited gauges with extended periods of record. **Table 3.5** summarizes the climate station data used in each study basin model. Note that all stations except for Fort McMurray had no data in the winter.

Table 3.5: Summary of EC gauges used in model development

Study Basin	Gauge Name	Period of Record	Winter Data Available	Percentage of Days Missing
House River	May LO	1957 -2011	No	59%
Hangingstone River	Fort McMurray A	1920 - 2016	Yes	3%
	Stoney Mountain LO	1954 – 2011	No	58%
Christina River	Algar LO	1959 - 2011	No	62%
	Christina LO	1966 – 2002	No	71%
	Conklin LO	1954 – 2011	No	59%
	Cowpar LO	1957 - 2011	No	60%

There is a corrected and homogenized data set of EC data available for select stations; of the above stations, only the Fort McMurray station had a corrected data set and this data set ended in 2008. This corrected data was used when available. The climate stations inputs used in the model are total precipitation, and daily maximum, minimum, and average temperatures. When available, the reported

average temperature was used. When not available, the average temperature was calculated as the average of the daily maximum and minimum temperature.

The Canadian Precipitation Analysis (CaPA) is a gridded precipitation product with data available after 2005. CaPA combines collected real time precipitation data from a variety of meteorological partners with the short term forecast from the Regional Deterministic Prediction System (Fortin 2014). Missing precipitation data at the May gauge after 2005 was filled in using CaPA data. The remaining days with missing precipitation were filled in using the Calling Lake, Lac La Biche, and Fort McMurray climate stations which had more complete records. Calling Lake is approximately 78 km from the House River WSC gauge, Lac La Biche is approximately 98 km away, and Fort McMurray is approximately 127 km away. These large distances are why these gauges were not included in the model, but they are the closest gauges that have data in the winter. **Figure 3.7** shows these 3 gauges in relation to the House River basin.

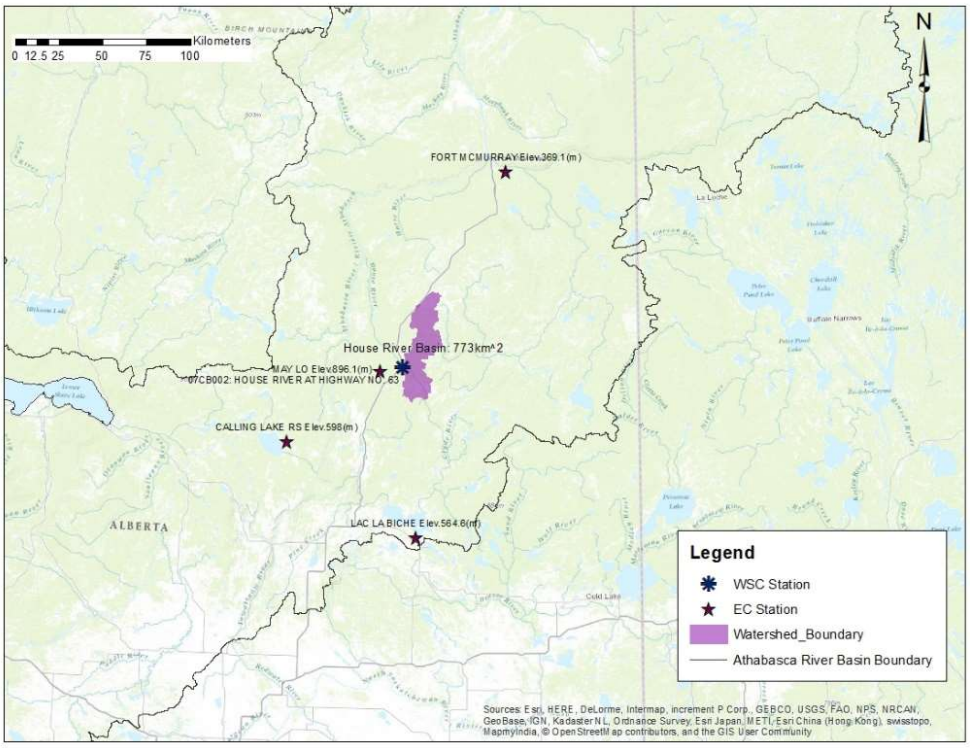

Figure 3.7: Map showing the location of the more complete EC gauges in relation to the House River Basin.

Prior to infill, the May station was compared to the Calling Lake, Lac La Biche, and Fort McMurray stations. Weekly total precipitation was calculated and the correlation between each station and the May station was determined by plotting these weekly precipitation values against one

another. The descending order of May station correlation with the other stations is Calling Lake (0.38), Lac La Biche (0.34), and Fort McMurray (0.24). A probability distribution function of the reported precipitation at the EC gauges is shown in **Figure 3.8**; note that May station has a higher mean total precipitation than the other gauges, likely part of the reason for the low correlation. Missing precipitation data was infilled directly from the station that had available data and the highest correlation. The daily temperature values were also compared in the same manner and while the correlation values were higher, the order remained the same. Missing maximum and minimum temperature data was infilled using the slope of the linear regression line between the two gauges and was filled using the same order of gauge preference as the precipitation data.

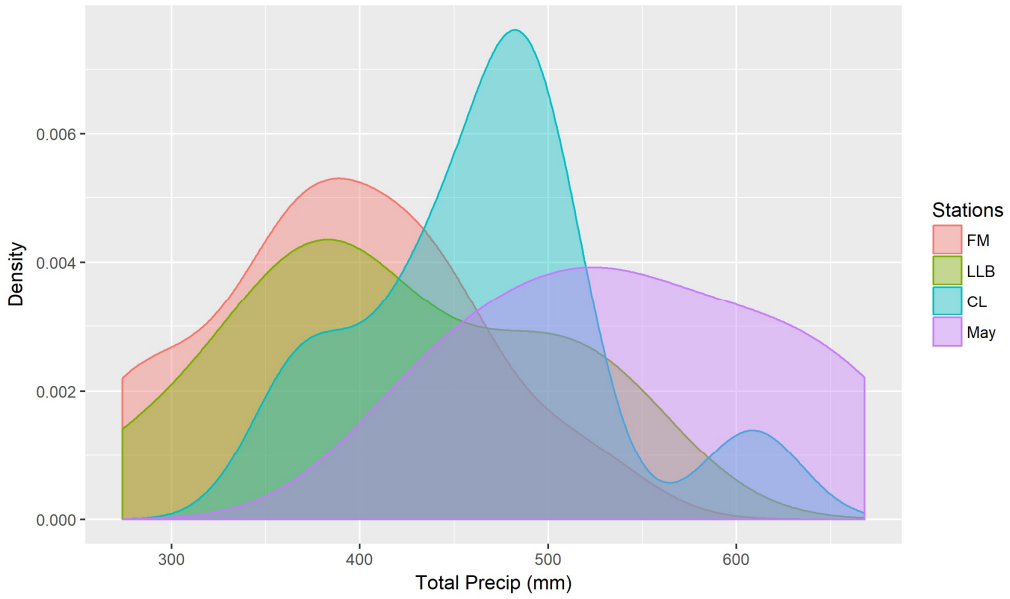

Figure 3.8: Probability distribution function of annual total precipitation for the 2001-2011 water years.

The completed data set, including the infilled data, was compared to the Alberta Climate Information Service (ACIS) historic interpolated data set. There was strong agreement between the two and thus the ACIS data was used to infill missing data at the gauges used in the other study basins. The ACIS data was not used initially since it was unclear how the data was interpolated due to minimal available documentation. To minimize the number of interpolated values the gauge records were not extended past 2011 since this would result in years where 100% of the data was interpolated from gauges that were further away since the closer gauges were discontinued.

Table 3.6 summarizes available hydrometric gauges in the study basins from WSC and the Regional Aquatics Monitoring Program (RAMP). Gauges used in the model have a star beside the

gauge number. Unfortunately, since the EC climate data ends in 2011, the RAMP gauges could not be used. Note that WSC flow data marked with the 'B' flag was removed from the observation data set in the models. This 'B' flag indicates that backwater effects were observed at the gauge, usually due to ice effects, making the reported discharge unreliable as it will not fall on the open water rating curve used to determine the gauge discharge rate.

Table 3.6: Summary of available hydrometric gauge data.

Study Basin	Gauge Source	Gauge Number	Gauge Name	Period of Record	Measurement
House River	WSC	07CB002*	House River at Highway No. 63	1982 - 2016	Flow
Hangingstone River	WSC	07CD004*	Hangingstone River at Fort McMurray	1965 - 2018	Flow
Christina River	WSC	07CE002*	Christina River near Chard	1982 - 2018	Flow
	WSC/RAMP	07CE005*	Jackfish River below Christina Lake	1982 – 1995 2010 – 2017	Flow
	WSC	07CE006*	Birch Creek near Conklin	1984 - 1995	Flow
	WSC	07CE906*	Christina Lake near Winefred Lake	2001 - 2018	Level
	RAMP	S57	Sunday Creek above Christina Lake	2011 - 2015	Flow
	RAMP	S60	Unnamed Creek South of Christina Lake	2012 - 2017	Flow
	RAMP	S61	Christina River above Statoil Leismer	2012 - 2017	Flow
	RAMP	S62	Birch Creek at Hwy 881	2012 - 2017	Flow
	RAMP	S63	Sunday Creek at Hwy 881	2012 - 2017	Flow
	RAMP	S64	Unnamed Creek East of Christina Lake	2012 - 2017	Flow

A new set of AWS models were created, which has the same parameter set and algorithms as the original AWS models but has the updated forcing and subbasin and HRU discretization that was used in the study basin models. These updated AWS models will henceforth be referred to as the AWS baseline models. To allow comparison between the original AWS models and the AWS baseline

models and to see the impacts of the changes, the baseline model was run for the same time period (2003 - 2014) as the original AWS models. **Table 3.7** summarizes the diagnostics of this updated model and compares them to the original AWS model results originally reported in **Table 3.1.** These AWS baseline models were also run for the same time period as the models of this thesis; these results are also summarized in **Table 3.7**. All future comparisons between the thesis models and the AWS baseline model will refer to the baseline model run for the thesis time period. When the subbasin and forcing data was updated there is an improvement in model NSE performance Christina study basins, while the House River and Hangingstone River basins see a decline in performance. Model NSE values dropped in the Christina River and House River basin when the baseline model was run for the same period as the thesis models while the Hangingstone River model improved. The reason for this change in model performance is unclear, one possibility could be that at such low NSE values, any minor increase in value may not correspond to better model performance as these numbers are too low to be interpreted.

Table 3.7: Summary of AWS baseline diagnostics.

Study Basin	Original AWS Model			Baseline Model – Original model period (2003 – 2014)			Baseline Model – Thesis model period			
	NSE	%Bias	R2	NSE	%Bias	R2	NSE	%Bias	R2	Model Period
House River	0.32	-15.4	0.35	-0.64	-10.2	0.07	-1.91	19.0	0.18	1982-2011
Hangingstone River	0.29	-11.9	0.30	0.24	-35.6	0.30	0.32	-8.97	0.35	1979-2011
Christina River	0.26	-22.2	0.32	0.33	-10.8	0.38	0.24	17.1	0.36	1982-2011

3.4 Model Evaluation

In addition to the quantitative hydrograph diagnostics described in **Table 2.3** in Section 2.4.1, various hydrologic signatures were used to qualitatively evaluate model performance. Each signature will be described in this section and the corresponding AWS baseline model performance in the House River will be presented. The information that each hydrologic signature can provide will be discussed. Note that in the figures observation values are bolded. Water years are defined as beginning on October 1st of the previous year and ending on September 30th of that year, so the 1991 water year would be defined from October 1st, 1990 to September 30th, 1991. Moving forward all years referred to are water years.

In addition to the subsequent hydrologic signatures, *a priori* assumptions, based on field observations in the Boreal Plains, were used to determine whether the model was behaving in a physically realistic manner. **Table 3.8** summarizes theses assumptions and the field sites where the behaviour was observed. Note that there is a strong reliance on URSA observations, although not all URSA observations were used as *a priori* assumptions. For instance, the URSA observation that snowmelt runoff in the forestlands is low was not taken as an assumption since there were contradicting field observations at other locations.

Table 3.8: Summary of a priori assumptions used when constraining model parameterization.

Wetlands		Forestlands	
Assumptions	**Field Sites**	**Assumptions**	**Field Sites**
Low ET losses unless it is a wet year (Smerdon et al. 2005)	URSA	Slow infiltration below the weathered surface (Devito et al. 2005b)	URSA
Lateral flow dominates (Ferone and Devito 2004, Smerdon et al. 2007, Thompson et al. 2015)	URSA	Vertical flow dominates (deepflow is the dominant flow path) (Gibson et al. 2002, Nijssen and Lettenmaier 2002, Redding and Devito 2010)	URSA, NE AB, BOREAS
Short shallow groundwater connections (quickflow is the dominant flow path) (Ferone and Devito 2004)	URSA	Regional groundwater discharge is low (Redding and Devito 2011), therefore most water in the forestlands should be lost to ET since deepflow is the dominant flow path	URSA
Increasing wetland coverage results in increased runoff (Prepas et al. 2006, McEachern 2016), implying that wetlands are a strong controller of surface runoff	FORWARD	Aspens move significant volumes of water and have high ET demands (Devito et al. 2012, Brown et al. 2014)	URSA
Groundwater tables are lower in the forestlands than in the wetlands (Devito et al. 2012)			URSA

3.4.1 Hydrograph

Hydrographs are one of the most commonly used hydrologic signatures. Hydrographs compare the modelled discharge time series to the observation hydrographs to determine model ability. Timing and magnitudes of events as well as general baseflow can be evaluated through this comparison. Baseflow can also be scrutinized in detail through baseflow separation approaches (Section 3.4.7). Figure 3.9 shows a hydrograph comparison between the AWS baseline model and the observed values for 5 of the 12 modelled years. Note that while the timing of the peaks is generally good the

magnitudes are flashier than what is observed at the WSC gauge. This may be attributed to the lack of wetland representation in the baseline model as wetlands can attenuate flood peaks. It is also possible that the model hydrograph timing, such as the missed peak in 1997, could be influenced by errors in the forcing data. As discussed in Watson et al. (2008), capturing local storm events is difficult with the existing climate gauge network.

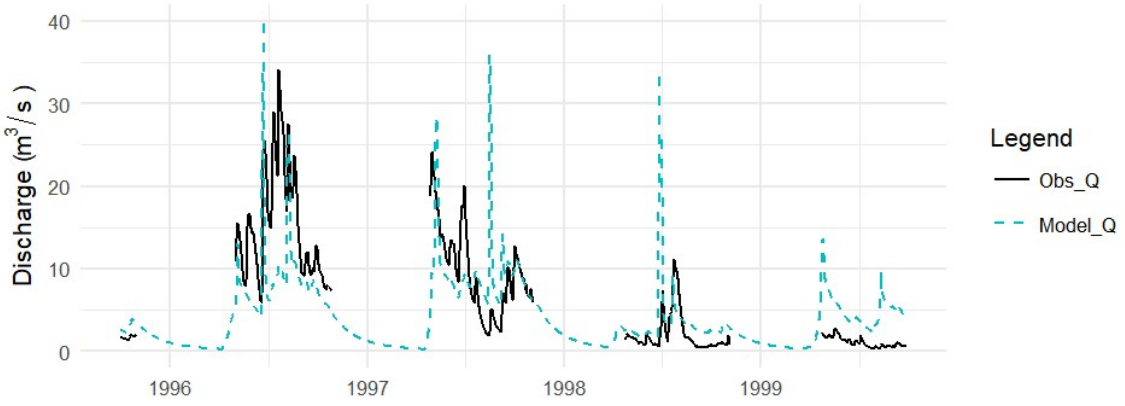

Figure 3.9: Hydrograph comparison between the observation values and the AWS modelled values in the House River Basin.

3.4.2 Regime Curves

Regime curves indicate the long-term monthly averages for a variety of fluxes. For this analysis, the examined fluxes are the modelled and observed outflow depths, modelled PET and AET, and modelled precipitation. **Figure 3.10** shows the regime curve for the AWS baseline model in the House River basin. Regime curves can indicate whether timing for major hydrologic events such as freshet, summer peaks, and fall recession are being met as well as determine if model ET is too high or low. The observed and modelled regime curves match fairly well except in August, implying the AWS model is not capturing the summer recession properly. The modelled AET is lower than the modelled precipitation, but the values are close, which is what is expected in the BPs, although the PET values seem high to achieve this.

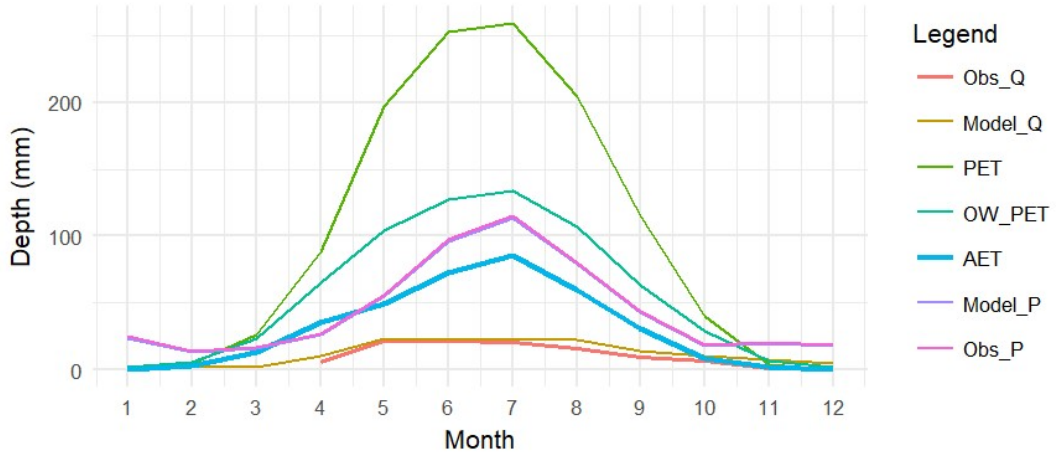

Figure 3.10: Regime curve for the AWS baseline model in the House River basin for the 1983 to 2011 water year

3.4.3 Budyko Curves

The Budyko Curve is a simple relationship that quantifies the partitioning of mean annual precipitation into ET and discharge. It was developed based on the assumption that water and vegetation co-evolved resulting in the Budyko pattern which been observed in multiple catchments around the world (Vereecken et al. 2015). The Budyko Curve has two axes: the aridity index and the evaporative index. The x-axis is the aridity index and is defined as the ratio between PET and precipitation while the evaporative index is the ratio between AET and precipitation. The curve is bound by two lines, the first is the energy limiting line which is the slope when the aridity index equals the evaporative index. The second bounding line is the water limiting line and occurs where AET equals precipitation, or in other words where the evaporative index equals 1.

An inherent assumption of the Budyko Curve is that at an annual timescale the change in storage is equal to 0, however, this is not true in the BPs. This means that there is more scatter expected in a BPs curve than in other catchments. This also means that a BPs Budyko Curve could have points above the water limiting line. The only way for points to be outside of the upper bound is for water to be introduced from outside the system. Since water from outside of each water year can be used in subsequent years this could result in points above this line. **Figure 3.11** is the Budyko Curve of the House River AWS baseline model compared to three EC stations with available modelled AET and PET data (ESRD 2013), the darker points show the long-term average. Note that the AWS cluster is much lower than the other stations, indicating that the model is underestimating AET and likely overestimating PET.

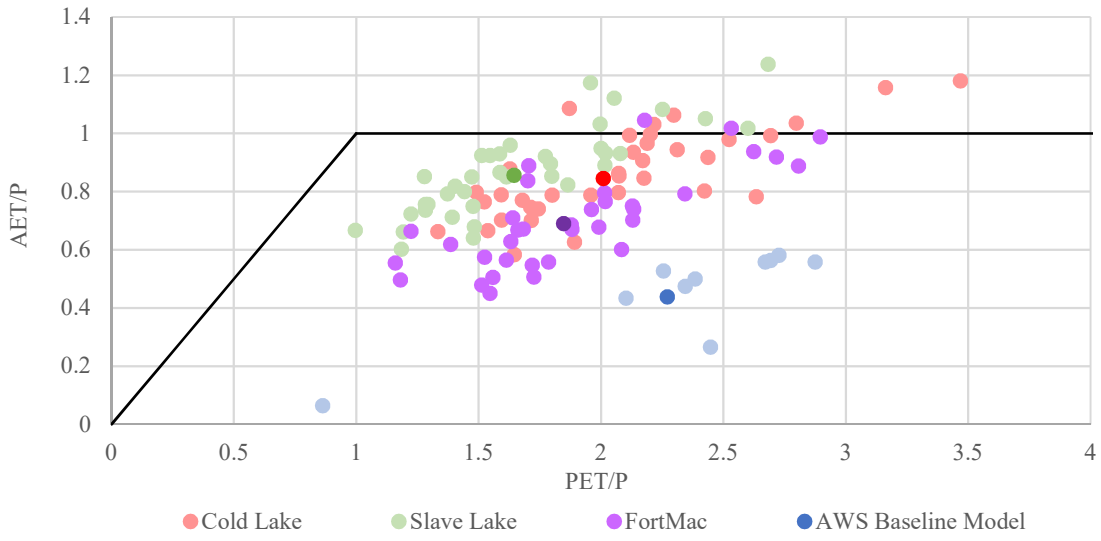

Figure 3.11: Budyko Curve for 3 EC climate stations and the AWS baseline model in the House River basin.

3.4.4 Annual Averages

It can be useful to see how the model is varying from year to year, therefore, the long-term water year averages were also examined. **Figure 3.12** shows these long-term averages for observed and modelled precipitation, modelled PET, modelled open water PET, observed water depths, and modelled water depths. Note that the AWS model on average has higher annual values and does not have as much interannual variability as the observed water depths, likely indicating that the model is not capturing the BPs storage correctly.

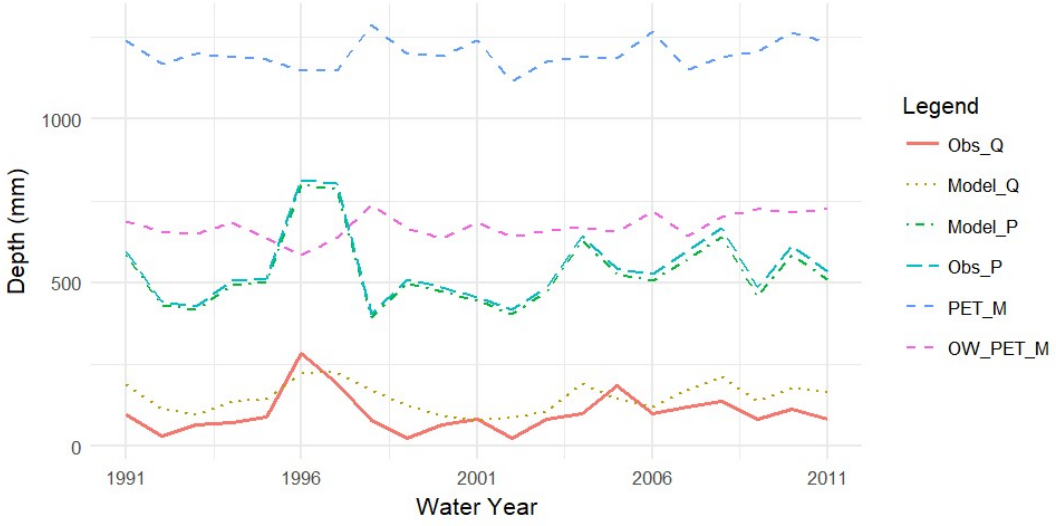

Figure 3.12: Annual plot comparing modelled and observed values.

3.4.5 Discharge Sources

The Raven model can track the source of all the water at the outlet which can be useful to determine if the model is performing in a way that makes physical sense. **Figure 3.13** shows the discharge sources for the AWS baseline model in the House River basin, note that deep groundwater flow (deepflow) is dominating this catchment, which does not make sense since in the BPs regional groundwater flow is low (Redding and Devito 2011) .

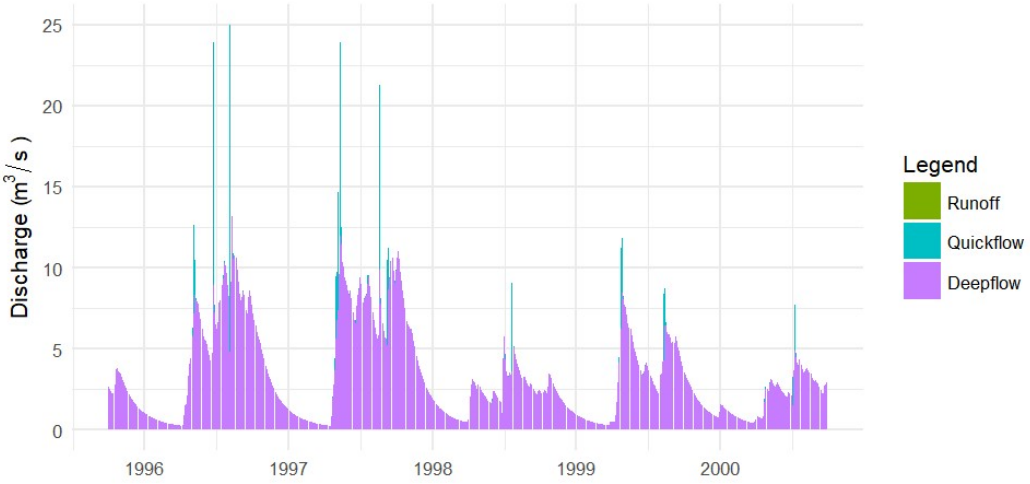

Figure 3.13: Discharge source at the outlet of the House River Basin (1996-200)

3.4.6 Soil Moisture

The Raven model can also report what the soil moisture content is in each modelled soil layer. The AWS baseline model has three soil layers. **Figure 3.14** and **Figure 3.15** show how the annual water year moisture content varies in the different soil layers. The moisture is presented by the main HRU groups: Coniferous Forest, Deciduous Forest, and Wetlands. Soil layer 0 is the topsoil and the layer numbers increase with depth. Note that the AWS baseline model was pushing most of the water to the deepest soil layer (soil 2) which is why the deepflow was so high.

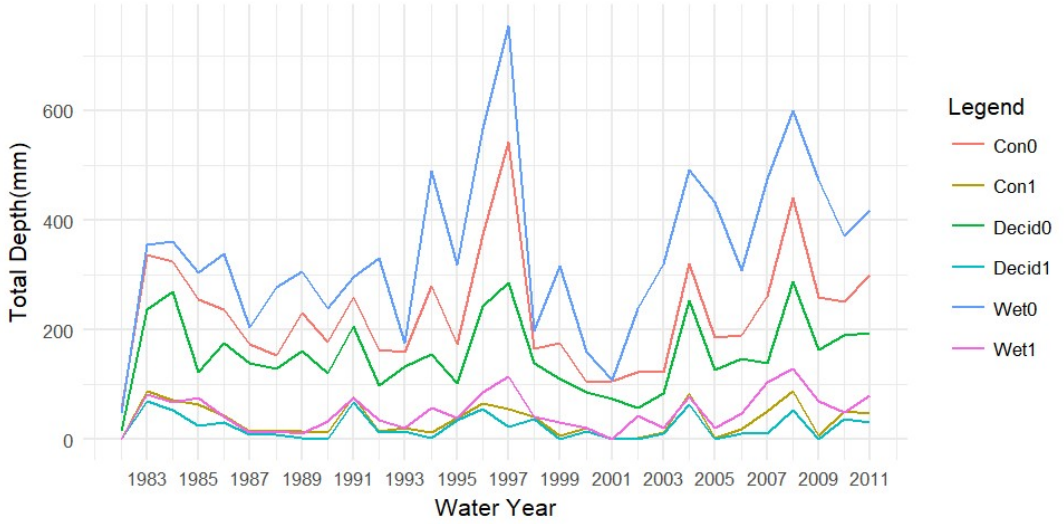

Figure 3.14: Annual soil moisture in the first two modelled soil layers in the AWS baseline model.

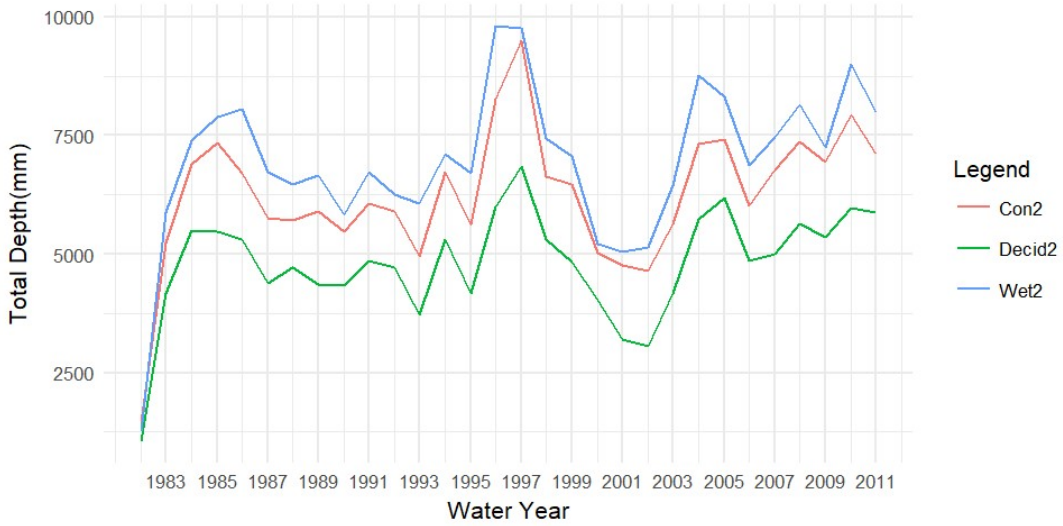

Figure 3.15: Annual soil moisture in the lowest modelled soil layers in the AWS baseline model.

3.4.7 Baseflow

The baseflow was separated from the observed and modelled hydrographs using the Lynne-Hollick filter method (Bond 2016). While no baseflow separation method is perfect, and the separation should be considered with some skepticism, it can provide insight into how the model is performing. **Figure 3.15** shows the baseflow comparison for the AWS baseline model in the House River basin. Note that the model appears to be underestimating baseflow in wet years and over estimating baseflow in dry years.

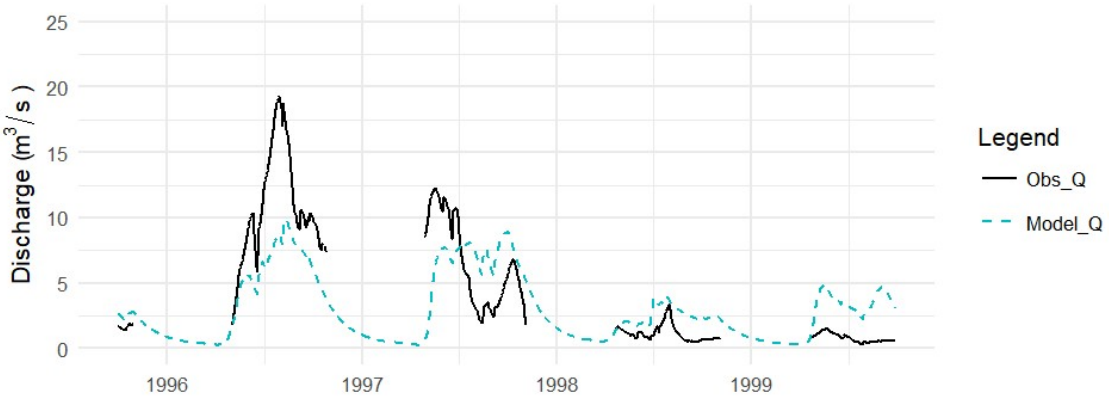

Figure 3.16: Separated baseflow hydrograph for the House River observed values and the AWS baseline model.

3.5 Model Structure Development

The model development followed the stepwise approach suggested by Fenicia et al. (2008) with the starting point being the AWS baseline model in the House River basin. The model structure was evaluated using the criteria discussed in Section 3.4 and then a single change, either parameter or structural, was made to the model in an iterative way until satisfactory performance was achieved. Then a combination of manual and autocalibration was used to improve model performance. If a specific process was not being properly represented after calibration, the model structure was revaluated, and the stepwise development approach applied. There were three model structures developed to determine the complexity necessary to model the BPs. Once satisfactory performance was achieved in the House River basin the models were deployed and calibrated in the remaining two study basins. Chapter 4 discusses this process in detail.

Chapter 4
Model Development

This chapter will discuss the final models that were developed, including development steps and reasoning behind model decisions.

4.1 Model Structures

Three primary model structures were developed for intercomparison and evaluation: Model 1 has a simpler structure while Model 2 and Model 3 have more complicated structures. The significant difference between Model 1 and Model 2 is that Model 2 parameterizes Deciduous and Coniferous forests differently and includes a function for Aspen tree transfer from the wetlands to the Deciduous forests as well as an unique evaporation algorithm. Model 2 and Model 3 have almost the same model structure, the key difference between them is there are two Hydrologically Equivalent Wetland (HEW) characterizations: one for wetland heavy subbasins (defined as wetland cover greater than 35%), and one for the other subbasins. The relevant model input files can be found in Appendices A, B, and C for Model 1, 2, and 3, respectively. While the number varies between study basins due to subbasin number, Model 1 for the House River has a total of 153 user-defined parameters, of these 24 were autogenerated by Raven: the saturated wilting point (6), the maximum canopy storage (6), the maximum canopy snow storage (6), and the relative leaf area index (LAI) (6). Note that the relative LAI was left at 1 in all instances. Model 2 has a total of 185 user-defined parameters, with 27 autogenerated, while Model 3 has a total of 191 user-defined parameters with 27 autogenerated. For comparison the AWS baseline models have 160 user-defined parameters with 40 auto-generated values. Of these user-defined parameters 20% were calibrated in Model 1, 23% in Model 2, and 23% in Model 3. **Figure 4.1** and **Figure 4.2** show schematics of Model 1 and Model 2 and 3, respectively.

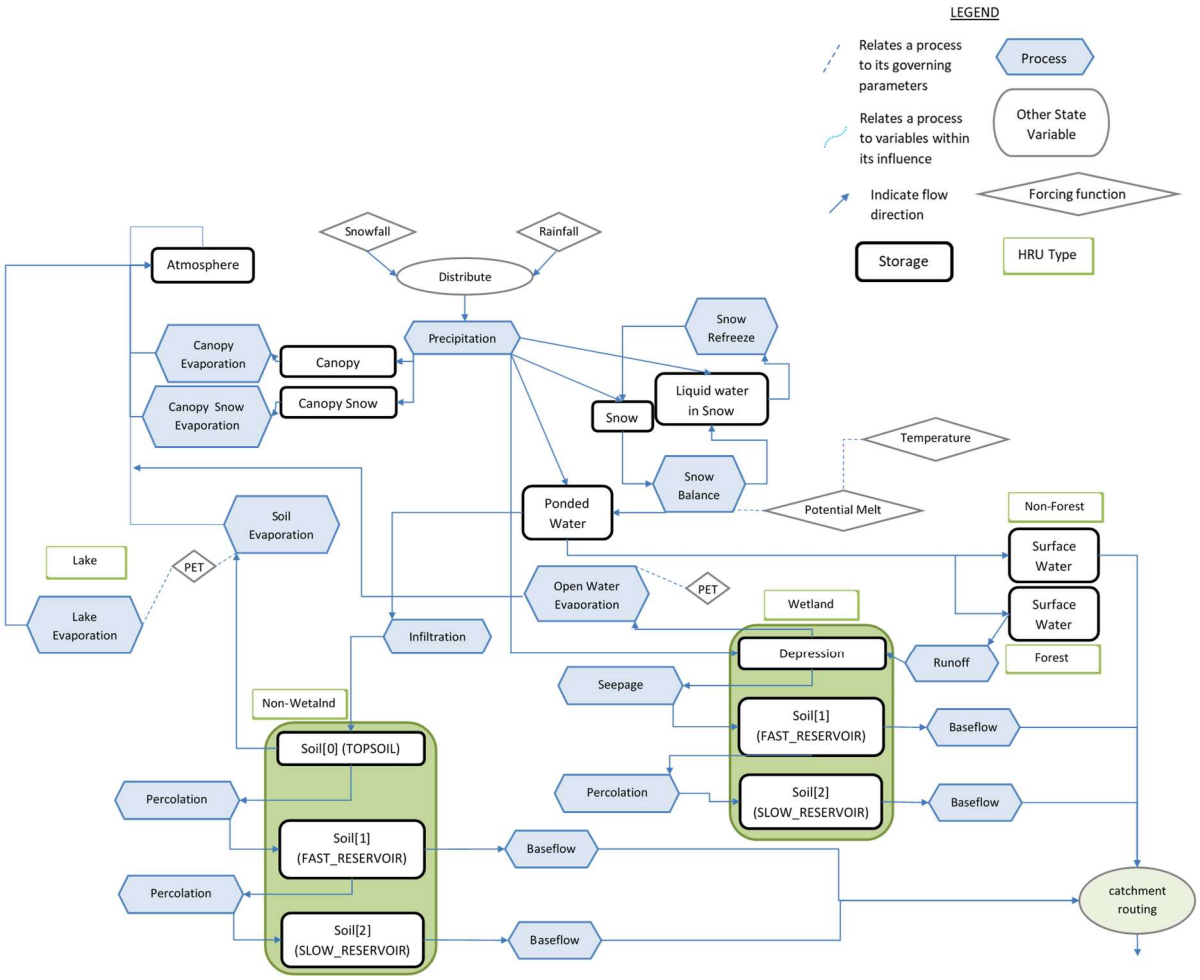

Figure 4.1: Schematic of the Model 1 structure. Green boxes indicate the specific HRU representations.

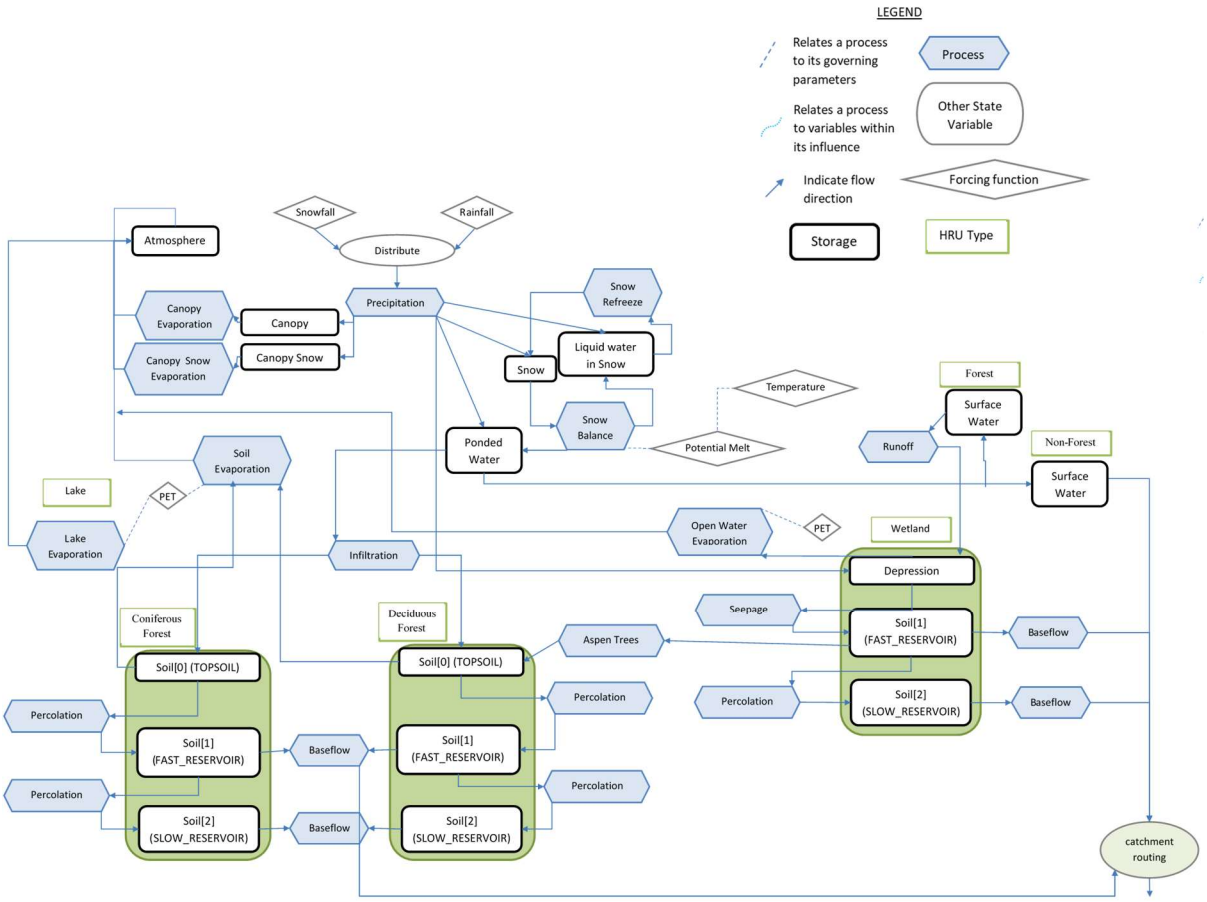

Figure 4.2: Schematic of the Model 2 and Model 3 structure. Green boxes indicate HRU representations.

At the HRU scale, water on the landscape is partitioned into different compartments and then moved via calculated fluxes for each time step. Precipitation can be distributed to canopy, canopy snow, snow, depression storage (for Wetlands), or ponded water for the other HRUS, which is a temporary storage compartment. This ponded water is partitioned either into the top soil layer via infiltration or to the surface water compartment as surface runoff which is then routed via in-channel routing to the outlet (Section 4.2.2).

There are six HRU landuse classes used in the models: Lakes, Bare, Grasslands, Wetlands, Coniferous Forest, and Deciduous Forest, the proportions of which are summarized in **Table 4.1**. Subbasins which were classified as wetland heavy in Model 3 have been highlighted. While Coniferous Forest is the dominant land class of all three study basins, Hangingstone has a significantly higher proportion of deciduous tree cover than the other two study basins. House River has the highest proportion of grassland and the lowest proportion of wetlands and almost the same

percentage of lakes as Christina River. Note that for the purpose of the model the Deciduous Forest class was treated as being entirely Aspen trees, which are predominant in the region (Barr et al. 2007, Michaelian et al. 2011).

Table 4.1: Summary of HRU area coverage for each subbasin

Study Basin	Sub Id	Sub Area (km^2)	% Lake	% Bare	% Grassland	% Wetland	% Coniferous	% Deciduous
House River	1	167.55	4.03	0.00	0.45	56.14	39.06	0.32
	2	262.06	4.22	0.04	0.11	40.51	51.36	3.75
	3	170.58	0.96	1.37	9.89	17.66	66.94	3.18
	4	174.30	0.86	0.12	0.16	10.84	2565.16	3.30
	Total	**774.49**	**2.71**	**0.34**	**14.39**	**28.49**	**51.26**	**2.72**
Hangingstone River	1	204.85	0.52	2.45	0.00	38.68	38.11	20.24
	2	65.67	0.00	0.20	0.00	46.25	20.77	32.79
	3	190.73	0.08	1.12	0.02	38.60	50.46	9.72
	4	89.6	0.22	1.32	0.00	29.40	45.95	23.11
	5	207.352	0.48	0.06	0.00	14.91	65.52	19.02
	Total	**758.202**	**0.32**	**1.13**	**0.01**	**31.72**	**48.14**	**18.68**
Christina River	1	852.36	2.12	1.73	3.85	28.53	39.90	23.87
	2	1355.45	3.21	0.08	0.37	39.98	53.44	2.93
	3	658.75	2.06	0.06	0.12	35.93	53.33	8.51
	4	677.7	2.28	3.33	16.62	29.60	42.83	5.34
	5	1158.77	947.84	0.82	3.71	27.51	53.16	9.55
	6	162.07	1.65	0.41	1.22	22.14	62.40	8.73
	Total	**4865.1**	**2.73**	**1.01**	**4.03**	**32.41**	**49.81**	**9.57**

Of the six HRU landuse classes, two are treated in Raven as special HRU classes. Lake classes represent the open water landuses that are not wetlands. Lakes do not interact with the soil and only have direct precipitation, evaporation, and routing applied to them. Wetland classes have no top soil class but instead the first layer is represented as depression storage. Precipitation automatically falls directly on the depression storage and does not require abstraction algorithms to move water from Ponded Water to depression storage as it would for non-Wetland HRUs. There are also specific algorithms to move water into and out of depression storage (Section 4.2.4). With one HRU group per subbasin, there is one HEW per subbasin in Model 1 and Model 2. These models parameterize all wetland HRUs the same, which would be the equivalent of having the same HEW for each subbasin with only the area changing. In Model 3 there are two HEWs, one for wetland heavy landscapes (highlighted in **Table 4.1**) and a second for the other basins. Runoff from the forestlands in the wetland heavy basins are routed through the wetlands while the other landscapes are without this lateral connection. Refer to Section 4.2.4 for more information on this process.

4.2 Model Structure and Parameterization

This section will discuss each aspect of the schematics presented in **Figure 4.1** and **4.2** in detail. Unless otherwise specified, the processes are the same in all model structures. More detailed information on any of the processes discussed here can be found in the Raven User manual (Craig et. al 2018).

4.2.1 Forcing Functions

The forcing data provided to the models include total precipitation and minimum, maximum, and average daily temperature. For the study basins with multiple climate stations the data was interpolated using the inverse distance weighting method which uses the distance from the centroid of the HRU to the climate gauge to weight the forcing data.

$$\alpha = 0.5 + \frac{T_{trans} - T_{ave}}{\Delta T} \quad \text{(eq. 3)}$$

Total precipitation is partitioned into rain and snow using a linear transition (eq 3.) that is applied when the average daily temperature is in the range from $T_{trans} - \Delta T/2$ to $T_{tran} + \Delta T/2$, where the transition temperature (T_{trans}) and the temperature range (ΔT) are specified by the user. The transition temperature was set to 0.27°C and the temperature range was set to 2°C, based on an analysis of the entire corrected data set from the Fort McMurray gauge. This data set was examined so the average temperature and standard deviation of average temperature were found for the days which had both rain and snow recorded.

$$T = T_g - \propto (z - z_g) \quad \text{(eq. 4)}$$

$$P = P_g \cdot (1.0 + \alpha(z - z_g) \quad \text{(eq.5)}$$

While elevation change is not significant in these basins, a number of the gauges are lookout stations which have significantly higher elevations than the surrounding areas. Therefore, there were corrections applied to the temperature data for these elevation changes between the HRUs and the climate stations. Temperature was corrected using (eq. 4) where T is the estimated HRU temperature, T_g is the measured gauge temperature, z is the elevation of the HRU, z_g is the elevation of the gauge, and α is the adiabatic lapse rate. The model adiabatic lapse rate was set to 6.5°C/km, which is the global average lapse rate (Dingman 2015). Precipitation was corrected in a similar way using (eq.5) where P is the precipitation rate applied to the HRUs, P_g is the gauge precipitation, and α is the

precipitation lapse rate (m^{-1}). The precipitation lapse rate was set to 0.5 m^{-1} which was the original value from the AWS baseline models. The models were not sensitive to the lapse rates.

The algorithm selected for intercepting precipitation in the canopy allows the interception fraction to be set by the user for both rain and snow. Rain interception was set to 0.12 in the deciduous HRUs and 0.10 in the coniferous HRUS, snow interception was set to 0.05 for deciduous 0.20 for coniferous HRUs. These values were set based on observation data at URSA as well as from a discussion in Dingman (2015) of different canopy interception values and were not calibrated.

Relative humidity and longwave and shortwave radiation were all estimated from the input forcing data. Relative humidity was calculated using (eq. 6) and assumes that the minimum daily temperature is equal to the dew point. The saturated vapour pressure (e_s) is a function of temperature and is calculated internally in Raven.

$$RH = \frac{e_s(T_{min})}{e_s(T_{ave})} \quad \text{(eq.6)}$$

$$S_{ET} = I_{sc} \cdot E_0 \cdot [\cos(\delta) \cdot \cos(\Lambda) \cdot \cos(2\pi t) + \sin(\delta) \cdot \sin(\Lambda)] \quad \text{(eq.7)}$$

$$S_{clear} = f_{atm} \cdot f_{asp} \cdot S_{ET} \quad \text{(eq.8)}$$

$$S_n = (1-\propto) \cdot f_{can} \cdot f_{cloud} \cdot S_{clear} \quad \text{(eq.9)}$$

$$L_n = \sigma \cdot \varepsilon_s \cdot (\varepsilon_{atm} \cdot T_{atm,K}^4 - T_{s,K}^4) \quad \text{(eq.10)}$$

$$f_{atm} = (\tau_{dir} + 0.5(1 - \tau_{diff})) \cdot (1 + 0.5(1 - \tau_{diff})\alpha)$$

$$f_{cloud} = 0.355 + 0.68 \cdot (1 - C_c) \quad \text{(eq.11)}$$

Extraterrestrial shortwave radiation (S_{ET}), net shortwave radiation (S_n), and longwave radiation (L_n) were calculated using the Raven default algorithms which require no additional user inputs; (eq. 7), (eq. 9), and (eq. 10), respectively. Where I_{sc} is the solar radiation constant (118.1 MJ/m^2d), E_0 is an eccentricity correction, t is the time of day in days, δ is the solar declination (rad), and Λ is the latitude (rad). In the longwave equation σ is the Stefan Boltzmann constant (4.9 x 10^{-9} MJ/m^2dK^4), $T_{atm,K}$ is the effective temperature of the atmosphere (°K), $T_{s,K}$ is the effective temperature of the ground surface (°K), and ε_s and ε_{atm} are the effective emissivities of the surface and atmosphere. This approach assumed that ground surface temperature is equal to the air temperature. Net shortwave

radiation is a function of the clear sky radiation (S_{clear}), the surface albedo (α), and canopy and forest correction factors. Clear sky radiation (eq.8) is a function of atmospheric refraction (f_{atm}) and slope/aspect (f_{asp}) correction factors and the extraterrestrial shortwave radiation. Total incident radiation (f_{atm}) is a function of the scattering correction factors for direct (τ_{dir}) and diffuse (τ_{diff}) solar radiation and the surface albedo (α), more information can be found in the Raven Users Manual (Craig et al. 2018). Additionally, cloud cover corrections were applied to shortwave radiation using (eq. 11) where C_c is the cloud cover and requires no user inputs. The cloud cover factor was left as 1 as no algorithm was used to calculate due to lack of data. No canopy correction factor was used in (eq. 8).

$$PET = \begin{cases} 0.013 \cdot \left(\frac{T_{ave}}{T_{ave}+15}\right) \cdot (23.88 \cdot S_n + 50) \cdot \left(1 + \frac{50-}{70}\right) for\ RH\ < 50\% \\ 0.013 \cdot \left(\frac{T_{ave}}{T_{ave}+15}\right) \cdot (23.88 \cdot S_n + 50) \qquad for\ RH\ \geq 50\% \end{cases} \quad \text{(eq. 12)}$$

$$PET = \frac{1}{\rho_w \lambda_v} \cdot S_{ET} \cdot 0.0023 \cdot \sqrt{T_{max} - T_{min}}(T_{ave} + 17.8) \quad \text{(eq. 13)}$$

Vegetation PET and open water PET were calculated using two empirical methods: Turc (1961) (eq. 12) and Hargreaves (1985) (eq. 13). Where PET is in mm/d, T_{ave} is the average daily temperature (°C), S_n is the daily net shortwave radiation (MJ/m^{2}d), S_{ET} is the extraterrestrial shortwave radiation (MJ/m^{2}d), λ_v is the latent heat of vaporization of water (MJ/kg), ρ_w is the density of water (kg/m^3), and RH is the relative humidity (%).

Six of the available PET algorithms in Raven were tested and the average PET for each algorithm for the modelled period (1982-2011) was compared to the reported PET ranges in the BPs. Of the available algorithms, the selected are the only ones that gave appropriate values, likely due to the other algorithms, such as the Penman-Monteith equation, relying on detailed vegetation data, which is not available in the study basins.

$$M_a' = C_f \cdot C_a(M_{a.min} + (M_{a.max} - M_{a.min}) \cdot \frac{1.0-\cos(\Gamma-\Gamma_s)}{2}) \quad \text{(eq.14)}$$

Potential snowmelt, the rate of melt if snow is present, is estimated from net energy inputs which are calculated using the HBV method (eq. 14). Here C_f is a forest correction factor, C_a is an aspect correction factor, $M_{a.max}$ and $M_{a.min}$ are user defined maximum and minimum potential melt rates, Γ is the day angle and Γ_s is the winter solstice angle (23.5°). The melt rates were calibrated while the

aspect correction factor was set to 0.25. The forest correction factors were kept constant in all models and study basins with Lakes set to 1.0, Bare at 0.95, Coniferous Forests having a value of 0.9, and Deciduous Forests, Wetlands, and Grasslands having a value of 0.89. These were the original values from the AWS baseline model. The models were not sensitive to either of the correction factors, so they were not calibrated.

4.2.2 Routing Functions

In Raven there is in-catchment routing between from HRUs to the subbasin outlet but generally not between HRU types unless it is explicitly added (Section 4.2.4). In the models, in-catchment routing was done using the triangular unit hydrograph approach (eq.15) where t_p is the time to peak and the total duration is specified by the time of concentration, t_c. The time of concentration for each subbasin was initially estimated using (eq.16) as recommended by Ball et. al (2016) where α is a global correction factor and A is the area of the subbasin (km^2). The correction factor was the same for each subbasin and was initially going to be determined through calibration, but the models were insensitive to this value, and thus were left as the values calculated in (eq.16). Time to peak is estimated internally in Raven and is set to one third of the time of concentration.

$$UH(t) = \begin{cases} \frac{2}{t_c}\frac{t}{t_p} & for\ t < t_p \\ \frac{2}{t_c}\left(\frac{t_c - t}{t_c - t_p}\right) & for\ t \geq t_p \end{cases} \quad \text{(eq.15)}$$

$$t_c = \alpha \cdot 0.0317 A^{0.38} \quad \text{(eq.16)}$$

$$UH'(t) = \frac{1}{2\sqrt{\pi D t}} \exp\left(-\frac{(L - c_{ref} t)^2}{4Dt}\right. \quad \text{(eq.17)}$$

There is also in-channel routing in the primary subbasin channels which was calculated in the model using an analytical solution to the diffusive wave equation, shown in (eq.17). The reference celerity (c_{ref}) is used to determine the mean travel time of the wave, while the channel diffusivity D (m^2/d) controls the smearing out of the wave. Here L is the channel reach length (m) and diffusivity is estimated from the channel reference flow, which is equivalent to the bankfull flow, and unless it is user-specified, it is calculated internally in Raven based upon the user-defined average annual runoff at the basin outlet.

The estimation method for the channel reference flow was selected in the models as there were no surveyed cross-sections to calculate bankfull flow. The average annual runoff for each study basin was calculated from the available gauge record and is summarized in **Table 4.2**, it is likely that all of these values are underestimated since there is no winter data for any of the WSC gauges and it is unlikely that any of the study basins main channels consistently dry out completely in the winter. However, the model was not particularly sensitive to these parameters since at a daily time step the peak timing becomes less important than at a finer temporal resolution.

Table 4.2: Summary of the annual runoff conditions in the study basins

Study Basin	Average Annual Runoff (mm)	Min Annual Runoff (mm)	Max Annual Runoff (mm)
House River	106	23	284
Hangingstone River	128	21	306
Christina River	96	21	228

4.2.3 Soil Properties

For non-Lake and non-Wetland HRUs there are three soil layers, top soil (soil 0), intermediate soil (soil 1) and deep soil (soil 2). Wetland HRUs possess the last two soil layers (but no topsoil) while soil moisture is not represented beneath lakes. Based upon reasonable ranges, the soil layer depths were determined through calibration during the model development process. **Table 4.3** summarizes the soil properties for each soil layer in Model 1 while **Table 4.4** summarizes the properties for Model 2 and Model 3. There are two soil classes in Model 1: Wetland soils and Forest soils and three soil classes in Model 2 and 3: Wetland soils, Coniferous Soils, and Deciduous soils. In accordance with the URSA observations (Devito et al. 2012) the soils in the forest HRUs were made deeper than the Wetland soils and porosity decreased in the deeper layers. The 6 HRU land classes are categorized by one of these soil types, except Lakes, as identified in the tables below. The mineral fractions were based on observations at a research site in the Taiga Plains (E. Devoie, personal communication 2018). While not in the Boreal Plains, the primary difference in composition will likely be thicker peat deposits, so the composition of the soils below the peat deposits should be an adequate starting point in the absence of site-specific data. The mineral fractions are used to internally estimate the field capacity and wilting point of the soil layer. Field capacity defines the soil moisture content where the soils will no longer drain due to gravity, while the wilting point defines the point where vegetation can no longer extract water from the soil (Dingman 2015). The field capacity was overwritten manually and initially set to the default values before being adjusted through calibration.

The model was not sensitive to wilting point so it was left as the autogenerated value. All the soil parameters in **Table 4.4** are constant between study basins and model structures.

Table 4.3: Summary of soil parameters for Model 1.

Soil Class	HRU Types	Soil Layer	Porosity	%Sand	%Clay	% Silt	% Organic
Wetland	Wetlands, Grasslands	0[1]	0.3	0.25	0.08	0.67	0.7
		1	0.25	0.25	0.08	0.67	0.2
		2	0.25	0.25	0.08	0.67	0.2
Forest	Bare, Coniferous Forest, Deciduous Forest	0	0.4	0.6	0.2	0.2	0.25
		1	0.25	0.6	0.2	0.2	0.15
		2	0.25	0.6	0.2	0.2	0.15

1. Only for the Grassland HRU class

Table 4.4: Summary of soil parameters for Model 2 and Model 3.

Soil Class	HRU Types	Soil Layer	Porosity	%Sand	%Clay	% Silt	% Organic
Wetland	Wetlands, Grasslands	0[1]	0.4	0.25	0.08	0.67	0.7
		1	0.3	0.25	0.08	0.67	0.2
		2	0.3	0.25	0.08	0.67	0.2
Coniferous Forest	Bare, Coniferous Forest	0	0.4	0.6	0.2	0.2	0.25
		1	0.3	0.6	0.2	0.2	0.15
		2	0.3	0.6	0.2	0.2	0.15
Deciduous Forest	Deciduous Forest	0	0.4	0.6	0.2	0.2	0.25
		1	0.3	0.6	0.2	0.2	0.15
		2	0.3	0.6	0.2	0.2	0.15

1. Only for the Grassland HRU class

4.2.4 Hydrologic Processes

The model option was selected that applies the hydrologic process in the order that they appear in the .rvi (model input) file for each time step. This is the order that they are presented in in this section. Any parameter values that were calibrated are summarized in Section 4.3.

Precipitation

At the beginning of each time step any applicable precipitation is applied to the appropriate storage compartments before the other hydrological processes are applied in sequence.

Canopy Processes

Any precipitation that is transferred to the canopy and canopy snow compartments as defined by the interception algorithm can be subsequently evaporated. Canopy evaporation in the model is defined by (eq.18) where F_c is the forest cover of the HRU defined by the user for each landuse.

$$M_{evap} = PET \cdot F_c \quad \text{(eq.18)}$$

The Coniferous and Deciduous forest HRUs both had forest covers of 1.0, while Wetland and Bare HRUs had a forest cover of 0.05, and Lakes and Grassland had a forest cover of 0. This algorithm was selected since it didn't automatically evaporate all the stored water and required less detailed vegetation information, such as trunk fraction, than the other available options.

Open Water Evaporation

Open water evaporation is applied to Lakes and Wetland HRUs and is equal to the open water PET multiplied by a correction factor that is intended to represent local factors such as wind shielding or wetland vegetation. Lake correction was left at 1 while the Wetland correction was set during calibration.

Snow Melt

The model uses a two-layer snowpack model with the top layer defined as the snow surface storage and the bottom layer defined as the snow pack. The snow algorithm tracks the snow liquid, snow water equivalent (SWE), and cold content of each layer. The user specifies the maximum SWE of the surface layer and the maximum liquid content the snowpack can hold as a fraction of SWE, which was set to the recommended Raven default of 0.05. The algorithm determines the SWE in the surface layer and adds new snow as SWE until the surface layer is full, after which the snow is added to the snow pack layer. This algorithm also allows for refreeze (Sgro 2016).

Seepage

Water in depression storage can seep into the confining soil layer (soil 1) via the seepage function (eq.19), where k_{seep} is the linear storage coefficient (1/d) and Φ_{dep} is the water in the depression (mm). This is the only available seepage algorithm in Raven.

$$M_{dflow} = k_{seep} \cdot \Phi_{dep} \quad \text{(eq.19)}$$

Infiltration

Water infiltrates from Ponded Water to soil layer 0 using the standard HBV modelling approach (eq.20).

$$M_{inf} = R \cdot (1 - (\frac{\Phi_{soil}}{\Phi_{max}})^{\beta}) \quad \text{(eq.20)}$$

Here, R is the rainfall/snowmelt rate (mm/d), β is a user-defined soil parameter, Φ_{soil} is the current soil water content (mm) and Φ_{max} is the maximum soil storage (mm). The β parameter was found through calibration. To account for frozen soils, β was made time-varying for summer and winter conditions. Summer conditions were defined as starting on May 1st and ending on September 30th with winter in October through April. While there was some debate in the literature (Chapter 2) about whether infiltration decreases in the winter it was observed that the spring freshet rates were being severely underestimated with a single infiltration value, implying that soil infiltration was too high during this time. When the parameter was made time varying, freshet representation was improved. The HBV algorithm was selected over the others because it requires limited soil information and while it is conceptual in nature, it has some physicality since it is a function of the antecedent moisture conditions.

Actual Evapotranspiration (AET)

In Raven, the AET in the basin from non-open water sources is taken from soil layer 0 and moved to the atmosphere. In Model 1 this is done using the HBV algorithm (eq. 21) which is a linear algorithm based on PET (mm/d), current soil water content Φ_{soil} (mm), and the maximum tension storage Φ_{tens} (mm).

$$M_{evap} = PET \cdot \min(\frac{\Phi_{soil}}{\Phi_{tens}}, 1) \quad \text{(eq.21)}$$

The tension storage is the difference between the soil field capacity and the wilting point. This algorithm was picked since it is purely a function of the antecedent conditions and PET and doesn't require any additional empirical parameters or detailed rooting information.

In Model 2 and 3 non-deciduous HRUs use (eq.21) while deciduous HRUs uses (eq.22) and (eq. 23) which is a two-layer evapotranspiration routine which allows evaporation from the topsoil and the deep groundwater reserve.

$$M_{evap}^{U} = PET \cdot (\frac{\Phi_{soil}^{U}}{\Phi_{tens}^{U}}) \quad \text{(eq. 22)}$$

$$M_{evap}^{L} = (PET - M_{evap}^{U}) \cdot (\frac{\Phi_{soil}^{L}}{\Phi_{tens}^{L}}) \quad \text{(eq.23)}$$

The upper layer (U) is the top soil layer 0 and the lower layer (L) is the bottom soil layer 2 and the remainder of the terms are defined above. This algorithm was written by the author specifically for this thesis and is used to represent the Aspen roots which can grow very deep and tap these groundwater reserves (Devito et al. 2012). Any of the PET that was not satisfied by the topsoil can then use water from the deep groundwater reserves to satisfy the high Aspen ET rates.

Depression Overflow

To model fill and spill, the depression storage in the Wetlands can overflow according to a threshold algorithm (eq. 24). This algorithm was selected over the other available algorithm based off model performance during the model development processes (Section 4.3.1).

$$M_{dflow} = M_{max} \cdot (\frac{\Phi_{dep} - \Phi_{th}}{\Phi_{max} - \Phi_{th}})^{n} \quad \text{(eq.24)}$$

Here, M_{max} is the maximum overflow rate (mm/d), Φ_{dep} is the water in the depression (mm), Φ_{th} is the threshold storage level, Φ_{max} is the maximum depression storage (mm), and n is an exponent. All of the overflow parameters were set during calibration. Currently in Raven there is no process that can freeze the water in the depressions, which created a challenge that is discussed in Section 5.4.

Baseflow

Once water reaches soil layer 1, it can either percolate to soil layer 2 or move to the Surface Water compartment via lateral flow (a.k.a quickflow) and be routed to the outlet. The algorithm chosen to represent quickflow is (eq.25), where k is the baseflow coefficient (1/d), Φ_{soil} is the available water (mm) and n is a user-defined parameter. The exponent *n* and the baseflow coefficient were set during calibration.

$$M_{base} = k\Phi_{soil}^{n} \quad \text{(eq.25)}$$

Once water reaches soil layer 2 it can only leave via baseflow to Surface Water, in the model this represents deepflow. In Model 1 the algorithm for deepflow is (eq.26) where M_{max} is the maximum baseflow rate at saturation (mm/d), Φ_{soil} is the available water (mm), Φ_{max} is the maximum soil

storage (mm), and *n* is a user-specified parameter. The maximum baseflow rate and *n* were determined during calibration.

$$M_{base} = M_{max}(\frac{\Phi_{soil}}{\Phi_{max}})^n \quad \text{(eq.26)}$$

$$M_{base} = M_{max} \cdot (\frac{\frac{\Phi_{soil}}{\Phi_{max}} - S_{th}}{1 - S_{th}})^n \quad \text{(eq. 27)}$$

In Model 2 and 3 the deepflow was represented using (eq.27) in the forestlands as a power law function of the soil moisture as well as a threshold (S_{th}) and (eq.26) for non-forested HRUs. The deep soil (layer 2) depth was set to 10 m and the threshold was initially set to 0.9. The deep soil was given an initial soil moisture at the threshold of 2700 mm in the forestlands. This allowed the Aspen trees to have a groundwater reserve to access since otherwise the layer would start dry and take longer than the spin up period to fill. The threshold was adjusted during calibration but the initial soil moisture was held fixed.

It is standard modelling practice to represent baseflow as either a linear or power law function. It would be impossible to test every possible representation in this thesis so the focus was placed on wetland representation which has typically been less explored in literature. As these representations are standard approaches, the assumption was made that they would be adequate since the power law functions do provide flexibility during model performance testing.

Percolation & Aspen Transfer

Vertical water movement between soil layers is determined by the percolation rate. A constant percolation rate was used in the models. More complicated algorithms were tested that were a function of antecedent conditions, but this resulted in either no baseflow or no percolation from soil layer 1 based on which algorithm was applied to the model first. In soil layer 0 the other percolation algorithms drained the soil layer faster than the water could be evaporated as AET, keeping too much water in the basin, or prevented any water from reaching the lower soil layers. The constant values were determined through calibration.

In Model 2 and 3 the Aspen tree transfer of additional water from adjacent HRUs is also modelled as a constant percolation rate moving water from Wetlands soil layer 1 to Deciduous Forest soil layer 0 which is consistent with the conceptual model. This new process was created during the

development process of this thesis and added to the Raven software framework by the author. The percolation value was determined through calibration.

Forested Runoff Routing

As mentioned in Section 4.2.2, there is no lateral exchange of water between HRUs unless explicitly added to the model. To allow the riparian wetlands to regulate and attenuate forestland runoff, runoff from the forest was "flushed" to wetland depression storage. In Model 1 and 2 all forest HRUs had their runoff transferred to the wetlands, while in Model 3 only the forests in wetland heavy subbasins had this transfer.

4.2.5 Reservoir Processes

The Christina River study basin has a large lake called Christina Lake that was represented as a reservoir. The lake is subject to direct precipitation and evaporation from the surface. To define the stage-discharge ($Q(h)$), stage-volume ($V(h)$), and stage-area ($A(h)$) relationships required by the model a stage discharge curve was developed. There is a WSC water level gauge at Christina Lake (07CE906) with data from 2001 – 2017. The RAMP gauge at the old WSC Jackfish River gauge (07CE005) downstream of the outlet of the lake had data available from 2010-2017. A scatterplot of stage vs discharge for the 7 overlapping years was fit with a powerlaw trendline that was used as a unique stage-discharge relationship needed in the model. It was assumed that the average surface area of the lake of 22.2 km^2 (DEAS 2018) was constant, which allowed the stage-volume and stage-area relations to be derived. Water is routed out of the lake using (eq.28) where h is the stage and $Q(h)$, $V(h)$, and $A(h)$, are defined above. The open water ET is defined by E and precipitation is added to Q_{in}.

$$\frac{V(h^{n+1})-V(h^n)}{\Delta t} = \frac{1}{2}\left(Q_{in}^{n} + Q_{in}^{n+1}\right) - \frac{1}{2}\left(Q(h^n) + Q(h^{n+1})\right) - \frac{E}{2}\left(A(h^n) + A(h^{n+1})\right) \quad \text{(eq.28)}$$

4.3 Calibration and Validation

The model structure development was an iterative approach, both manual and automatic calibration was used during the development process to identify areas where the model was underperforming and adjust the model accordingly. Once the model structure was fixed a refining calibration and validation was completed in all study basins. This section discusses both processes of calibration and the model validation. Over the course of this thesis, including model development, calibration, and validation in the three study basins, the models were run approximately 2.5 million times. A summary of a description of all of the calibration parameters can be found in Appendix D.

4.3.1 Structural Development Process

Model development was primarily focused upon the House River basin. For structural development, the calibration period was set from the 1991 water year to the 2000 water year, with an eight-year warm-up period from 1982-05-24 to 1990-09-30. This long spin-up period was chosen due to the potential for interannual storage changes in the BPs. The selected calibration period included both wet years (1996, 1997) and a dry year (1999) as recommended by the literature. The structural development process involved model adjustment followed by manual calibration, followed by automatic calibration, then evaluation, and the process was repeated until the structure was set. Note that with 30 years of available record, 10 years is not a standard split calibration approach, which would typically have 14 to 18 years of data in the calibration period. However, since the development stage required a combination of manual and automatic calibration, the period was restricted to 10 years to make it easier to manually interpret the results. The following sections summarize the iterative processes and testing that was used to finalize the model structures.

Starting with the AWS baseline model, algorithms were changed in Model 1 in a step-wise manner and evaluated using both the model diagnostics and hydrologic signatures defined in Section 3.4. Once a satisfactory model performance was achieved through manual calibration, automatic calibration techniques were deployed. The resulting model was evaluated, manual changes were made, and the processes repeated itself until the final model structure was achieved.

This thesis uses the Optimization Software Toolkit for Research Involving Computational Heuristics (OSTRICH) (Mattot 2016) to automatically calibrate the model. OSTRICH works for any text based model, including Raven, and provides a variety of optimization algorithms and tools.

Two autocalibration approaches were applied during model iteration. One autocalibration technique that was used to converge on a "best" parameter solution was the Dynamically Dimensioned Search (DDS) (Tolson and Shoemaker 2007) algorithm. During model development, this algorithm was used to optimize the NSE value while applying a penalty of 0.01 to the NSE if the Percent Bias was outside of a specified range. This range varied with each calibration depending on the starting Percent Bias. A second technique of multi-objective calibration that used the Pareto Archived DDS (PADDS) (Asadzadeh and Tolson 2009) search algorithm was also used. This approach was used to optimize two separate NSE values. During model development, the WSC gauge record was split into two gauges, one representing the freshet values, defined as the period when the 'B' flag is removed from the WSC gauge to May 31st and the other representing the summer values

defined from June 15 to September 30. As discussed in Section 3.3, the 'B' flag represents values which were impacted by backwater effects, and therefore do not fall on the open water rating curve used to report discharges and thus are not used in this thesis. The PADDS was used to optimize the NSE of each gauge period, producing a suit of non-dominated solutions. These non-dominated solutions were then run using the original WSC gauge data and the resulting model diagnostics and hydrologic signatures were used to determine the "best" of the non-dominated solution sets.

Another technique that was used was a basic sensitivity analysis. Selected parameters were first perturbed by a large amount (3000% to 99% depending on the stage of model development) to create an upper and lower value. The model was run with these perturbed values one at a time for each of the tested parameters and the difference in the NSE and Percent Bias was recorded. If models had a change that was deemed sensitive, which varied depending on current model performance, the parameter was perturbed again by a smaller amount. For example, early on in model development a change of an NSE value of 0.45 by 67% was considered insensitive, while later in model development a change of an NSE value of 10% was considered sensitive. This was done iteratively to create a tiered ranking system of how sensitive a parameter was and inform structural changes moving forward. This approach was applied once the structure was finalized and is summarized in Section 4.3.2.

The final technique used to evaluate model performance during the development process was a mass balance on specific HRU groups. This was used to see if certain process were getting turned off in calibration, such as infiltration, in specific HRU groups. The primary focus of these mass balances were on wetland, coniferous forest, and deciduous forest mass balances.

In general, either a DDS or PADDS calibration was performed, followed by manual changes and evaluation of signatures and evaluation metrics. Once major changes were made, the above process was repeated. Some of the key changes that were tested are summarized in **Table 4.5**. Change type can be either parameter (a parameter value was changed significantly), algorithm (a different algorithm was used than the previous iteration), or structural (a new process was added to the model). Change types with a * after the type indicate an automatic calibration was done after the change. Successful changes were left in the model, while unsuccessful changes were removed. Two examples of successful changes during the model development process was the determination that a time-varying wetland seepage and forest infiltration were required. During model development when the PADDS was run, the resulting model either matched the freshet or the summer peaks but not both.

There was no compromise between the two within a single parameter set. When the summer values were correct the freshet was underrepresented, which was interpreted to mean too much water was infiltrating during freshet likely due to the lack of representation of frozen soils. Since frozen soils could limit infiltration, the decision was made to make seepage and infiltration time-varying to represent the frozen soils during the winter months.

Once the Model 1 structure was set the other two model structures were developed. Model 2 builds off of Model 1 and Model 3 builds off of Model 2. In Model 2 additional parameters were added to the model so that Deciduous and Coniferous forests soils could be parameterized differently and there could be an Aspen transfer between the Wetland HRUs and the Deciduous Forest HRUs. A unique Aspen ET algorithm was written to allow the Aspen trees to access the deep groundwater reserves. Model 3 defined any subbasin with wetland cover greater than 35% as a wetland heavy subbasin. These wetland heavy subbasins were given a different HEW representation than the other subbasins and forest runoff was only redirected to wetlands in the wetland heavy subbasins.

Table 4.5: Summary of key model changes during model development.

Change Type	Change Description	Successful (Y/N)
Structural	Added the Wetland HRU class with corresponding wetland algorithms	Yes
Algorithm	Changed the snow balance algorithm from the HBV default to the two-layer algorithm	Yes
Parameter	Changed the soil layers to be deeper (originally 0.1 m thick soil 0)	Yes
Algorithm	Removed an HBV algorithm which flushed ponded water to soil 1	Yes
Algorithm	Changed PET algorithm from Priestly-Taylor to Turc	Yes
Parameter*	Parameterize wetland soils and forestland soils differently (the same before)	Yes
Algorithm	Change percolation algorithm from constant percolation to one that was a function of soil moisture	No
Algorithm	Remove capillary rise from the model	Yes
Structural	Add lateral runoff transfer from the forestlands to the wetlands; included baseflow and runoff	Yes
Algorithm*	Change wetland overflow representation from linear to the power law representation	Yes
Parameter*	Change infiltration and seepage to time-varying	Yes
Parameter*	Change wetland threshold to time-varying	Yes
Structural*	Move baseflow before percolation in hydrologic process order	Yes
Parameter	Changed adiabatic lapse rate from AWS value of 5.1 to the global average of 6.5	Yes
Algorithm	Removed PET orographic correction	Yes
Algorithm	Remove temperature orographic correction	No

Change Type	Change Description	Successful (Y/N)
Algorithm	Remove precipitation orographic correction	No
Algorithm	Remove cloud cover correction	No
Algorithm*	Change infiltration algorithm to PRMS	No
Algorithm*	Change soil evaporation algorithm to UBC	No
Parameter*	Remove the relative LAI parameterization (monthly value to adjust max LAI), set to auto generate a value of 1	Yes
Algorithm*	Re-test two percolation algorithms which are functions of soil moisture	No
Structure	Add user defined canopy interception	Yes
Parameter*	Change the mineral fractions from AWS baseline to the Taiga Plain values	Yes
Parameter	Add user defined time of concentration to the model	Yes
Parameter*	Add user defined field capacity to the model	Yes
Parameter*	A warm-up period (with 0 weighting for diagnostics) was added to the calibration run	Yes
Parameter*	Remove time-varying infiltration	No
Structural	Change the lateral transfer from forests to wetlands to only be runoff as opposed to runoff and baseflow	Yes
Parameter*	Remove time-varying threshold	Yes
Structural*	Change deepflow baseflow algorithm to be threshold dependent	No
Structural*	Change percolation from soil 0 to moisture dependent	No
Model 2		
Structural	Added additional soil class for Deciduous Trees	Yes
Structural*	Added an Aspen transfer function from the Wetlands to the deciduous forests	Yes
Algorithm	Changed the deepflow baseflow algorithm from the Model 1 algorithm to the threshold algorithm for the forests	Yes
Parameter	Deepened forest soils to 10 m for ample storage	Yes
Parameter*	Initialized the soil water content in forest soil layer 2 to the threshold value	Yes
Parameter*	Added PET correction factors to deciduous trees so AET can be greater than PET	Yes
Algorithm*	Test soil infiltration from top soil with moisture dependent algorithm	No
Structural*	Added a new soil evaporation algorithm that allows Aspen trees to tap the soil layer 2 groundwater table if the water content in soil 0 is below the field capacity	Yes
Model 3		
Structural*	Added second HEW representation, 1 for wetland heavy subbasins, 1 for other subbasins	Yes
Structural*	Updated transfer to wetlands so only forests in wetland heavy subbasins would runoff into wetlands, other forest runoff directed to surface water	Yes

4.3.2 Refining Calibration and Validation

Once the model structures were finalized they were deployed in all three study basins. **Table 4.6** summarizes the warm-up, calibration, and validation period, for each study basin. The same periods were used for all model structures. Note that a warm-up period of 5 years was used in all study basins. This is longer than usual, but since the BPs have a long memory it was deemed important to have a longer warm-up period. The calibration and validation periods were selected such that there were wet and dry years in both the of the data sets, as shown in **Table 4.7**. The results for calibration and validation are presented in Chapter 5.

Table 4.6: Summary of refining calibration and validation periods.

Study Basin	Warm-up	Calibration	Validation
House River	28-May-1982 to 30-Sep-1988	1-Oct-1988 to 30-Sep-2000	1-Oct-2000 to 30-Sep-2011
Hangingstone River	6-Nov-1979 to 30-Sep-1984	1-Oct-1984 to 30-Sep-2000	1-Oct-2000 to 30-Sep-2011
Christina River	20-May-1982 to 30-Sep-1988	1-Oct-1988 to 30-Sep-2000	1-Oct-2000 to 30-Sep-2011

Table 4.7: Summary of wet and dry years in calibration and validation for all study basins.

Study Basin	Wet or Dry	Calibration			Validation		
		Year	Annual Runoff (mm)	Average Daily Discharge (m^3/s)	Year	Annual Runoff (mm)	Average Daily Discharge (m^3/s)
House River	Wet	1996	284	8.69	2005	184	5.35
		1997	193	5.89			
	Dry	1992	32	0.97	2002	26	0.82
		1999	23	0.66			
Hangingstone River	Wet	1996	250	6.00	2005	171	4.11
		1997	216	5.20			
	Dry	1999	21	0.52	2006	68	1.63
Christina River	Wet	1996	206	47.29	2005	167	38.39
		1997	195	44.81			
	Dry	1992	27	6.38	2002	45	10.27
		1999	21	4.71			

The refining calibration consisted of two phases, the first phase involved all the calibration parameters and the second only involved the sensitive model calibration parameters. Before the final model structures were calibrated in each basin a sensitivity analysis, as described above, was completed on the full parameter set. Appendix E summarizes the results of this sensitivity analysis. The first calibration optimized the NSE value with no other penalties applied and was run for 5000

evaluations. The second calibration also optimized the NSE but penalties were applied, depending on the performance after the first calibration and was run for 5000 evaluations. Penalties were applied either to the Percent Bias, KGE, a calculated NSE for fit to the regime curve, or a calculated NSE for baseflow. Note that if a calibration was unsuccessful in that it yielded unrealistic results, such as completely turning off infiltration in the forests, the calibration was re-done after some manual adjustments to parameter values for a shorter evaluation period. Note than in the case of insensitive parameters, such as the baseflow coefficient of forests in soil layer 1, values were calibrated in Model 1 but then may not have been calibrated in subsequent Model structures.

Table 4.8, **4.9**, and **4.10** summarize the parameters that were calibrated and the calibrated value for each of the study basins for each model structure. A full description of each parameter and which equation it applies to can be found in Appendix A.

Table 4.8: Summary of calibrated Model 1 parameters for each study basin.

Parameter Name	Sensitive?	Lower Bound	Upper Bound	Final Calibrated Value		
				House River	Hangingstone River	Christina River
BETA_S	Yes	0.75	1.5	0.986	0.77	0.97
BETA_W	Yes	0.3	0.8	0.326	0.77	0.798
BETA_G	No	0.5	2	1.00	0.64	1.48
PERCW0	No	0.005	1.5	0.0287	1.243	0.0219
PERCW1	No	0.01	0.1	0.015	0.03	0.05
PERCF0	No	0.01	0.1	0.08	0.08	0.04
PERCF1	No	0.1	5	1.75	3.07	2.13
BASEW1	Yes	0.1	2	0.102	0.102	0.514
WN1	Yes	0.1	3	1.22	2.35	2.02
BASEW2	No	0.1	2	0.124	0.101	0.104
WN2	No	0.1	3	1.94	2.94	2.96
BASEF1	No	0.1	5	0.87	1.34	0.677
FN1	No	0.1	3	1	1.27	2.56
BASEF2	Yes	0.1	10	6.49	3.49	2
FN2	Yes	0.1	3	0.534	1.14	1.6
FC_W0	Yes	0.17	0.4	0.17	0.37	0.18
FC_F0	Yes	0.17	0.4	0.33	0.33	0.36
DEPTHW0	No	0.4	1.5	0.73	1.24	1.08
DEPTHW1	No	0.5	2	1.3	0.62	1.14
DEPTHW2*	No	-	-	8	8	8
DEPTHF0	No	0.4	1.5	0.4	1.32	0.53

Parameter Name	Sensitive?	Lower Bound	Upper Bound	Final Calibrated Value		
				House River	Hangingstone River	Christina River
DEPTHF1	No	0.5	2	0.5	1.26	1.58
DEPTHF2*	No	-	-	8	8	8
SEEP_S	Yes	0.01	0.1	0.015	0.062	0.024
SEEP_W	No	0.00001	0.1	0.0001	0.097	0.0195
MELT1	Yes	1.5	20	19.99	3.05	1.91
MELT2	No	0.1	1.2	1	0.99	0.1
SWE1	Yes	2.5	50	49.97	2.5	44.99
DEPT1	Yes	25	400	92.26	54.41	224.97
DEPMF1	Yes	5	55	31.53	46.34	43.98
DEPM1	No	850	1200	915	973	854.2
DEPN1	Yes	0.1	1.1	1.01	0.34	0.64
OW1	No	0.6	1	0.7	0.6	0.624

Table 4.9: Summary of calibrated Model 2 parameters for each study basin.

Parameter Name	Sensitive?	Lower Bound	Upper Bound	Final Calibrated Value		
				House River	Hangingstone River	Christina River
BETA_CS	Yes	0.7	1.5	1.09	0.726	0.8
BETA_CW	Yes	0.3	0.8	0.3	0.649	0.516
BETA_DS	Yes	0.8	3.5	1.46	0.92	3.09
BETA_DW	Yes	0.8	3.5	1.199	1.1	2.5
BETA_G	No	0.5	2	1.85	0.626	1.48
PERCW0	No	0.1	3	2.5	2.17	1.15
PERCW1	No	0.01	0.08	0.054	0.012	0.02
PERCCF0	No	0.01	1	0.06	0.339	0.05
PERCCF1	No	0.5	2.5	0.521	1.95	2.15
PERCDF0	No	0.05	1	0.09	0.62	0.15
PERCDF1	No	0.5	2.5	1.04	1.17	1.07
BASEW1	Yes	0.1	2	0.766	0.379	0.259
WN1	Yes	0.1	3	0.39	2.49	2.85
BASEW2	No	0.1	2	0.4	0.1	0.104
WN2	No	0.1	3	0.149	2.94	2.96
BASECF1	No	0.05	2.5	0.05	1.34	0.05
CFN1	No	0.1	3	2.7	1.27	2.56
BASECF2	Yes	0.1	5	3.89	4.98	0.108
CFN2	Yes	0.1	5	0.449	4.99	1.61

Parameter Name	Sensitive?	Lower Bound	Upper Bound	Final Calibrated Value		
				House River	Hangingstone River	Christina River
BASEDF1	No	0.05	2.5	0.05	1.34	0.05
DFN1	No	0.1	3	1.83	1.27	2.56
BASEDF2	Yes	0.1	5	1.51	4.27	4.85
DFN2	Yes	0.1	5	0.728	3.69	0.126
BASETCF1	No	0.8	0.99	0.88	0.891	0.8
BASETDF1	No	0.8	0.99	0.88	0.811	0.8
FC_W0	No	0.18	0.4	0.33	0.39	0.221
FC_CF0	No	0.17	0.4	0.33	0.38	0.38
FC_DF0	No	0.17	0.4	0.17	0.378	0.2
FC_DF2	No	0.15	0.4	0.172	0.178	0.244
ASPENP1	Yes	0.5	1.2	0.607	0.96	0.769
DEPTHW0	No	0.1	1.5	0.1	1.37	0.489
DEPTHW1	No	0.4	2.5	0.5	2.17	1.45
DEPTHW2*	No	-	-	4	4	4
DEPTHCF0	No	0.4	1.5	0.498	1.36	1.41
DEPTHCF1	No	0.5	2.5	1.92	1.91	1.49
DEPTHCF2*	No	-	-	10	10	10
DEPTHDF0	No	0.3	1.5	0.3	0.75	0.45
DEPTHDF1	No	0.5	2.5	1.03	2.24	2.32
DEPTHDF2*	No	-	-	10	10	10
SEEP_S	Yes	0.02	0.08	0.02	0.0581	0.021
SEEP_W	No	0.00001	0.4	0.00001	0.0156	0.017
MELT1	Yes	2	25	22	2.096	2.34
MELT2	No	0.1	2.2	1.74	1.58	0.11
SWE1	Yes	5	50	49.99	8.81	8.07
DEPT1	Yes	25	400	90.3	57.997	249.3
DEPMF1	Yes	5	55	40.34	27.49	49.38
DEPM1	No	850	1200	1127	1172	854.26
DEPN1	Yes	0.2	1.2	0.981	0.203	0.677
OW1	No	0.6	1	0.625	0.58	0.6

Table 4.10: Summary of calibrated Model 3 parameters for each study basin.

Parameter Name	Sensitive?	Lower Bound	Upper Bound	Final Calibrated Value		
				House River	Hangingstone River	Christina River
BETA_CS	Yes	0.9	3	2.21	0.904	1.01
BETA_CW	Yes	0.3	0.9	0.38	0.899	0.617
BETA_DS	Yes	0.2	3	2	0.22	1.74
BETA_DW	Yes	0.2	3	1.498	0.217	0.987
BETA_G	No	0.5	2.5	2.19	0.716	1.43
PERCW0	No	0.1	3	2.99	2	1.49
PERCW1	No	0.0005	0.05	0.0005	0.002	0.037
PERCCF0	No	0.01	0.5	0.261	0.297	0.0289
PERCCF1	No	0.1	2.5	1.24	1.33	2.22
PERCDF0	No	0.01	2.5	2.5	0.109	0.0204
PERCDF1	No	0.1	3	3	2.94	1.09
BASEW1	Yes	0.1	2	0.163	0.596	0.395
WN1	Yes	0.1	3	1.08	2.2	2.998
BASEW2	No	0.1	0.5	0.4	0.1	0.104
WN2	No	0.1	3	0.149	2.94	2.96
BASECF1	No	0.05	3	0.05	1.34	0.677
CFN1	No	0.1	3	2.7	1.27	2.56
BASECF2	Yes	0.1	5	1.5	3.869	0.2
CFN2	Yes	0.1	3	0.8	2.4	0.295
BASEDF1	No	0.05	3	0.05	1.34	0.677
DFN1	No	0.1	3	1.83	1.27	2.56
BASEDF2	Yes	0.1	4	2.5	3.414	1.7
DFN2	Yes	0.1	3	2.07	0.71	0.16
BASETCF1	No	0.8	0.99	0.908	0.911	0.8
BASETDF1	No	0.8	0.99	0.99	0.817	0.846
FC_W0	No	0.17	0.4	0.18	0.344	0.356
FC_CF0	No	0.17	0.4	0.17	0.37	0.38
FC_DF0	No	0.17	0.4	0.17	0.27	0.18
FC_DF2	No	0.17	0.25	0.172	0.205	0.174
ASPENP1	Yes	0.3	1.5	0.517	0.32	0.77
DEPTHW0	No	0.4	1.5	1.12	1.24	1.35
DEPTHW1	No	0.5	2.5	1.24	2.4	1.27
DEPTHW2*	No	-	-	4	4	4
DEPTHCF0	No	0.4	1.5	0.494	1.37	1.48
DEPTHCF1	No	0.5	2.5	1.96	0.54	1.03
DEPTHCF2*	No	-	-	10	10	10

Parameter Name	Sensitive?	Lower Bound	Upper Bound	Final Calibrated Value		
				House River	Hangingstone River	Christina River
DEPTHDF0	No	0.3	1.5	0.314	0.55	1.3
DEPTHDF1	No	0.5	2.5	1.59	1.75	1.92
DEPTHDF2 *	No	-	-	10	10	10
SEEP_S1	Yes	0.02	0.1	0.02	0.082	0.022
SEEP_W1	No	0.000001	0.02	0.00003	0.0294	0.021
SEEP_S2	Yes	0.018	0.1	0.079	0.0633	0.019
SEEP_W2	No	0.000001	0.02	0.000996	0.0001	0.00017
MELT1	Yes	2.5	25	20.9	4.66	2.85
MELT2	No	0.1	2.2	1.48	1.78	0.127
SWE1	Yes	3	50	23.67	25.51	4.8
DEPT1	Yes	5	400	77.42	39.39	41.53
DEPT2	Yes	5	400	122.67	168.35	154.35
DEPMF1	Yes	5	55	37.93	44.19	54.11
DEPMF2	Yes	5	55	47.09	48.91	11.23
DEPM1	No	850	1500	1226	1430	1195
DEPM2	No	850	1500	1009	1400	907.9
DEPN1	Yes	0.1	1.2	0.899	0.337	0.685
DEPN2	Yes	0.1	1.2	1.11	0.879	0.326
OW1	No	0.58	1	0.6	0.58	0.6

Chapter 5
Model Performance Results & Discussion

This section presents the results from the refining calibration and validation for Model 1, 2, and 3. An interpretation of the results is provided and the challenges that were faced during the model development process are discussed. To allow fair comparison between the AWS baseline models and the thesis models the AWS models were calibrated and validated using the same period as the thesis models. The AWS calibration consisted of 10 parameters and was run for 5000 evaluations optimizing the NSE with no penalties. This was done to simulate a standard calibration. Moving forward references to the AWS baseline models refer to these calibrated models.

5.1 Model Diagnostics

The calibration and validation results for all the AWS baseline models and the three thesis model structures are summarized in **Tables 5.1**, **5.2**, and **5.3** for House River, Hangingstone River, and Christina River, respectively. All the stream gauges in Christina River are presented, however, the discussion will be centered around the gauge at the primary outlet. Note that the Birch Creek and Jackfish River gauges do not have observed data after 1995 and are therefore not presented in validation in the table.

Table 5.1: Summary of daily model diagnostics for the House River basin.

Model Run	Calibration					Validation				
	NSE	Percent Bias	KGE	R2	RMSE	NSE	Percent Bias	KGE	R2	RMSE
Calibrated AWS	0.54	26.1	0.51	0.57	3.38	0.5	20.1	0.49	0.54	2.91
Model 1	0.72	1.41	0.8	0.72	2.93	0.39	-18	0.58	0.45	3.33
Model 2	0.71	-0.85	0.81	0.72	2.97	0.37	-20.9	0.58	0.46	3.37
Model 3	0.68	-2.21	0.71	0.69	3.12	0.36	-18.55	0.48	0.41	3.41

With the limited number of deciduous trees in the House River basin it was expected that Model 2 and Model 3 would only have minor changes in performance when compared to Model 1. The calibration NSE values are similar in the thesis models, with Model 1 having the best value and the AWS baseline model having a much lower value. In calibration the percent bias values indicate that the thesis models have similar performance while the AWS baseline model overestimates flow volumes. The KGE and R^2 values are similar to the NSE results with the AWS baseline model having much worse performance than the thesis models. The RMSE also indicates that Model 1 performs better than the other thesis models or the AWS baseline model, although the difference between

Model 1 and Model 2 is minor. Therefore, based on the model diagnostics in calibration, Model 1 appears to be the best model structure. However, there is a noticeable drop in performance between the calibration and validation periods in the thesis models that is not observed in the AWS baseline model. The NSE values changed by over 40% in all thesis models and the percent bias changed by over 1000% in Model 1 and Model 2. Note that a significant change between the two periods can be an indication that the model was overfit during calibration. In validation the volumes are being underestimated in all the thesis model structures.

Table 5.2: Summary of daily model diagnostics for the Hangingstone River basin.

Model Run	Calibration					Validation				
	NSE	Percent Bias	KGE	R2	RMSE	NSE	Percent Bias	KGE	R2	RMSE
Calibrated AWS	0.52	9.31	0.52	0.54	5.71	0.30	-0.30	0.47	0.32	4.70
Model 1	0.67	-5.44	0.70	0.67	4.78	0.28	-11.70	0.62	0.41	4.76
Model 2	0.65	-6.96	0.71	0.66	4.86	0.21	-4.91	0.62	0.39	4.97
Model 3	0.60	-17.10	0.59	0.63	5.21	0.24	-15.50	0.56	0.36	4.91

Out of all the study basins the Hangingstone River had the worst model diagnostic performance, however, there are larger changes between the Model 1 and Model 2 performance than in the House River. In calibration the thesis models performed better than the AWS baseline model in the NSE, KGE, R^2 and RMSE values. The thesis model's percent bias values indicate that flow volumes are being underestimated more so than in the House River basin with the largest discrepancy observed in Model 3. The AWS baseline model is overestimating flow in calibration but not by as large an amount as in the House River basin. The minimum change in NSE value between calibration and validation was 58%, while the minimum change in percent bias was 9.36% in Model 3. However, the percent bias started off poor to begin with, so a minor change may not be significant to interpreting model performance. Looking solely at the diagnostics it is not possible to say which model structure was best suited for the Hangingstone River basin.

Table 5.3: Summary of daily model diagnostics for the Christina River basin.

Gauge	Model Run	Calibration					Validation				
		NSE	Percent Bias	KGE	R2	RMSE	NSE	Percent Bias	KGE	R2	RMSE
Christina River	Calibrated AWS	0.59	8.8	0.58	0.61	14.3	0.50	-11.7	0.52	0.52	15.5
	Model 1	0.75	1.1	0.72	0.77	12.0	0.49	-18.4	0.52	0.56	15.7
	Model 2	0.81	3.9	0.82	0.81	10.5	0.48	-15.7	0.57	0.52	15.9
	Model 3	0.77	-0.29	0.75	0.78	11.6	0.45	-22.0	0.52	0.53	16.3
Birch Creek	Calibrated AWS	0.44	11.1	0.40	0.49	0.9	-	-	-	-	-
	Model 1	0.40	-15.2	0.37	0.44	1.0	-	-	-	-	-
	Model 2	0.37	-13.2	0.37	0.39	1.0	-	-	-	-	-
	Model 3	0.13	-25.7	0.28	0.19	1.2	-	-	-	-	-
Jackfish River	Calibrated AWS	0.15	72.3	0.22	0.50	3.7	-	-	-	-	-
	Model 1	0.47	56.2	0.39	0.65	3.2	-	-	-	-	-
	Model 2	0.45	59.5	0.38	0.67	3.3	-	-	-	-	-
	Model 3	0.19	70.7	0.24	0.52	3.9	-	-	-	-	-

At the outlet of the basin, the Christina River has better diagnostics than the other study basins, it also sees more of a difference in performance between Model 1 and Model 2 than the House River, as expected. From the model diagnostics, Model 2 appears to be the best model structure in the Christina River basin, however, as with the other study basins there was a sharp drop in performance between the calibration and validation periods. Once again the validation period underestimates the flow volumes and saw decreases in all diagnostics. Model 1 saw the smallest decrease in NSE with a 35% difference, while the other two model structures had changes over 40%. The percent difference in percent bias was the smallest for the Model 2 structure with a difference of 500%. In the two smaller subbasins, model performance was not well captured in any of the models.

For comparison to other published BPs models, the monthly NSE values are also reported for the primary outlets in **Table 5.4**. Note that in all the thesis models, except Model 3 in the Hangingstone River basin, the validation monthly NSE is worse than the daily NSE. This is very counterintuitive as typically, monthly NSE values are higher than the daily NSE values, as is observed in the calibration periods and the AWS models. It is unclear why this is observed here. One possible reason could be the freshet representation is particularly bad in validation, as will be discussed in subsequent sections. Since freshet only occurs during one or two months a large difference could lead to this lower value.

Table 5.4: Monthly NSE values in calibration and validation.

Study Basin	AWS		Model 1		Model 2		Model 3	
	Cal	Val	Cal	Val	Cal	Val	Cal	Val
House River	0.57	0.60	0.74	0.37	0.74	0.36	0.71	0.39
Hangingstone River	0.54	0.23	0.69	0.19	0.68	0.19	0.61	0.30
Christina River	0.60	0.45	0.79	0.44	0.85	0.43	0.83	0.43

To explore this more thoroughly the average monthly RMSE was calculated for each study basin for the calibration period for the AWS baseline and thesis models, shown in **Figure 5.2**. There were less values to compare to in April and November due to the lack of observation data during these months. In all the models, the RMSE is the highest in April during freshet. This is most noticeable in the Hangingstone River basin where the April RMSE is over twice as large as the other months in all models. The AWS baseline models have consistently higher monthly RMSE values while there are only small differences between the thesis models. There is the largest difference in RMSE values between the thesis models in the Christina River basin where Model 2 has lower error through the early summer months than the other model structures. In the House River and Hangingstone River basins the RMSE generally decreases as the year progresses, while the Christina River sees an increase in RMSE in September, possible indicating a poor match to the summer recession.

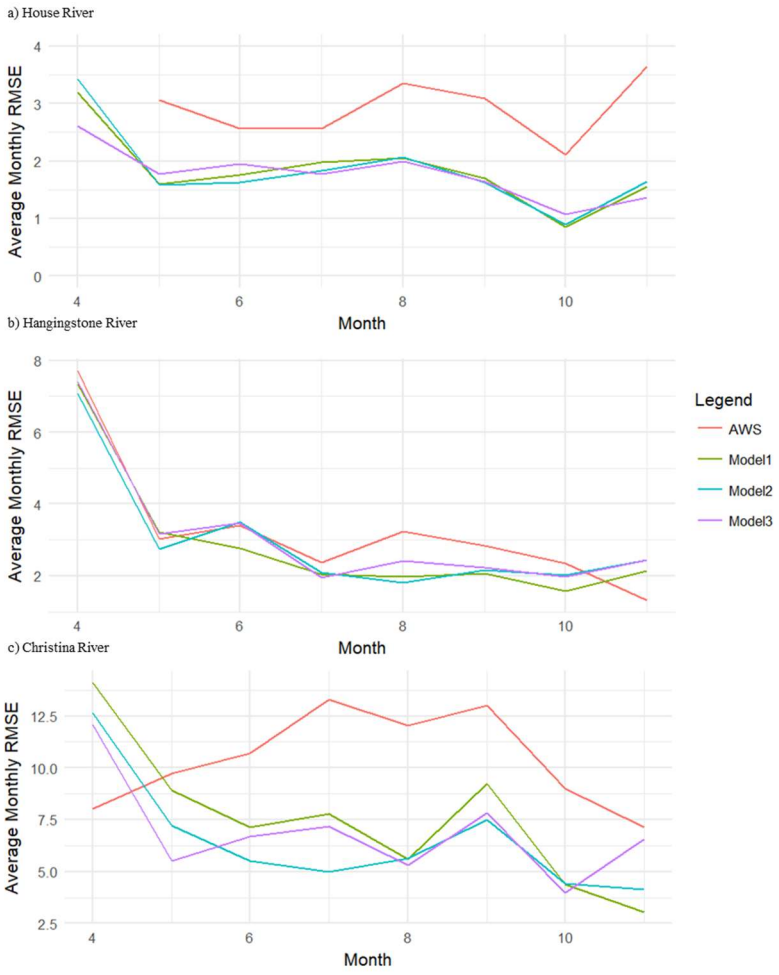

Figure 5.1: Monthly RMSE values for the calibration period in each study basin for all model structures.

As expected, there was a decrease in model performance between calibration and validation, however, the magnitude of the decrease indicates that the model structures were overfit during the calibration period. All the thesis model structures in all of the study basins resulted in underestimated flows in validation. Conversely, while the AWS baseline models had poorer calibration performance, they did not experience as large of a drop during validation. Looking at just the model diagnostics it is unclear if one model structure is better than the others.

This large drop in performance has been reported in literature in BPs models. While the SWATBF model had better results in calibration (Watson et al. 2008), they saw a much sharper decline during validation. Their daily calibration NSE dropped from 0.81 to 0.27 in validation, a change of 67%. The monthly calibration NSE dropped from 0.89 to 0.44, a difference of 44%. The SWATBF model also saw the percent bias increase from less than 15% in calibration to over 40% in validation (Watson et

al. 2008). The fact that there is less of a decline in performance in the thesis models than in the SWATBF model supports the idea that the thesis model structures may be more physically representative of the BPs. It is likely that since the SWATBF was applied and tested in a well instrumented basin their input data was of higher quality than the models in this thesis, which could explain their higher calibration values. However, this also demonstrates the importance of validation, since the thesis models performed better here than the SWATBF model. It should also be acknowledged that while the SWATBF model basin was well instrumented they also had a shorter run time, which meant there was less data for calibration. The model had a four year warm-up period, three years for calibration and two years for validation. There was a wet and dry year in calibration but no description of the years in validation. Additionally, it did not report results in the winter months. This shorter run time and lack of representation of seasonality could also be part of the explanation why the SWATBF model performed poorly in validation.

5.2 Model Hydrologic Signatures

To explore whether the model structures are more physically representative of the BPs, the additional hydrologic signatures introduced in Chapter 3 were used to evaluate the AWS baseline model, Model 1, Model 2, and Model 3. While numerous signatures were examined during model development and calibration only a select few will be presented here to support model comparison discussions.

5.2.1 Hydrographs

Figures 5.2, **5.3**, and **5.4** show a comparison of a hydrographs in calibration and validation for the three study basins. There are minimal differences between Model 1 and 2 while Model 3 is consistently flashier with higher peaks.

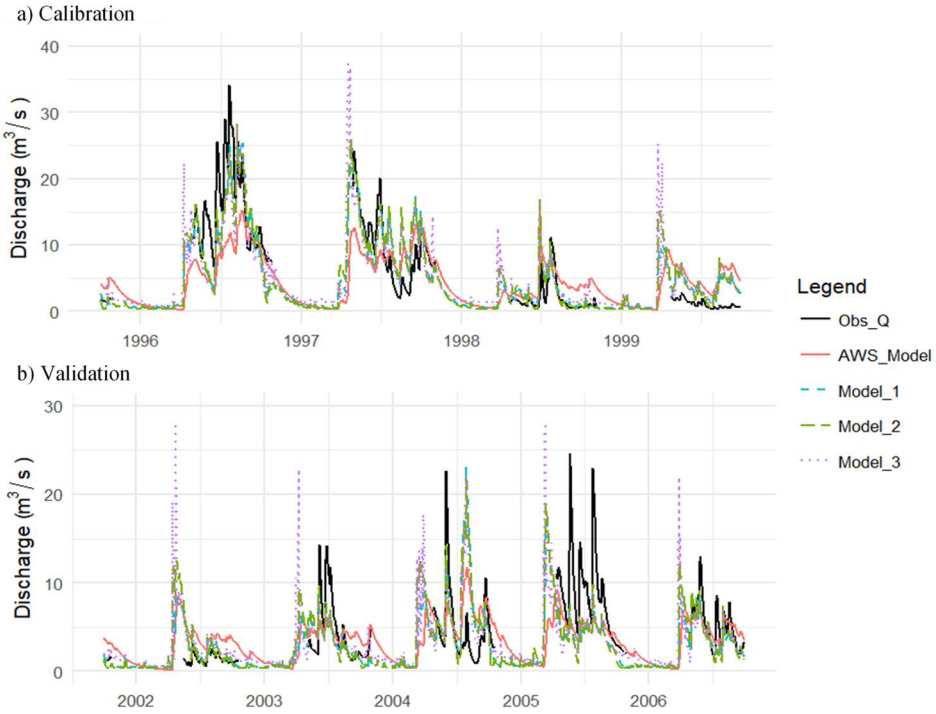

Figure 5.2: Hydrographs for a select 5 years in the House River basin for calibration (a) and validation (b).

Figure 5.2 shows that the freshet timing in the thesis models in the House River basin is generally too early and the magnitude is too high in validation; this is most pronounced in Model 3. Additionally, the thesis models do not capture the summer peaks very well in wet years in both calibration and validation. The dry years are overestimated in both model periods as well. Comparatively, the AWS baseline model is muted with limited variability, and does not capture the peaks well in calibration or validation.

The Hangingstone River basin had the poorest hydrograph performance of the three study basins, which are shown in **Figure 5.3**. In validation the freshet is early and the magnitudes are too high. Model 3 is flashier than the other two and the magnitudes of the peak events in both calibration and validation are too high. Again, the AWS model does not have the same variation that the thesis models have and generally underestimates the peaks in the wet years.

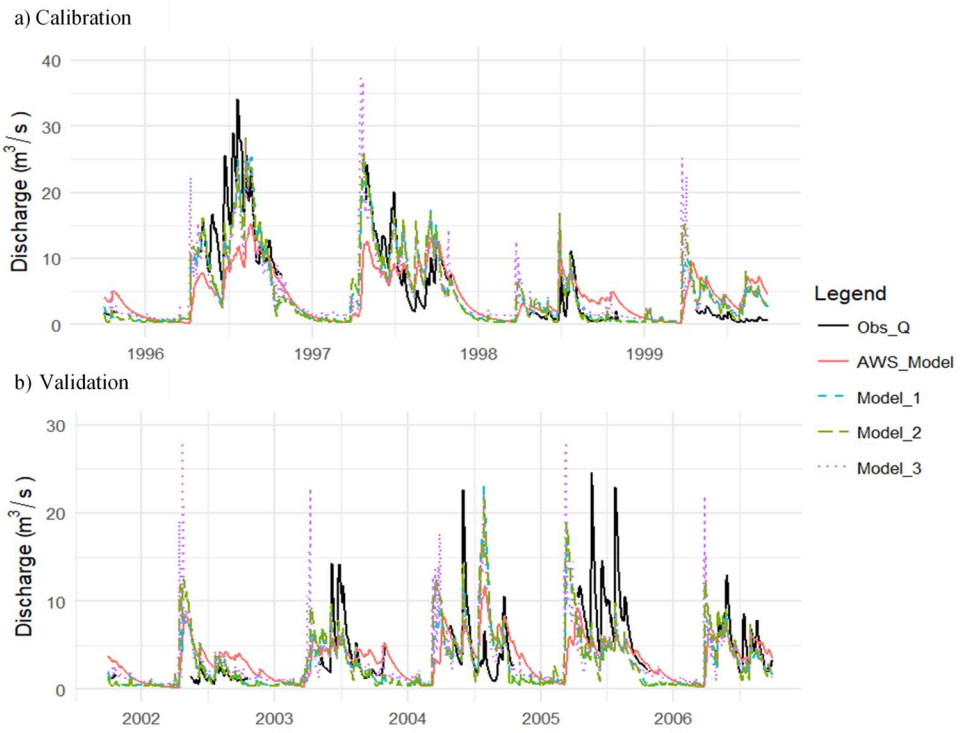

Figure 5.3: Hydrographs for a select 5 years in the Hangingstone River basin for calibration (a) and validation (b).

In the Christina River basin (**Figure 5.4**) during calibration, the thesis models capture the freshet very well except in the dry year. The summer peaks don't match as well as the freshet but they are better than what is observed in the other two study basins. In validation the freshet magnitudes are generally over-estimated, except in wet years, although there is not the same shift in timing observed here as there is in the other two study basins. The AWS model doesn't have the variability that the thesis models have. The thesis models also appear to capture the summer recession in both calibration and validation better than the AWS baseline model.

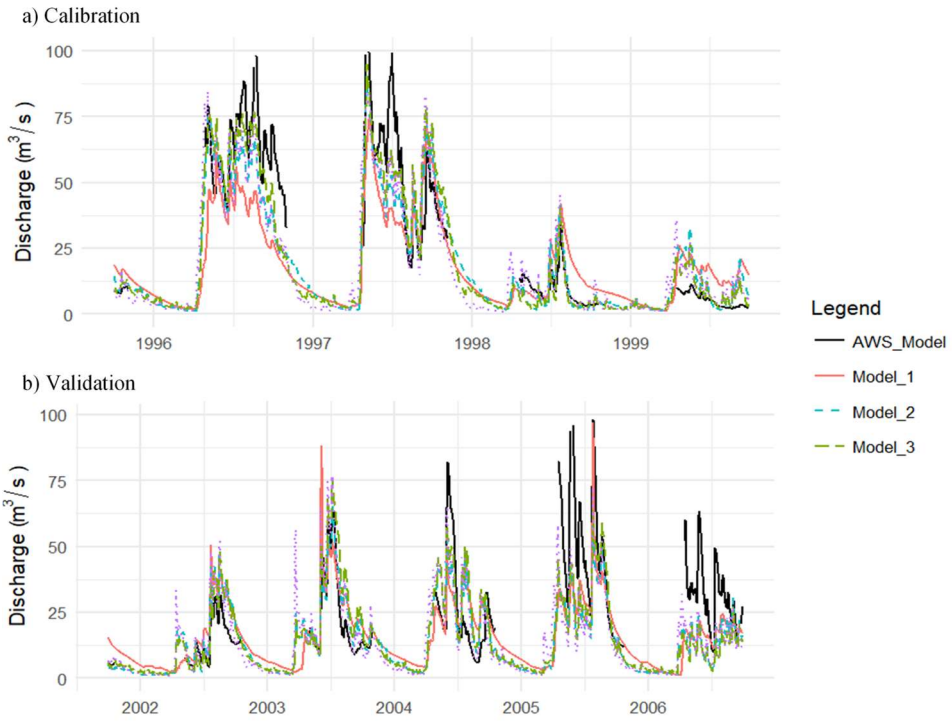

Figure 5.4: Hydrographs for a select 5 years in the Christina River basin for calibration (a) and validation (b).

5.2.2 Regime Curves

An example of a regime curve is shown in **Figure 5.5** for Model 1 in calibration and validation for the House River basin. Only months with gauge data are shown in the observed discharge regime curve. In calibration the freshet timing is too early, but the magnitude is close to what is observed. In validation the modelled freshet has shifted to a month earlier although the magnitudes are also close to the observed values. The precipitation shifts from peaking in May in calibration to peaking in July in validation while the modelled AET and PET peaks in July in both calibration and validation.

Note that between the calibration and validation period there is a shift in the observed regime curves. In validation the flow depth regime curve's freshet is the largest peak, compared to calibration where both the freshet and summer have significant peaks in the regime. While not shown here, a regime shift was observed in all observed regime curves in all study basins. A shift in regime could partially explain the error in timing of the freshet in validation of the thesis models. These shifts could occur for several reasons such as climate change or anthropogenic impacts in the basin (for example significant land cover changes). The model assumes the landcover presented in the GIS data is representative of the landcover throughout the course of the model run. Any significant changes could

impact model performance. This observed shift also raises the question of whether the split calibration approach used is the best way to validate the results, since different regimes may not result in a fair comparison.

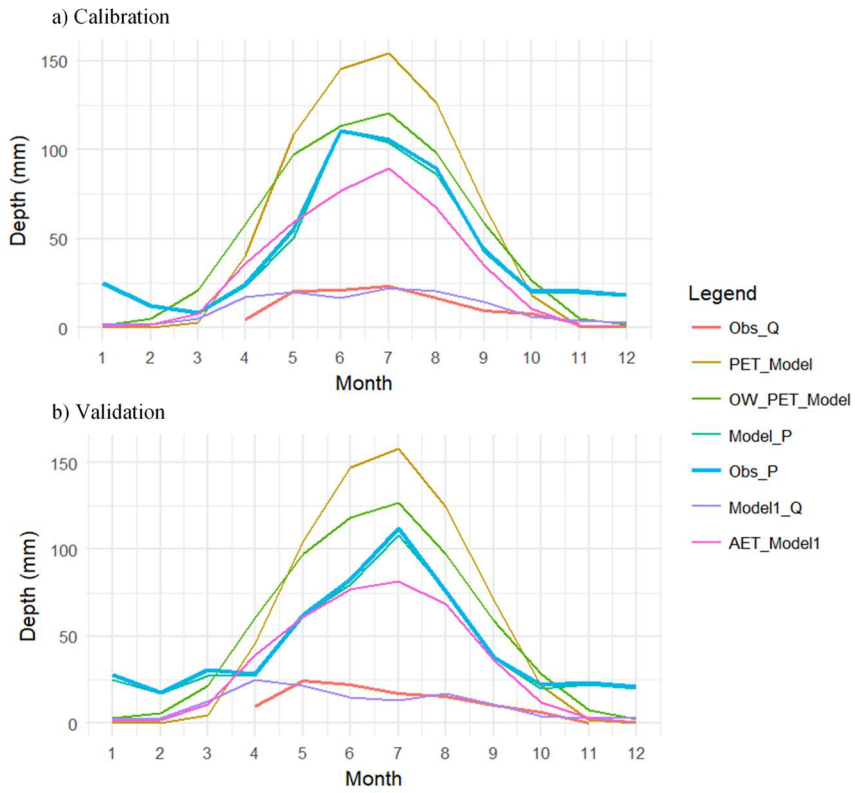

Figure 5.5: Regime curve for the House River basin for the calibration period (a) and validation period (b).

As shown in Chapter 3, the AWS modelled PET was consistently higher than expected in the regime curve. At URSA, for example, the average annual rainfall is 481 mm/year and the average annual PET is 518 mm/year (Redding and Devito 2008). **Table 5.5** summarizes the model PET and AET in each basin. Note that the AWS model PET is almost double what is observed at URSA.

Table 5.5: Modelled PET and AET in each study basin.

Study Basin	AWS		Model 1		Model 2		Model 3	
	PET	AET	PET	AET	PET	AET	PET	AET
House River	1237	359	673	389	673	385	673	379
Hangingstone River	1114	315	674	364	674	357	674	372
Christina River	1142	359	688	376	688	381	688	386

5.2.3 Discharge Sources

Figure 5.6 shows the discharge sources for the AWS, Model 1, Model 2, and Model 3 for 5 years of the calibration period in the House River basin. Deepflow is lower in Model 1 and Model 2 than it is in Model 3, while overflow events are reduced in Model 3 when compared to the other two. The AWS baseline model is mostly deepflow, which, as discussed in Chapter 3, is not consistent with the expected hydrology of BPs basins since observed deep groundwater flow in the BPs is low(Redding and Devito 2011). Additionally, the AWS flow peaks are less than what is observed in the thesis models. There are overflow events occurring in the winter months in the thesis models, which should not happen since this water should be held as ice during this time.

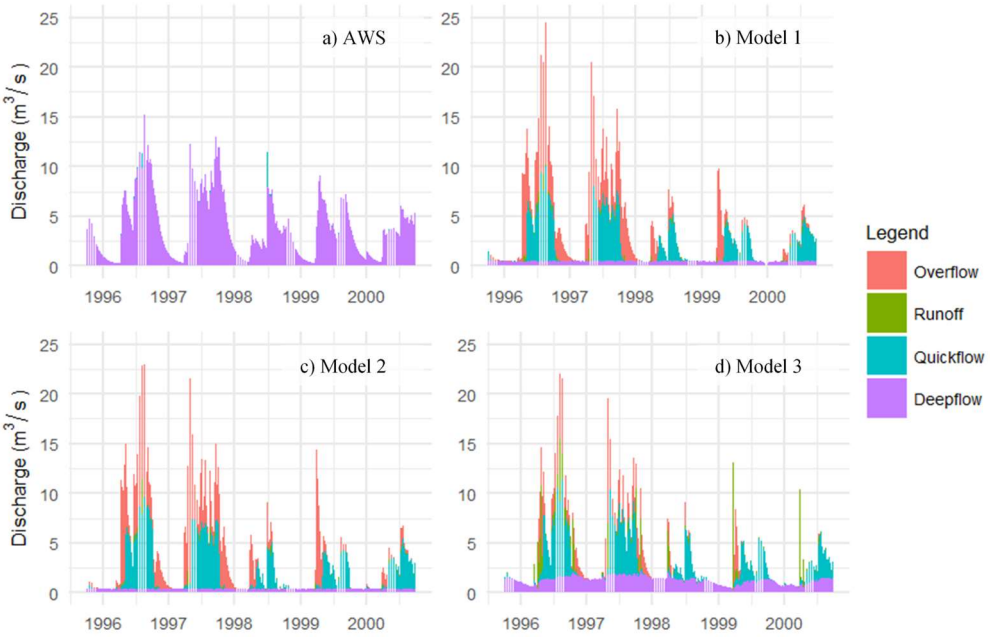

Figure 5.6: Discharge source hydrographs for 5 years of the calibration in the House River basin.

Figure 5.7 shows the percentage of each flow source for the entire model period in the House River basin. Model 1 and Model 2 have very similar proportions of each flow source, while deepflow and runoff are increased in Model 3.

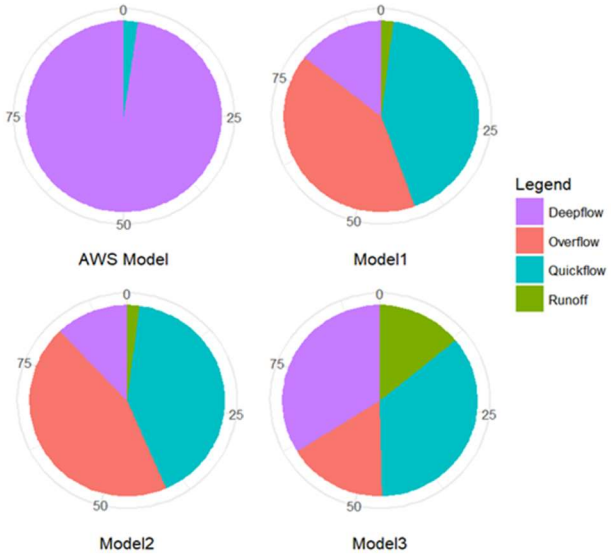

Figure 5.7: Discharge source in the House River basin for the full modelled period (1982-2011) for the AWS baseline model and Model 1, 2 and 3.

Figure 5.8 shows the same period as **Figure 5.5** for the Hangingstone River basin for the 3 thesis models and the AWS baseline model. The AWS model is primarily deepflow while the thesis models are primarily quickflow with overflow and runoff events supplying the peaks. Model 2 and 3 have a higher proportion of deepflow than Model 1.

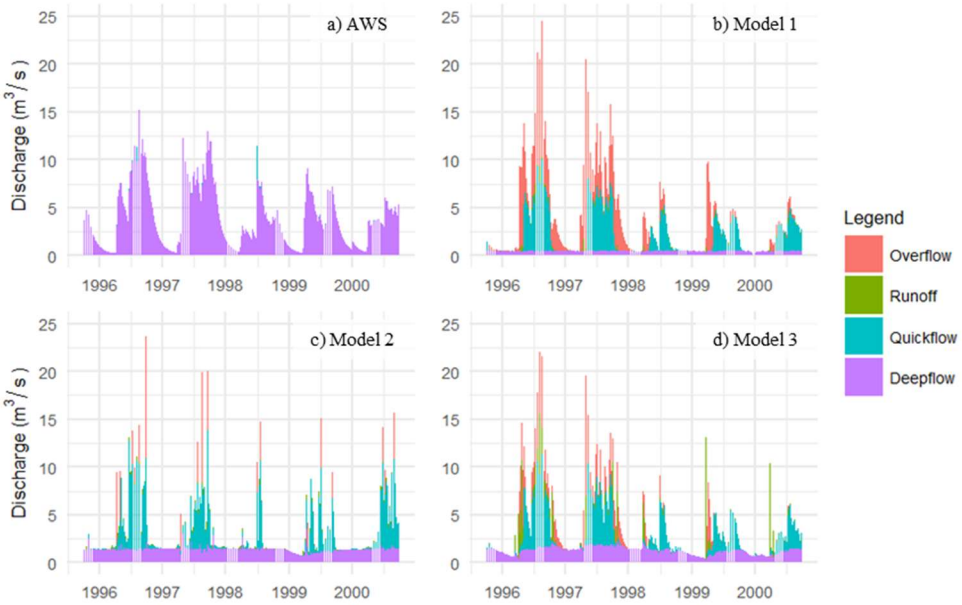

Figure 5.8: Discharge source hydrographs for 5 years of the calibration in the Hangingstone River basin.

Figure 5.9 shows the breakdown of discharge source for each model. Note that Model 2 is mostly wetland overflow events, while Models 1 and 2 are more balanced and are likely more representative of reality.

Figure 5.9: Discharge source in the Hangingstone River basin for the full modelled period (1979-2011) for the AWS baseline model and Model 1, 2 and 3.

Figure 5.10 shows the discharge sources for the AWS, Model 1, Model 2, and Model 3 for 5 years of the calibration period in the Christina River basin. Note that overflow from the wetlands was mostly turned off in all the thesis models. In Model 3, the peaks are composed primarily of the surface runoff that was not directed to the wetlands. Model 2 and 3 also have a slightly higher deepflow proportion than Model 1.

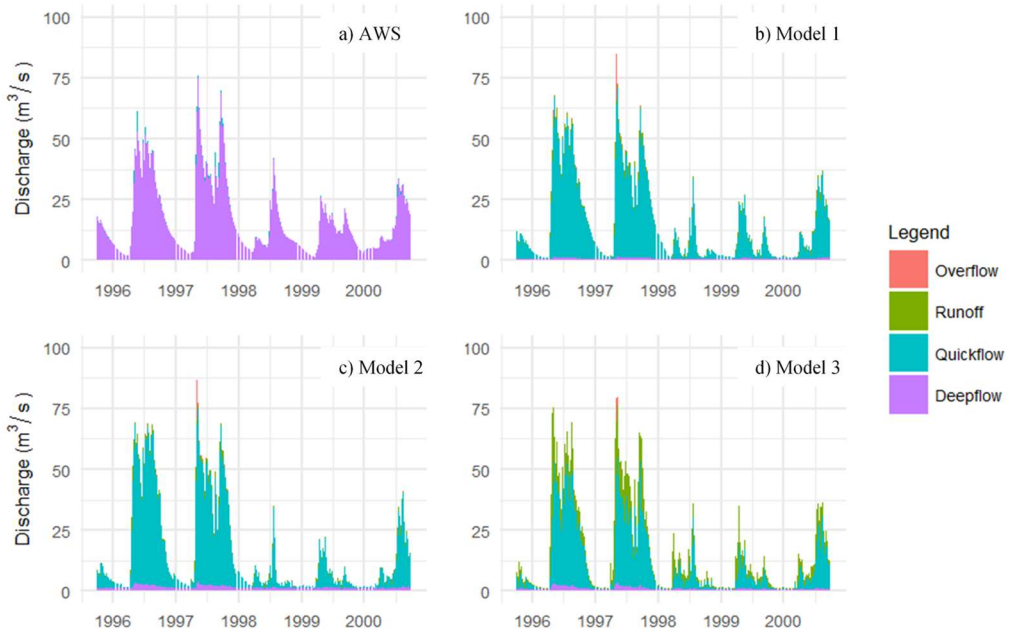

Figure 5.10: Discharge source hydrographs for 5 years of the calibration in the Christina River basin.

Figure 5.11 shows the discharge proportions for the entire period in the Christina River basin. Wetland overflow is low in all the thesis models and that runoff increases in Model 3. The AWS model is once again primarily deepflow.

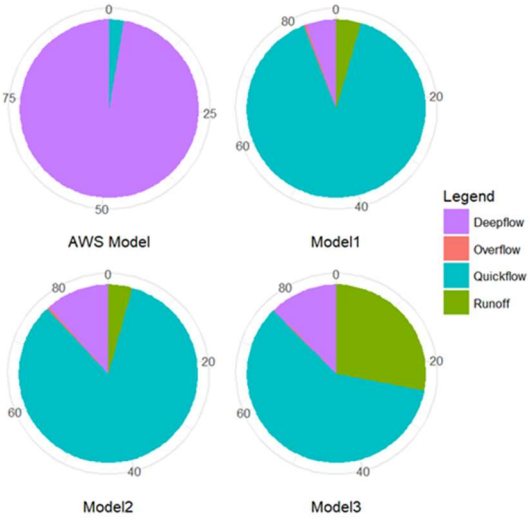

Figure 5.11: Discharge source in the Christina River basin for the full modelled period (1982-2011) for the AWS baseline model and Model 1, 2 and 3.

5.2.4 Baseflow

Figures 5.12, **5.13**, and **5.14** show the baseflow separated hydrographs for the calibration and validation periods of the study basins. The baseflow was separated from the observed and modelled hydrographs using the method described in Section 3.4.7. However, baseflow separation is an approximate method and therefore should be considered with some skepticism.

In calibration in the House River (**Figure 5.12**) the thesis models match well, although the peaks are low in the wet years and overestimated in the dry year. The AWS baseline model does not have the same variability that the observed flows and thesis models have. In validation the timing and magnitude of the peaks of the thesis models are off in most years and the average baseflow appears to be too high in Model 3. This could be an indication that baseflow was increasing with time in the model, which was observed during model development.

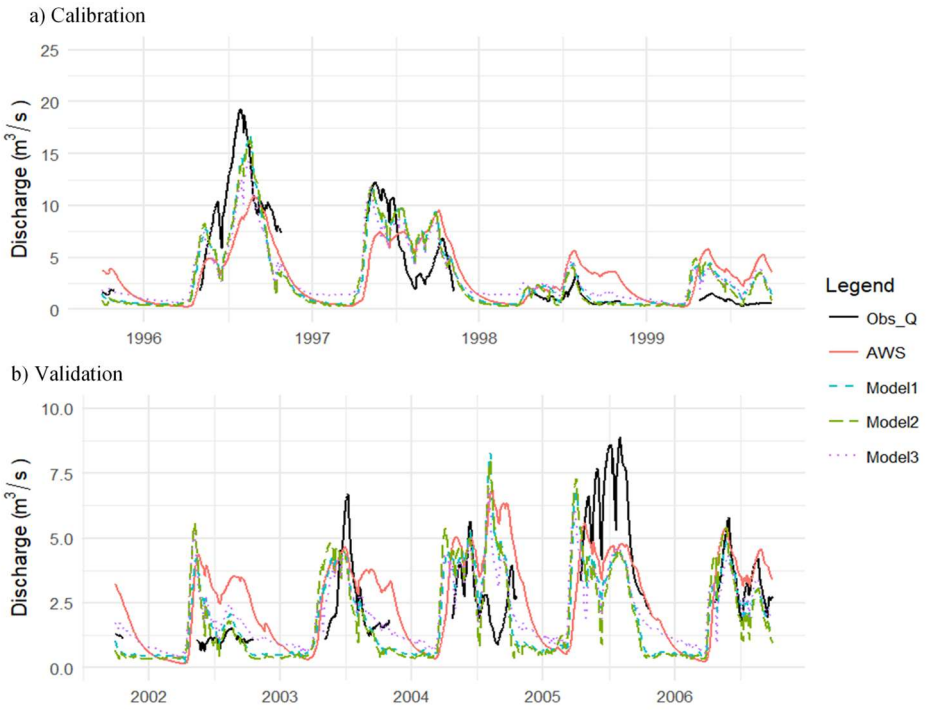

Figure 5.12: Separated baseflow hydrographs for a 5-year period in the House River basin for calibration (a) and validation (b)

Figure 5.13 shows the separated baseflow hydrograph for the Hangingstone River basin. Model 3 has average baseflow rates that are too high, both in calibration and validation. Models 1 and 2 have better separated baseflow representations in both calibration and validation as the recession more closely matches the observed separated baseflow hydrograph.

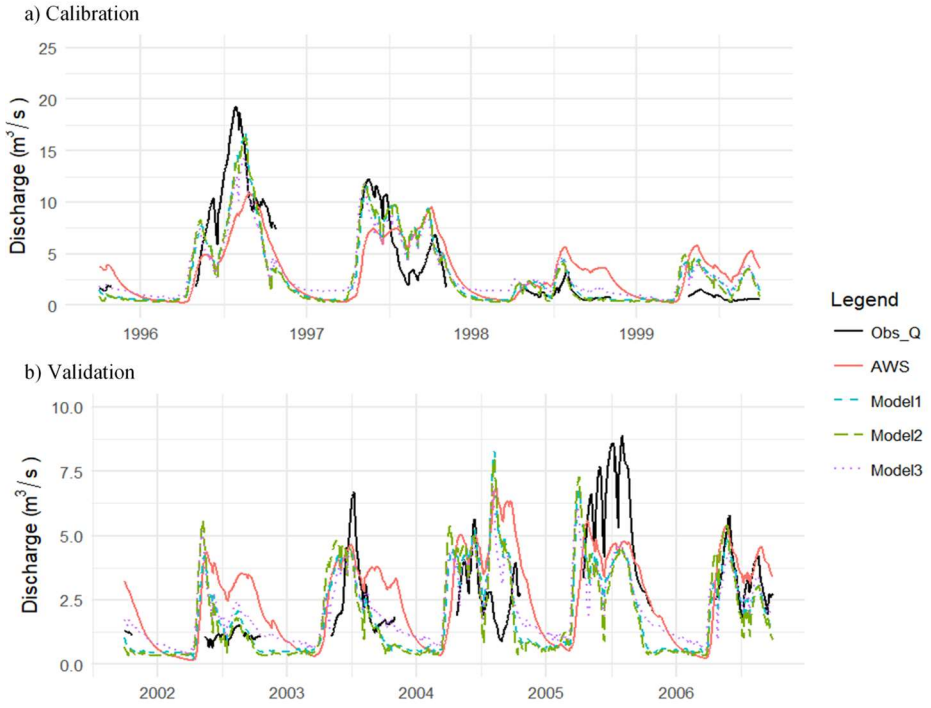

Figure 5.13: Separated baseflow hydrographs for a 5-year period in the Hangingstone River basin for calibration (a) and validation (b)

The baseflow in the Christina River basin is very well matched by the thesis models in calibration, as shown in **Figure 5.14**. There is a decline in performance in validation, although it is not as noticeable as in the other two basins. Model 2 most closely matches the baseflow in calibration, while in validation there is not much difference between the thesis models' performance.

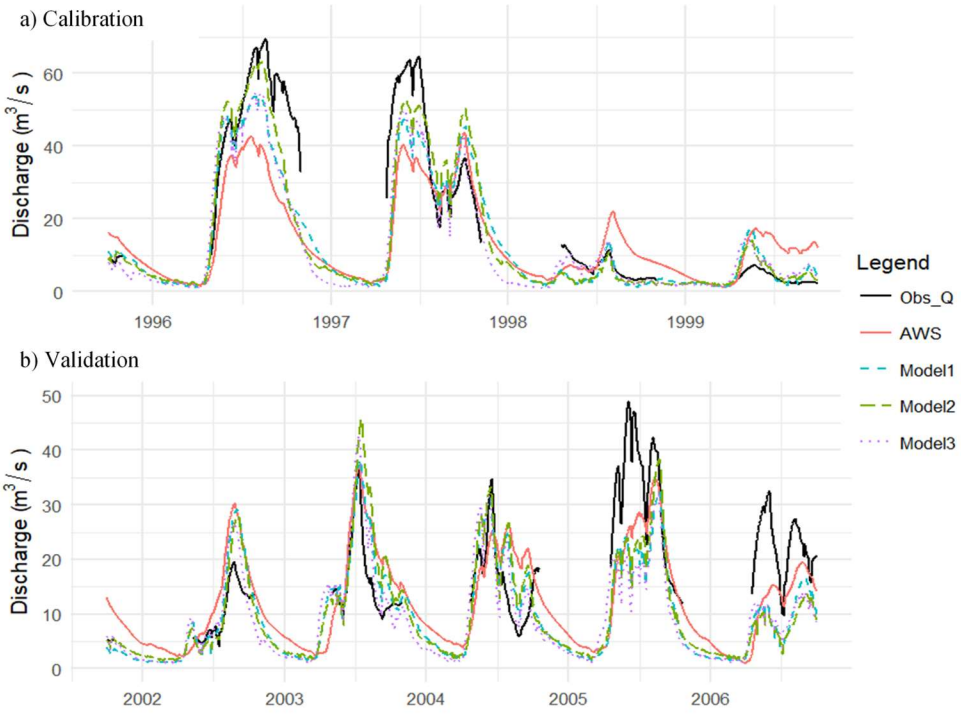

Figure 5.14: Separated baseflow hydrographs for a 5-year period in the Christina River basin for calibration (a) and validation (b).

5.2.5 Annual Runoff Depths

In the BPs there is large interannual variability in annual runoff between years, as shown in **Figure 5.15**. The figure shows that the average runoff depths are generally too high in all basins, yet the percent biases reported in Section 5.1 are typically negative, implying an underestimation in flow volume. This discrepancy could be attributed to the fact that Raven only calculates diagnostics when there is observed data, while **Figure 5.15** uses the entire hydrograph period. The observed hydrographs are typically missing data from October to April, so the depths shown in **Figure 5.15** should be lower than the modelled depths since the modelled hydrographs have a continuous output record. Therefore, the comparison should be made based on trends in variability and not based on the magnitudes.

The thesis models consistently capture the interannual variability better than the AWS baseline models, especially Model 2 in the Christina River basin. All the models in the Hangingstone River basin are failing to capture the interannual variability of the basin, which sees more significant interannual variation than what was observed in the House River or Christina River basins.

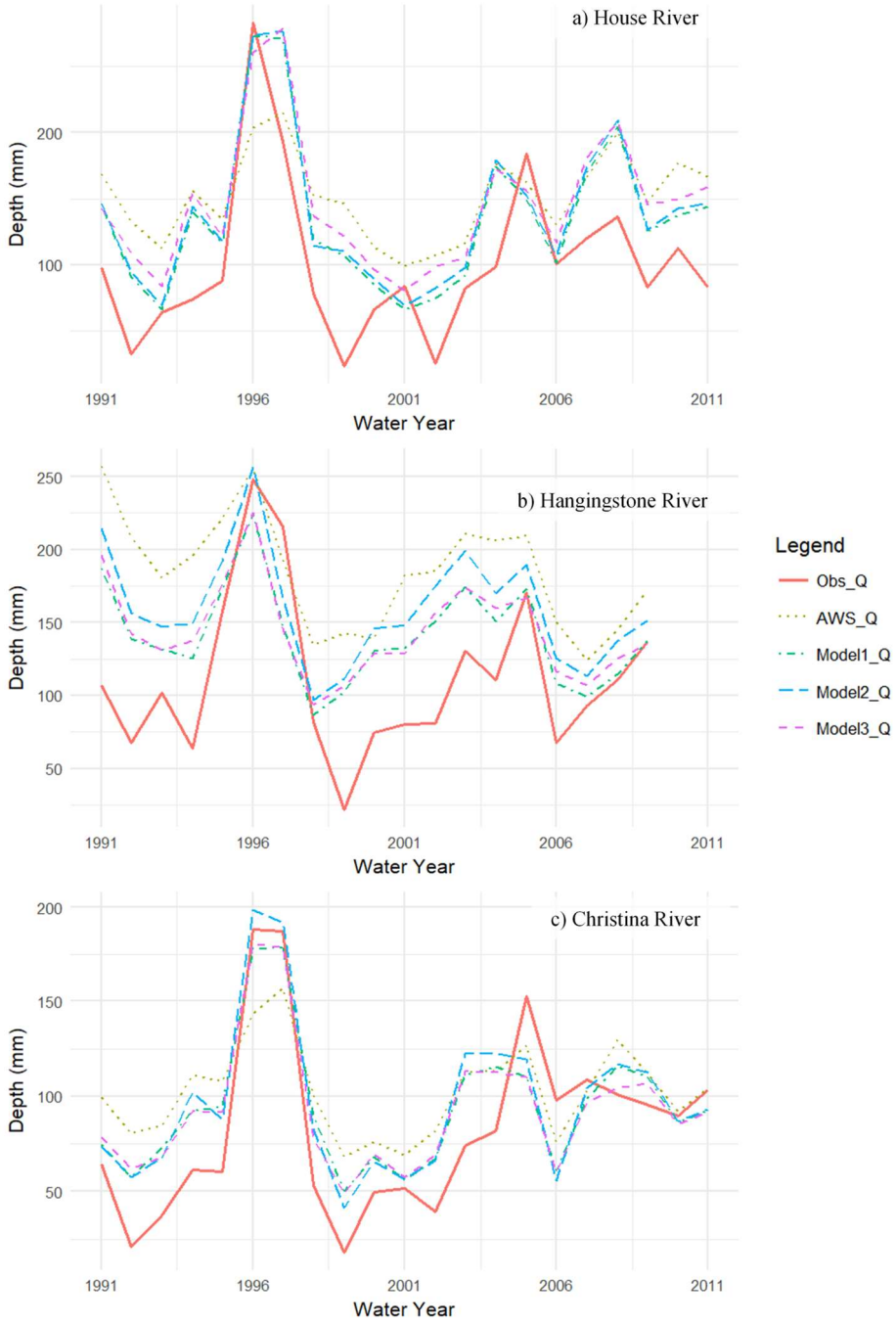

Figure 5.15: Annual average runoff comparison between the observed runoff, the AWS baseline model, and the three thesis models for the House River (a), Hangingstone River (b) and Christina River (c) study basins.

Evaluating annual runoff can also be done through comparison of the runoff coefficient, which is described by the average annual runoff divided by the average annual precipitation. **Figure 5.16** summarizes the runoff coefficients for each study basin and model structure. The observed runoff coefficients are likely underestimated since there is no runoff reported during the winter months even though there is flow during this period. The thesis models match the runoff coefficient well in the Christina River basin but are high in the Hangingstone River and House River basins. The AWS baseline models consistently overestimate runoff.

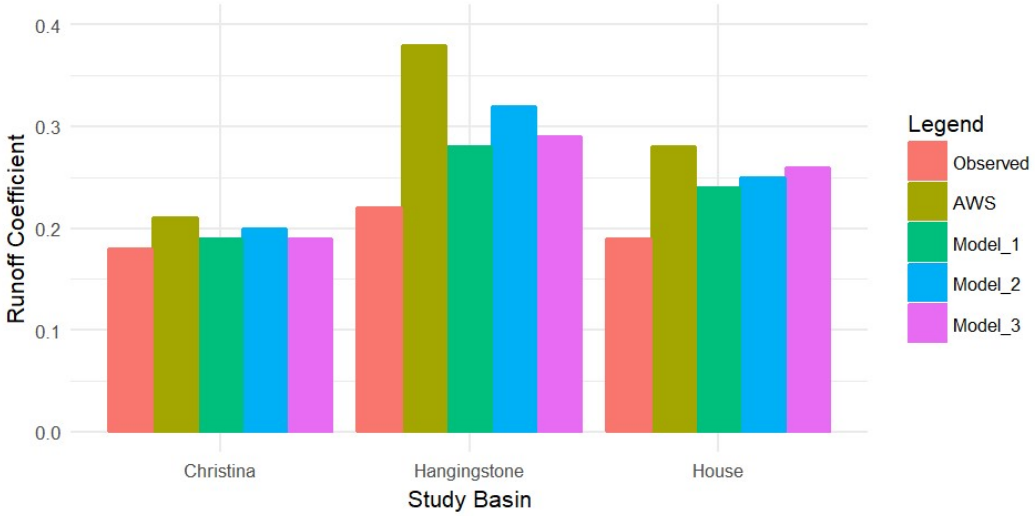

Figure 5.16: Runoff coefficients in each study basin for observed and modelled values.

5.3 Model Complexity and Performance

One of the objectives of this thesis was to evaluate conceptual model structures and make recommendations based on this evaluation. It is clear from the change between calibration and validation that the models were overfit in calibration, however, there is still useful insight provided by the model comparison and hydrologic signatures. While the AWS baseline models had better performance in validation, the fully calibrated values were still very low. Additionally, from the evaluation of hydrologic signatures, it appears that the baseline models are getting the "right" answers for the wrong reasons. Most of the water reaching the outlet is deepflow and it does not have the same variability that the thesis models were able to capture. Therefore, these models should not be considered physically representative of the BPs study basins. It is clear that additional effort is required to find an ideal model configuration which can accurately represent the hydrological function of these basins. Better calibration performance could have been achieved in the thesis models if the constraints on physical representativeness had not been enforced with manual checks

during calibration. The author identified multiple model configurations which led to better hydrograph fits in terms of NSE, but these sacrificed physical appropriateness, and were thus excluded.

There is a trade-off with increasing model parameters and model complexity, as the greater the number of parameters, the greater the challenge of equifinality becomes. Model 1 was the simplest model structure, adding explicit wetland representation and allowing forest runoff to be attenuated by the wetlands. Model 2 accounted for Aspen trees, which according to observations at URSA, play a significant role in the BPs water balance (Devito et al. 2012). During model development it became clear that the wetlands were controlling the summer peaks and these peaks were too low. Thus, Model structure 3 was added which only routes water to wetlands in wetland heavy subbasins. This model structure also allowed the hypothesis of whether multiple HEW representations would improve model performance to be tested. This increase in surface water availability was theoretically supposed to allow for better matching of summer peaks, in practice this was not the case.

Increasing model complexity did not necessarily (or consistently) result in increased model performance. Model 1 was the best model representation of the House River basin, which makes sense as this basin has the lowest percentage of deciduous forest coverage, and therefore Aspen representation should not be as important. Model 2 was the best representation in the Christina River basin based both on model diagnostics and hydrologic signatures. While the diagnostics were inconclusive, with respect to the hydrologic signatures, the best model representation in the Hangingstone River basin was Model 1 since it had a realistic discharge source proportion and best matched the baseflow. This is surprising, since this is the basin with the most deciduous tree cover, which should make Aspen tree representation important. The Hangingstone river basin was the steepest basin, with over 300 m of elevation change, so this may have impacted model performance since the BPs conceptualization is for flat basins. The poorer performance of Model 2 in the Hangingstone River basin could indicate that the Aspen trees were not properly represented in the model structures, although with the better performance in Christina River this seems less likely.

The thesis models were able to represent the wetland functions and the variable contributing area fairly well since most of the water reaching the outlet was a function of antecedent conditions. However, the representation of winter processes was lacking. This is evident not only from the poor freshet performance in validation but also from the calibrated values of the winter parameters. There was large variability in surface SWE of the snowpack and melt parameters between study basins and

between model structures, which shouldn't be the case with the three basins so geographically close together. Additionally, changing between model structures, which have constant snowmelt representations, should not impact the way snow accumulates and melts. Therefore, it is possible the snow representation in all of the thesis models was under performing. However, since storage is such a crucial component to BPs hydrology, snowmelt is likely closely intertwined with other processes. This could mean that the snowmelt was well represented in one or more of the basins, but since the other processes, such as infiltration, may not have been, the overall winter representation suffered.

Based on the evaluation of model structures either Model structure 1 or 2 could be recommended over the existing AWS of SWATBF model structures, but neither is conclusively optimal and therefore both more testing is required.

5.4 Modelling Challenges

This section will discuss the challenges that were faced during the model development process and how they were addressed. Proposed future solutions to these challenges and potential areas of future work will be discussed in Chapter 6.

5.4.1 Data Limitations

One of the primary challenges of model development was the limited availability of data for the study basins, which is quite common in the BPs. The openly available data was limited to sparse EC climate stations, few WSC hydrometric stations, and poor resolution DEM and landcover data. There was no detailed data available for soil mineral fractions, cloud cover or solar data, or vegetation parameters. A model can only be as good as its input data, so having limited data automatically limits the potential of any model. Only one of the seven EC climate gauges used had data in the winter months, meaning the other six gauges only had interpolated winter data for the entire 30 year run time. There are already errors associated with collecting precipitation data, especially in the winter, and interpolating introduces additional error. Snowmelt is a crucial component to the water cycle in the BPs and this lack of winter data limited the potential to better constrain the model and therefore increased the likelihood of overfitting during calibration. Additionally, it has been suggested that precipitation intensity and distribution is more important than precipitation volumes in the BPs (Devito et al. 2012). Watson et al. (2008) also noted that not properly capturing local precipitation variability may have impacted the SWATBF model performance. Therefore, having interpolated data, instead of local measurements, and a minimal number of gauges, likely further limits model performance potential. This limited climate data was partially mitigated by stopping the model period

in 2011 when most of the EC gauges were discontinued. This reduced the amount of days that would have been interpolated if the model run time was extended and thus limited some of the potential error. More available climate data, such as a greater spatial distribution of climate gauges and gauges which report winter data, would likely have helped reduce modelling uncertainty.

The WSC streamflow gauges also had data availability issues. House River and Hangingstone River only had one gauge available and, due to ice effects, the overwinter flows and freshet were not fully captured. While Christina River had more gauges, including RAMP gauges, they also suffered from ice effects. Additionally, data collected at the RAMP gauges is only reported after 2011, which is when most of the EC gauges stopped reporting data, making them ineligible to use in model training. While it should be acknowledged that all three models had at least 30 years of available data, which is better than published models like the SWATBF model had (Watson et al. 2008), the lack of winter data likely contributed to model equifinality.

Limited availability of readily available GIS data was also challenging. The 50k resolution DEM was not hydrologically conditioned, and due to its coarseness, combined with the flat landscape, available tools to condition DEMs were ineffective. This resulted in the need for basins and subbasins to be manually delineated based on contours and satellite imagery, introducing the potential for human error. The available landcover data set was also fairly coarse, which combined with the 50k DEM, made delineating between riparian and GIW wetlands impractical. It also limited the ability to delineate which upland forests were contributing to the wetlands and identify GIWs that were upland of forestlands. Having more detailed landcover data would have enabled proper identification of forestlands that runoff into wetlands (instead of the arbitrary selection of subbasins with wetland coverage greater than 35% that was used). A more informed delineation could have potentially resulted in better performance in Model 3 as it would have likely resulted in more physically meaningful HEW representations. Additionally, detailed landcover data could determine the proportion of the deciduous forest that was Aspen trees. With no additional data the assumption was made that all of the deciduous forests were Aspen trees, which is likely an overestimate. This could have resulted in decreased model performance of Model 2 and Model 3 by moving more water than necessary.

The discrepancy between the wetland and open water HRU classification is a bit arbitrary in the BPs since these waterbodies can act either more like open water sources with large evaporative fluxes or wetlands with smaller evaporative fluxes depending on the wetness of the year (Devito et al. 2012).

The United States has a wetland inventory that can be used to identify wetlands and their function type (USEPA 2015), and it would be useful if such an inventory existed in Canada. Ducks Unlimited do occasionally publish wetland inventories but their scope is typically limited, reducing their usefulness.

Without any soil data in the BPs, the mineral fraction from a field site in the Taiga Plain was used. There is high soil heterogeneity and variability in both regions, also, the Taiga Plains have deeper peatland deposits and permafrost while the BPs do not. However, in the absence of site specific data, it was a better starting point than random mineral fractions. These mineral fractions controlled how the model calculated field capacity and wilting point, and this lack of data resulted in the field capacity becoming a calibration parameter. While the overall impact this had on the model was minimal it is worth noting that this was an area of data limitation since increased parameters during calibration can lead to greater problems with equifinality. Additionally, lack of detailed information on things such as soil types, solar radiation, and vegetation characteristics, forced the developed model structures to use simpler algorithms, since these were the only ones that could be justified by the data.

The objective of this model was to be practical, meaning that any hydrologic modeller could use this structure as opposed to having data requirements that only detailed field sites could provide. This meant that only freely available data could be used to inform model structure development and constrain the model during calibration, thus creating this challenge of data limitation. This may have limited the use of more complicated algorithms but that was one of the purposes of the thesis, to develop a structure with these simpler algorithms that can effectively and efficiently represent the BPs at the catchment scale. Since, modelling in data poor areas, such as the BPs, often means relying on these simpler algorithms.

5.4.2 Current Understanding of the Physical Environment and Upscaling

As discussed at length in Chapter 2 the hydrology of the BPs is quite complicated which creates its own modelling challenges, especially when compared to the many basins that are well represented using standard rainfall-runoff models. There is also a lack of understanding of the physical processes in the BPs at the catchment scale. A majority of the observations of BPs hydrology occur at the field scale at URSA, which is in the Peace River Basin (PRB) and from satellite imagery it appears to have more areas of GIW than the Athabasca River Basin (ARB). URSA observations, such as vertical flow dominating the forestlands, were used as *a priori* assumptions to determine if the model was

performing in a physically realistic manor. However, it is unclear if observations in a different basin at the field scale are representative of basins in the ARB at the catchment scale. With limited research data at other field sites and the limited understanding of catchment scale performance, it is unclear if the model is representing reality. This question remains unanswered even though the best attempts were made to use multiple hydrologic signatures to verify model performance. However, these signatures are subject to any errors associated with the WSC gauges and the limited availability of other data that could be used to verify performance.

5.4.3 Modelling and Delineating Wetlands

Data limitations meant explicitly representing wetlands and wetland catchment areas at large scales impossible, thus the assumption was made that the HEW approach is applicable in the study basins, even though there are arguments that the spatial distribution of storage matters more than the magnitude (Spence 2010). The original model development plan included the use of separate HEW representations for GIW and riparian wetlands. As discussed in Section 5.4.1, the limited data made delineating between the two wetland functional groups impractical. However, it is also possible that the ARB doesn't have a significant number of GIW when compared to the PRB. The HEW approach was also modified for the models developed in this thesis. The HEW approach is supposed to have one unique HEW per subbasin, however, the way it was deployed in this thesis is a modified approach. While each subbasin does have its own HEW, with the exception of Model 3, they are all parameterized the same, making the area of the HEW the only difference between subbasins. Model 3 did not perform as well as the other two model structures but how the HEWs were characterized was arbitrary and it is possible that more detailed delineation could have resulted in better model performance. Therefore, it is unclear if having multiple HEWs can improve model performance and the testing of this more complicated HEW representation should be an area of future study.

5.4.4 Variable Contributing Area

Hydrologic connectivity and variable contributing area are important concepts to BPs hydrology. The models implicitly take this into account through the selection of algorithms which dictate how water can reach the outlet. In the developed models, hydrologic connectivity is dictated by antecedent moisture conditions and storage capacity, which is what is expected in this region. As demonstrated in **Figures 5.7**, **5.9**, and **5.11**, traditional overland runoff is limited in the models. Additionally, **Figure 5.15** shows that the interannual variability is closer to what is observed in the BPs than what

the standard AWS baseline models produced. Therefore, this challenge seems to have been adequately addressed.

5.4.5 Maintaining Physical Realism and Reducing Equifinality

One of the biggest challenges during the model development process was balancing appropriately constraining the model parameters during calibration with allowing enough flexibility for the calibration to explore the parameter space. The best way to constrain the model during calibration such that the model respects physical reality is still unclear. There were multiple parameter sets identified during development calibration that could have been selected, demonstrating the problem with equifinality.

Although equifinality is a problem, it was mitigated by using multiple signatures and model evaluation criteria. For example, there was one model parameter set in Model 1 in the House River basin that had higher diagnostics than the final model presented in this thesis (calibration NSE of 0.79). However, when the mass balance was checked it became apparent that the calibration had turned off infiltration in the forest, forcing all precipitation to runoff into the wetlands and then overflow into the channel. Since multiple field studies concluded runoff from the forestlands should be minimal (Gibson et al. 2002, Nijssen and Lettenmaier 2002, Redding and Devito 2010) this was eliminated as a possible solution set, despite its higher performance in calibration. If only traditional evaluation metrics had been used this likely would have been selected as the final model representation, even though it is less physically accurate.

5.4.6 Limited Algorithm Availability

Raven is a powerful hydrologic modelling tool and its flexible nature allowed model development to evolve past the standard fixed model approach. While it is continually adding new algorithms and is actively being developed, there exist some limitations that need to be addressed, such as how Raven represents winter and wetland processes. For example, sublimation routines are not fully developed, and there is no current way to represent frozen soils or freeze water in depressions. In an attempt to work around this the wetland overflow threshold was changed to time-varying to force water to stay in the depressions over winter. However, the date where the wetland threshold switched from winter to summer conditions strongly dictated the freshet timing and magnitude as there was a large release of water all at once on that day. The model was too sensitive to this date and so the threshold was changed back to a constant value, this resulted in the possibility of wetlands drying out in the winter and of overflow events in the winter months. It would have been better to have a more

gradual release that was a function of melt timing. At URSA, overwinter wetland ice plays an important role in the freshet (Devito et al. 2012) so not being able to represent this limited the physical realism of the model. From the validation and calibrated values of the snowmelt parameters it is obvious that the winter processes were not accurately captured in the model structures. Freshet is a major component of the regime in these basins and not representing the winter processes properly likely led to decreased model performance.

Additionally, there is limited wetland representation algorithms. For example, wetland seepage only has one possible algorithm option. While it does not appear to be a limiting factor in model performance, without other algorithm options to test it can't be concluded that this is the best algorithm to represent seepage. Furthermore, Raven assumes that Lake HRU classes do not have significant groundwater interactions, however, it has been observed in the BPs that lakes can act as "evaporation windows" for groundwater and in some shallow lakes groundwater is a major input (Smerdon et al. 2005). Therefore, the physical representation of the smaller lakes may have been limited.

5.4.7 Applicability of Split Calibration and Model Assumptions

There are some inherent assumptions made during the modelling process that may not be true in the three study basins for the entire modelled period. Two of theses assumptions are that the landuse acquired from the GIS information is constant in the basins and the hydrology in the basin is consistent for the entire modelled period. As demonstrated by the regime curve shift discussed in Section 5.2 these assumptions may not be valid. A greater emphasis on freshet was observed in the validation period and peak precipitation timing shifted, meaning that conditions in the basin, whether due to landuse changes, climate changes, or other factors, occurred between these two periods. Split sampling calibration is a common approach, however, it may not be entirely appropriate in this situation because of these changes. Therefore, the validation used in this thesis may not have been a true indication of model performance. The AWS baseline models were also subject to these regime changes and therefore, the changes cannot completely excuse the overfitting which occurred in the thesis models. However, this regime shift needs to be acknowledged and future work should consider other ways to validate in basins which do not maintain a steady regime.

Chapter 6
Summary & Conclusions

The Boreal Plains (BPs) are characterized by their abundance of wetlands and forestlands underlain by deep soil deposits. In this region in an average year, the AET is greater than precipitation, with the deep soils providing stored water to support this moisture deficit. This unique characteristic combined with the large quantities of water moved by Aspen trees, fill and spill wetland dynamics, and variable hydraulic connectivity make developing hydrologic models in the region very challenging. This is a concern because the BPs are an area of high ecologic sensitivity and are expected to be greatly impacted by climate change. They are also the location of major industrial activity, including the Athabasca Oil Sands (AOS) extraction projects. The projects result in large disturbed areas that are required by the Government of Alberta to be reclaimed to pre-disturbed conditions. However, with the unique hydrology of the region, what this undisturbed condition is is not well understood. Hydrologic models are tools that are used to not only aid in reclamation projects such as those in the AOS but to also inform policy decisions. Thus, there is a need for physically realistic models that can capture the unique hydrology of the region. There have been some attempts to specifically model the BPs. These attempts used fixed modelling approaches and had poor performance in validation, demonstrating the continued need for a better modelling methodology in the region.

There were two primary goals of this thesis: 1) To demonstrate the need for improved modelling methods in the Boreal Plains through a literature review and evaluation of existing models; and 2) To propose and rigorously evaluate modelling methods for hydrologic models developed in typical BPs ecoregion watersheds with limited data availability.

The first goal was met in Chapter 2 which discussed in detail the challenging hydrology of the BPs as well as presenting modelling challenges that would need to be overcome. It also summarized existing standard modelling approaches, with examples which performed poorly in the BPs.

The second goal was achieved in Chapters 4 and 5 where the methodology to generate more physically realistic model structures were presented along with the results. Using a flexible and iterative step-wise modelling approach, three model structures with varying complexity and performance were developed and tested in three study basins.

6.1 Contributions to Literature

This thesis presents two main contributions: 1) the novel approach of using a flexible step-wise modelling approach to develop a model structure, and 2) the development and rigorous testing of physically-based model structures for the BPs region. To the author's knowledge this is the first documented demonstration of using a flexible model approach to develop a model structure from scratch. Literature discussing flexible modelling approaches appears to focus more on the advantages of flexible model structure instead of its application. Additionally, while there have been numerous studies which create model structures, these studies typically introduce one or two new algorithms to a pre-existing fixed model structure. Therefore, the use of a flexible step-wise modelling approach is unique.

The literature review showed why BPs hydrology is challenging for hydrologic models. The annual variability, wetland fill and spill, and changing hydrologic connectivity, are some of the challenges that standard modelling approaches have failed to represent in this region. Additionally, existing models in the BPs which have used standard fixed modelling approaches have demonstrated relatively poor performance. A study by Watson et al (2008) developed a SWAT model in the BPs called the SWATBF model in a well instrumented research basin in the FORWARD project. While the model had very good performance in calibration (daily NSE of 0.81, and monthly NSE of 0.89) there was a significant decrease of 67% in validation, indicating that even though only 15 parameters were calibrated, the model was over fit or not capturing the hydrology of the region. Another model of the BPs was created using the integrated groundwater-surface water model HydroGeoSphere (Hwang et al. 2018). This was a large-scale model with six subbasins for the entire ARB that simulate steady-state long-term surface and groundwater conditions. While the reported R^2 value was 0.96 for the six 40-year average discharge values reported, since the model did not output daily or even monthly discharge values, it is likely to not be useful in informing water management decisions.

The three model structures developed in this thesis were thoroughly and repeatedly evaluated through the use of multiple model diagnostics, multiple hydrologic signatures, and qualitative "reality checks" through *a priori* assumptions informed by research in the BPs. Each model structure was deployed in three study basins and the results were compared to the standard fixed modelling approach of the AWS baseline models. Over the course of this thesis the models were run approximately 2.5 million times. The thesis models saw a sharp decline in performance between calibration and validation, although it was not as large of a decrease that was observed in the

SWATBF model. While the AWS baseline model did not see as sharp of a decline in performance in the validation, the model was not physically realistic and was therefore likely getting the "right" answers for the wrong reasons. Through hydrologic signatures the thesis models showed that they were more physically representative than the standard modelling approach, although there is room for improvement. Ultimately, two of the structures, Model 1 and Model 2, could be recommended as more physically realistic representations of BPs hydrology. More testing with more detailed delineation is required before a decision can be made about the Model 3 structure.

Additionally, as a part of the model development process, two new algorithms were written and added to the Raven modelling framework that allow for explicit representation of Aspen trees, which are significant component of the BPs water balance (Devito et al. 2012). The first algorithm allows Aspen trees to access water in adjacent wetlands via a constant percolation rate. The second algorithm allows for a two-layer evapotranspiration routine. Since Aspen roots can grow very deep this algorithm allows Aspens to access the groundwater for evapotranspiration if the surface soils and wetland transfer cannot meet the water demand.

Different hydrologic models have different purposes, for example, a model focused on flood mitigation would emphasize the peak flows, while a model focused on irrigation demands would focus on low flows. It would therefore be crucial for these models to adequately represent these specific components of the hydrograph. The use of hydrologic signatures as presented in this thesis demonstrates a method that can be used in addition to traditional model diagnostics to aid in verifying whether the specific components of the hydrograph that are important to the goal of the model are adequately being represented. Thus, these signatures can have implications for multiple engineering applications outside of the work completed in this thesis.

6.2 Opportunities for Future BPs Modelling Progress

There are obvious areas where the existing model performance was restricted due to the challenges presented in Section 5.4. One potential solution to the challenge of data availability could be to deploy the current model structures in some of the URSA basins, which are heavily instrumented and well-studied. By using the more detailed URSA data, one could then test the physical realism of the proposed model structures and likely improve the BPs representation. Additionally, detailed elevation data such as LiDAR could be deployed to better delineate basins and wetland types. More detailed elevation data could also allow wetland catchments to be delineated. This could result in more physically realistic proportions of forest runoff reaching the wetlands instead of the arbitrary

proportions used in this thesis. More detailed data could also allow the importance of GIW and their structural representation to be explored. Since the original goal was to create a practical model, the more detailed information would be used to verify and improve the existing structure. It would not be used to apply more complicated algorithms that could not be supported by freely available data.

One source of freely available data that was not explored is the suite of satellite and remote sensing products that are increasingly becoming available. Parameters such as snow cover and LAI could potentially be informed by using this data. Although most of this data is only available in recent years and thus limits its applicability in basins with flow and climate data observation periods ending before the satellite data is available.

Equifinality and properly constraining models is a topic much discussed in literature and there does not appear to be a clear and obvious solution (Beven 2006). However, Shafii and Tolson (2015) introduced an interesting approach. Instead of using hydrologic signatures to evaluate parameter sets after calibration, hydrologic signatures were used to inform the calibration itself. This was done by transforming different hydrologic signatures into fitness metrics that then informed parameter selection during calibration. The study observed improved model performance with this calibration approach and could be used in future work to improve the BPs model structure. This was partially attempted in the refining calibration by calculating an NSE value for the observed discharge regime curve and the separated baseflow hydrograph. However, the result this had on calibration performance was minimal. The Shaffi and Tolson (2015) paper utilized multiple hydrologic signatures in one performance metric which is more stringent than what was applied in the refining calibration here. However, to get these quantitative hydrologic signatures requires abundant and high-quality data which, as discussed previously, is not readily available in the BPs.

As discussed in Chapter 5 there was a change in regime observed between the calibration and validation periods, raising questions about the validity of the split sample approach used to evaluate the models. Future work should take this into consideration and examine alternatives. One such alternative could be similar to the approach presented by Zheng et al. (2018) where the calibration and validation years were selected differently. The years were ranked from wettest to driest and then split into validation and calibration. The wettest year would be in the calibration period and the second wettest year would be in the validation period and so on. This approach was applied to an automated neural network model where having a broken time-series would not present the same problems as it would in a physically-based model, such as those presented in this thesis. However,

since there are long records available, one could test using this division approach but on longer time scales. This approach could also make sure that the splitting resulted in similar regimes between calibration and validation.

One area that was not explored during model development was the lumped HRU approach that was used. It could be tested if having disaggregated HRUs could improve model performance through better routing or timing or if additional subbasins affected model performance. Additional subbasins, and therefore additional HEWs, could test whether spatial distribution of storage is significant in controlling basin behaviour, and thus verify whether the HEW approach is valid or not.

The Raven modelling team is currently developing better winter routines. As discussed in Chapter 5 the winter representation in the model was poor. Future work on BPs representation would likely benefit from these updated winter representations. Additionally, it has been observed at URSA that shallow lakes can have significant groundwater connections (Smerdon et al. 2005). Raven assumes that all lakes do not have such connections, therefore, an area of future work could be to examine whether these connections are important in a BPs hydrologic model.

Another area of increasing research focus is the use of isotopes to verify hydrologic models. By using measured hydrogen and oxygen isotopes one can infer the source of the water reaching the outlet (Stadnyk 2018). This information could then be coupled with the discharge source hydrologic signatures to verify that the right proportions of runoff, quickflow, and deepflow are reaching the outlet which could lead to improved BPs representation.

While not perfect, the model structures presented in this thesis provide insight into how physically representative model structures could be developed in the complicated BPs region. If the areas of suggested work are applied, particularly the improved representation of winter processes, it is likely possible to achieve even better model performance, and thus provide better information to inform water management decisions in the region.

References

Alberta Environment and Sustainable Resource Development (ESRD). 2013. Evaporation and evapotranspiration in Alberta. Alberta Government. Edmonton, AB. ISBN: 978-1-4601-1121-5. http://www.agric.gov.ab.ca/acis/docs/mortons/mortons-evaporation-estimates.pdf

Ali, G., Oswald, C.J., Spence, C., Cammeraat, E.L.H., McGuire, K.J., Meixner, T., and Reaney, S.M. 2013. Towards a unified threshold-based hydrological theory: necessary components and recurring challenges. Hydrological Processes, **27**(2): 313–318. doi:10.1002/hyp.9560.

Asadzadeh, M., and Tolson, B.A. 2009. A new multi-objective algorithm, pareto archived DDS. Proceedings of the 11th annual conference companion on Genetic and evolutionary computation conference - GECCO '09, (January): 1963. doi:10.1145/1570256.1570259.

Balland, V., Bhatti, J., Errington, R., Castonguay, M., and Arp, P.A. 2006. Modeling snowpack and soil temperature and moisture conditions in a jack pine, black spruce and aspen forest stand in central Saskatchewan (BOREAS SSA). Canadian Journal of Soil Science, **86**: 203–217.

Barr, A.G., Black, T.A., Hogg, E.H., Griffis, T.J., Morgenstern, K., Kljun, N., Theede, A., and Nesic, Z. 2007. Climatic controls on the carbon and water balances of a boreal aspen forest, 1994-2003. Global Change Biology, **13**(3): 561–576. doi:10.1111/j.1365-2486.2006.01220.x.

Barr, A.G., van der Kamp, G., Black, T.A., McCaughey, J.H., and Nesic, Z. 2012. Energy balance closure at the BERMS flux towers in relation to the water balance of the White Gull Creek watershed 1999–2009. Agricultural and Forest Meteorology, **153**: 3–13. Elsevier B.V. doi:10.1016/j.agrformet.2011.05.017.

Beven, K. 2006. Searching for the Holy Grail of scientific hydrology : Qt = H(S, R, t)A as closure. Hydrology and Earth System Sciences Discussions, European Geosciences Union, **10**(5): 609–618.

Blöschl, G., and Sivapalan, M. 1995. Scale issues in hydrological modelling: A review. Hydrological Processes, **9**(3–4): 251–290. doi:10.1002/hyp.3360090305.

Bracken, L.J., and Croke, J. 2007. The concept of hydrological connectivity and its contribution to understanding runoff-dominated geomorphic systems. Hydrological Processes, **21**(13): 1749–1763. doi:10.1002/hyp.6313.

Bracken, L.J., Wainwright, J., Ali, G.A., Tetzlaff, D., Smith, M.W., Reaney, S.M., and Roy, A.G. 2013. Concepts of hydrological connectivity: Research approaches, pathways and future

agendas. Earth-Science Reviews, **119**: 17–34. Elsevier B.V. doi:10.1016/j.earscirev.2013.02.001.

Brown, S.M., Petrone, R.M., Chasmer, L., Mendoza, C., Lazerjan, M.S., Landhäusser, S.M., Silins, U., Leach, J., and Devito, K.J. 2014. Atmospheric and soil moisture controls on evapotranspiration from above and within a Western Boreal Plain aspen forest. Hydrological Processes, **28**(15): 4449–4462. doi:10.1002/hyp.9879.

Chasmer, L., Hopkinson, C., Montgomery, J., and Petrone, R. 2016. A physically based terrain morphology and vegetation structural classification for wetlands of the Boreal Plains, Alberta, Canada. Canadian Journal of Remote Sensing, **42**(5): 521–540. doi:10.1080/07038992.2016.1196583.

Chu, X. 2017. Delineation of pothole-dominated wetlands and modeling of their threshold behaviors. Journal of Hydrologic Engineering, **22**(1): 1–11. doi:10.1061/(ASCE)HE.1943-5584.0001224.

Clark, M.P., Bierkens, M.F.P., Samaniego, L., Woods, R.A., Uijlenhoet, R., Bennett, K.E., Pauwels, V.R.N., Cai, X., Wood, A.W., and Peters-Lidard, C.D. 2017. The evolution of process-based hydrologic models: Historical challenges and the collective quest for physical realism. Hydrology and Earth System Sciences, **21**(7): 3427–3440. doi:10.5194/hess-21-3427-2017.

Clark, M.P., McMillan, H.K., Collins, D.B.G., Kavetski, D., and Woods, R.A. 2011. Hydrological field data from a modeller's perspective: Part 2: process-based evaluation of model hypotheses. Hydrological Processes, **25**(4): 523–543. doi:10.1002/hyp.7902.

Dadaser-Celik, F., Stefan, H.G., and Brezonik, P.L. 2006. Dynamic hydrologic model of the Örtülüakar Marsh in Turkey. Wetlands, **26**(4): 1089–1102.

Devito, K., Creed, I., Gan, T., Mendoza, C., Petrone, R., Silins, U., and Smerdon, B. 2005a. A framework for broad-scale classification of hydrologic response units on the Boreal Plain: is topography the last thing to consider? Hydrological Processes, **19**(8): 1705–1714. doi:10.1002/hyp.5881.

Devito, K., Mendoza, C., and Qualizza, C. 2012. Conceptualizing Water Movement in the Boreal Plains Implications for Watershed Reconstruction.

Devito, K.J., Creed, I.F., and Fraser, C.J.D. 2005b. Controls on runoff from a partially harvested aspen-forested headwater catchment, Boreal Plain, Canada. Hydrological Processes, **19**(1): 3–25. doi:10.1002/hyp.5776.

Devito, K.J., Mendoza, C., Petrone, R.M., Kettridge, N., and Waddington, J.M. 2016. Utikuma Region Study Area (URSA) – Part 1: Hydrogeological and ecohydrological studies (HEAD). The Forestry Chronicle, **92**(1): 57–61. doi:10.5558/tfc2016-017.

Donnelly, M., Devito, K.J., Mendoza, C., Petrone, R., and Spafford, M. 2016. Al-Pac Catchment Experiment (ACE). The Forestry Chronicle, **92**(1): 23–26.

van Esse, W.R., Perrin, C., Booij, M.J., Augustijn, D.C.M., Fenicia, F., Kavetski, D., and Lobligeois, F. 2013. The influence of conceptual model structure on model performance: a comparative study for 237 French catchments. Hydrology and Earth System Sciences, **17**(10): 4227–4239. doi:10.5194/hess-17-4227-2013.

Euser, T., Winsemius, H.C., Hrachowitz, M., Fenicia, F., Uhlenbrook, S., and Savenije, H.H.G. 2013. A framework to assess the realism of model structures using hydrological signatures. Hydrology and Earth System Sciences, **17**(5): 1893–1912. doi:10.5194/hess-17-1893-2013.

Evenson, G.R., Golden, H.E., Lane, C.R., and D'Amico, E. 2016. An improved representation of geographically isolated wetlands in a watershed-scale hydrologic model. Hydrological Processes, **30**(22): 4168–4184. doi:10.1002/hyp.10930.

Faramarzi, M., Srinivasan, R., Iravani, M., Bladon, K.D., Abbaspour, K.C., Zehnder, A.J.B., and Goss, G.G. 2015. Setting up a hydrological model of Alberta: Data discrimination analyses prior to calibration. Environmental Modelling & Software, **74**: 48–65. Elsevier Ltd. doi:10.1016/j.envsoft.2015.09.006.

Fenicia, F., Kavetski, D., and Savenije, H.H.G. 2011. Elements of a flexible approach for conceptual hydrological modeling: 1. Motivation and theoretical development. Water Resources Research, **47**(11): 1–13. doi:10.1029/2010WR010174.

Fenicia, F., Savenije, H.H.G., Matgen, P., and Pfister, L. 2008. Understanding catchment behavior through stepwise model concept improvement. Water Resources Research, **44**(1): 1–13. doi:10.1029/2006WR005563.

Ferone, J.M., and Devito, K.J. 2004. Shallow groundwater–surface water interactions in pond–peatland complexes along a Boreal Plains topographic gradient. Journal of Hydrology, **292**(1–4): 75–95. doi:10.1016/j.jhydrol.2003.12.032.

Fossey, M., Rousseau, A.N., Bensalma, F., Savary, S., and Royer, A. 2015. Integrating isolated and riparian wetland modules in the PHYSITEL/HYDROTEL modelling platform: model

performance and diagnosis. Hydrological Processes, **29**(22): 4683–4702. doi:10.1002/hyp.10534.

Freeze, R.A. 1972. Role of Subsurface Flow in Generating Surface Runoff 2. Upstream Source Areas. Water Resources Research, **8**(5): 1272–1283.

Gao, H., Hrachowitz, M., Schymanski, S.J., Fenicia, F., Sriwongsitanon, N., and Savenije, H.H.G. 2014. Climate controls how ecosystems size the root zone storage capacity at catchment scale. Geophysical Research Letters, **41**(22): 7916–7923. doi:10.1002/2014GL061668.

Gassman, P.W., Reyes, M.R., Green, C.H., and Arnold, J.G. 2007. The Soil and Water Assessment Tool : historical development, applications, and future research directions. *In* Transactions of the ASAE. doi:10.1.1.88.6554.

Gibson, J.J., Birks, S.J., Yi, Y., and Vitt, D.. 2015. Runoff to boreal lakes linked to land cover, watershed morphology and permafrost thaw: A 9-year isotope mass balance assessment. Hydrological Processes, **29**(18): 3848–3861. doi:10.1002/hyp.10502.

Gibson, J.J., Prepas, E.E., and McEachern, P. 2002. Quantitative comparison of lake throughflow, residency, and catchment runoff using stable isotopes: modelling and results from a regional survey of Boreal lakes. Journal of Hydrology, **262**: 128–144.

Golden, H.E., Creed, I.F., Ali, G., Basu, N.B., Neff, B.P., Rains, M.C., McLaughlin, D.L., Alexander, L.C., Ameli, A.A., Christensen, J.R., Evenson, G.R., Jones, C.N., Lane, C.R., and Lang, M. 2017. Integrating geographically isolated wetlands into land management decisions. Frontiers in Ecology and the Environment, **15**(6): 319–327. doi:10.1002/fee.1504.

Golden, H.E., Lane, C.R., Amatya, D.M., Bandilla, K.W., Raanan Kiperwas, H., Knightes, C.D., and Ssegane, H. 2014. Hydrologic connectivity between geographically isolated wetlands and surface water systems: A review of select modeling methods. Environmental Modelling & Software, **53**: 190–206. Elsevier Ltd. doi:10.1016/j.envsoft.2013.12.004.

Golden, H.E., Sander, H.A., Lane, C.R., Zhao, C., Price, K., D'Amico, E., and Christensen, J.R. 2016. Relative effects of geographically isolated wetlands on streamflow: a watershed-scale analysis. Ecohydrology, **9**(1): 21–38. doi:10.1002/eco.1608.

Granger, R.J., and Pomeroy, J.W. 1997. Sustainability of the western Canadian boreal forest under changing hydrological conditions. II. Summer energy and water use. *In* Sustainability of Water Resouces under Increasing Uncertainty (Proceedings of the Rabat Symposium S1). IAHS. pp.

243–249.

Gupta, H. V., Kling, H., Yilmaz, K.K., and Martinez, G.F. 2009. Decomposition of the mean squared error and NSE performance criteria: Implications for improving hydrological modelling. Journal of Hydrology, **377**(1–2): 80–91. Elsevier B.V. doi:10.1016/j.jhydrol.2009.08.003.

Harms, T.E., and Chanasyk, D.S. 1998. Variability of snowmelt runoff and soil moisture recharge. Nordic Hydrology, **29**: 179–198.

Hartmann, A. 2016. Putting the cat in the box: why our models should consider subsurface heterogeneity at all scales. WIREs Water, **3**(August): 478–486. doi:10.1002/wat2.1146.

Hillman, G., and Rothwell, R. 2016. Spring Creek representative and experimental watershed project. The Forestry Chronicle, **92**(1): 43–46.

Hogg, E.H., and Hurdle, P.A. 1995. The aspen parkland in western Canada: A dry-climate analogue for the future boreal forest? Water, Air, & Soil Pollution, **82**(1–2): 391–400. doi:10.1007/BF01182849.

Hrachowitz, M., Fovet, O., Ruiz, L., Euser, T., Gharari, S., Nijzink, R., Freer, J., Savenije, H.H.G., and Gascuel-Odoux, C. 2014. Process consistency in models: The importance of system signatures, expert knowledge, and process complexity. Water Resources Research, **50**(9): 7445–7469. doi:10.1002/2014WR015484.

Huang, S., Young, C., Abdul-Aziz, O.I., Dahal, D., Feng, M., and Liu, S. 2013. Simulating the water budget of a Prairie Potholes complex from LiDAR and hydrological models in North Dakota, USA. Hydrological Sciences Journal, **58**(7): 1434–1444. Taylor & Francis. doi:10.1080/02626667.2013.831419.

Hvenegaard, G., Carr, S., Clark, K., Dunn, P., and Olexson, T. 2015. Promoting sustainable forest management among stakeholders in the Prince Albert Model Forest, Canada. Conservation and Society, **13**(1): 51–61. doi:10.4103/0972-4923.161222.

Hwang, H.-T., Park, Y.-J., Sudicky, E.A., Berg, S.J., McLaughlin, R., and Jones, J.P. 2018. Understanding the water balance paradox in the Athabasca River Basin, Canada. Hydrological Processes, **32**(6): 729–746. doi:10.1002/hyp.11449.

Ireson, A.M., Barr, A.G., Johnstone, J.F., Mamet, S.D., van der Kamp, G., Whitfield, C.J., Michel, N.L., North, R.L., Westbrook, C.J., DeBeer, C., Chun, K.P., Nazemi, A., and Sagin, J. 2015. The changing water cycle: the Boreal Plains ecozone of Western Canada. Wiley

Interdisciplinary Reviews: Water, **2**(5): 505–521. doi:10.1002/wat2.1098.

Jepsen, S.M., Walvoord, M.A., Voss, C.I., and Rover, J. 2016. Effect of permafrost thaw on the dynamics of lakes recharged by ice-jam floods: case study of Yukon Flats, Alaska. Hydrological Processes, **30**(11): 1782–1795. doi:10.1002/hyp.10756.

Johnson, E.A., and Miyanishi, K. 2008. Creating new landscapes and ecosystems. The Albera Oil Sands. Annals of the New York Academy of Sciences, **1134**(1): 120–145. doi:10.1196/annals.1439.007.

Kampf, S.K., and Burges, S.J. 2007. A framework for classifying and comparing distributed hillslope and catchment hydrologic models. Water Resources Research, **43**(5). doi:10.1029/2006WR005370.

Kerkhoven, E., and Gan, T.Y. 2006. A modified ISBA surface scheme for modeling the hydrology of Athabasca River Basin with GCM-scale data. Advances in Water Resources, **29**(6): 808–826. doi:10.1016/j.advwatres.2005.07.016.

Ketcheson, S.J., Price, J.S., Carey, S.K., Petrone, R.M., Mendoza, C.A., and Devito, K.J. 2016. Constructing fen peatlands in post-mining oil sands landscapes: Challenges and opportunities from a hydrological perspective. Earth-Science Reviews, **161**: 130–139. Elsevier B.V. doi:10.1016/j.earscirev.2016.08.007.

Kirchner, J.W. 2006. Getting the right answers for the right reasons: Linking measurements, analyses, and models to advance the science of hydrology. Water Resources Research, **42**(3): 1–5. doi:10.1029/2005WR004362.

KlemeŠ, V. 1986. Operational testing of hydrological simulation models. Hydrological Sciences Journal, **31**(1): 13–24. doi:10.1080/02626668609491024.

Lehmann, P., Hinz, C., McGrath, G., Tromp-van Meerveld, H.J., and McDonnell, J.J. 2006. Rainfall threshold for hillslope outflow: an emergent property of flow pathway connectivity. Hydrology and Earth System Sciences Discussions, **3**(5): 2923–2961. doi:10.5194/hessd-3-2923-2006.

Leibowitz, S.G., Mushet, D.M., and Newton, W.E. 2016. Intermittent surface water connectivity: fill and spill vs. fill and merge dynamics. Wetlands, **36**(S2): 323–342. Wetlands. doi:10.1007/s13157-016-0830-z.

Liu, G., Schwartz, F.W., Wright, C.K., and McIntyre, N.E. 2016. Characterizing the climate-driven collapses and expansions of wetland habitats with a fully integrated surface–subsurface

hydrologic model. Wetlands, **36**(S2): 287–297. Wetlands. doi:10.1007/s13157-016-0817-9.

El Maayar, M., and Chen, J.M. 2006. Spatial scaling of evapotranspiration as affected by heterogeneities in vegetation, topography, and soil texture. Remote Sensing of Environment, **102**(1–2): 33–51. doi:10.1016/j.rse.2006.01.017.

McDonnell, J.J., Sivapalan, M., Vaché, K., Dunn, S., Grant, G., Haggerty, R., Hinz, C., Hooper, R., Kirchner, J., Roderick, M.L., Selker, J., and Weiler, M. 2007. Moving beyond heterogeneity and process complexity: A new vision for watershed hydrology. Water Resources Research, **43**(7): 1–6. doi:10.1029/2006WR005467.

McEachern, P. 2016. Forest Watershed and Riparian Disturbance Project (FORWARD). The Forestry Chronicle, **92**(1): 29–31.

McMillan, H., Gueguen, M., Grimon, E., Woods, R., Clark, M., and Rupp, D.E. 2014. Spatial variability of hydrological processes and model structure diagnostics in a 50 km2 catchment. Hydrological Processes, **28**(18): 4896–4913. doi:10.1002/hyp.9988.

Mekonnen, B.A., Nazemi, A., Mazurek, K.A., Elshorbagy, A., and Putz, G. 2015. Hybrid modelling approach to prairie hydrology: fusing data-driven and process-based hydrological models. Hydrological Sciences Journal, **60**(9): 1473–1489. Taylor & Francis. doi:10.1080/02626667.2014.935778.

Michaelian, M., Hogg, E.H., Hall, R.J., and Arsenault, E. 2011. Massive mortality of aspen following severe drought along the southern edge of the Canadian boreal forest. Global Change Biology, **17**(6): 2084–2094. doi:10.1111/j.1365-2486.2010.02357.x.

Neff, B.P., and Rosenberry, D.O. 2018. Groundwater connectivity of upland-embedded wetlands in the prairie pothole region. Wetlands, **38**(1): 51–63. Wetlands. doi:10.1007/s13157-017-0956-7.

Nicholls, E.M., Carey, S.K., Humphreys, E.R., Clark, M.G., and Drewitt, G.B. 2016. Multi-year water balance assessment of a newly constructed wetland, Fort McMurray, Alberta. Hydrological Processes, **30**(16): 2739–2753. doi:10.1002/hyp.10881.

Nijssen, B., and Lettenmaier, D.P. 2002. Water balance dynamics of a boreal forest watershed: White Gull Creek basin, 1994-1996. Water Resources Research, **38**(11): 1–12. doi:10.1029/2001WR000699.

Office of Research and Development, U.S.E.P.A. (USEPA). 2015. Connectivity of Streams & Wetlands to Downstream Waters: A Review & Synthesis of the Scientific Evidence (Final

Report). *In* EPA/600/R-14/475F. *Edited By*Intergovernmental Panel on Climate Change. Cambridge University Press, Cambridge. doi:10.1017/CBO9781107415324.004.

Paniconi, C., and Putti, M. 2015. Physically based modeling in catchment hydrology at 50: Survey and outlook. Water Resources Research, **51**(9): 7090–7129. doi:10.1002/2015WR017780.

Park, J., Botter, G., Jawitz, J.W., and Rao, P.S.C. 2014. Stochastic modeling of hydrologic variability of geographically isolated wetlands: Effects of hydro-climatic forcing and wetland bathymetry. Advances in Water Resources, **69**: 38–48. Elsevier Ltd. doi:10.1016/j.advwatres.2014.03.007.

Petrone, R., Devito, K.J., and Mendoza, C. 2016. Utikuma Region Study Area (URSA) - Part 2: Aspen harvest and recovery study. The Forestry Chronicle, **92**(1): 62–65. doi:10.5558/tfc2016-018.

Petrone, R.M., Silins, U., and Devito, K.J. 2007. Dynamics of evapotranspiration from a riparian pond complex in the Western Boreal Forest, Alberta, Canada. Hydrological Processes, **21**(11): 1391–1401. doi:10.1002/hyp.6298.

Pomeroy, J.W., and Granger, R.J. 1997. Sustainability of the western Canadian boreal forest under changing hydrological conditions. I. Snow accumulation and ablation. *In* Sustainability of Water Resouces under Increasing Uncertainty (Proceedings of the Rabat Symposium S1, April 1997). IAHS. pp. 237–242.

Prepas, E.E., Burke, J.M., Whitson, I.R., Putz, G., and Smith, D.W. 2006. Associations between watershed characteristics, runoff, and stream water quality: hypothesis development for watershed disturbance experiments and modelling in the Forest Watershed and Riparian Disturbance (FORWARD) project. Journal of Environmental Engineering and Science, **5**(Supplement 1): S27–S37. doi:10.1139/s05-033.

Price, D.T., Alfaro, R.I., Brown, K.J., Flannigan, M.D., Fleming, R.A., Hogg, E.H., Girardin, M.P., Lakusta, T., Johnston, M., Mckenney, D.W., Pedlar, J.H., Stratton, T., Sturrock, R.N., Thompson, I.D., Trofymow, J.A., and Venier, L.A. 2013. Anticipating the consequences of climate change for Canada's boreal forest ecosystems. Environmental Reviews, **21**: 322–365. doi:dx.doi.org/10.1139/er-2013-0042.

Price, J.S., Branfireun, B.A., Michael Waddington, J., and Devito, K.J. 2005. Advances in Canadian wetland hydrology, 1999-2003. Hydrological Processes, **19**(1): 201–214. doi:10.1002/hyp.5774.

Quinn, N.W.T., Heinzer, T.J., and Diane Williams, M. 2012. Breathing new life into legacy

integrated surface groundwater models using gisbased adaptive mesh, hydrology refinement and data mapping tools. *In* International Environmental Modelling and Software Society (iEMSs) 2012 International Congress on Environmental Modelling and Software Managing Resources of a Limited Planet, Sixth Biennial Meeting. *Edited by* R. Seppelt, A.. Voinov, S. Lange, and D. Bankamp. Leipzig, Germany. pp. 1391–1398. Available from http://www.scopus.com/inward/record.url?eid=2-s2.0-84894112559&partnerID=tZOtx3y1.

Redding, T., and Devito, K. 2010. Mechanisms and pathways of lateral flow on aspen-forested, Luvisolic soils, Western Boreal Plains, Alberta, Canada. Hydrological Processes, **24**(21): 2995–3010. doi:10.1002/hyp.7710.

Redding, T., and Devito, K. 2011. Aspect and soil textural controls on snowmelt runoff on forested Boreal Plain hillslopes. Hydrology Research, **42**(4): 250. doi:10.2166/nh.2011.162.

Redding, T.E., and Devito, K.J. 2008. Lateral flow thresholds for aspen forested hillslopes on the Western Boreal Plain, Alberta, Canada. Hydrological Processes, **22**(21): 4287–4300. doi:10.1002/hyp.7038.

Rowe, J.S., and Coupland, R.T. 1984. Geological history of the Interior Plains. Prairie Forum: Journal of the Canadian Plains Research Center, **9**(2): 231–248.

Shaw, D.A., Martz, L.W., and Pietroniro, A. 2005. A methodology for preserving channel flow networks and connectivity patterns in large-scale distributed hydrological models. Hydrological Processes, **19**(1): 149–168. doi:10.1002/hyp.5765.

Shaw, D.A., Vanderkamp, G., Conly, F.M., Pietroniro, A., and Martz, L. 2012. The fill-spill hydrology of prairie wetland complexes during drought and deluge. Hydrological Processes, **26**(20): 3147–3156. doi:10.1002/hyp.8390.

Shook, K., Pomeroy, J.W., Spence, C., and Boychuk, L. 2013. Storage dynamics simulations in prairie wetland hydrology models: evaluation and parameterization. Hydrological Processes, **27**(13): 1875–1889. doi:10.1002/hyp.9867.

Shrestha, N.K., and Wang, J. 2018a. Predicting sediment yield and transport dynamics of a cold climate region watershed in changing climate. Science of The Total Environment, **625**: 1030–1045. Elsevier B.V. doi:10.1016/j.scitotenv.2017.12.347.

Shrestha, N.K., and Wang, J. 2018b. Current and future hot-spots and hot-moments of nitrous oxide emission in a cold climate river basin. Environmental Pollution, **239**: 648–660. Elsevier Ltd.

doi:10.1016/j.envpol.2018.04.068.

Singh, V.P., and Woolhiser, D.A. 2002. Mathematical modeling of watershed hydrology. Journal of Hydrologic Engineering, **7**(4): 270–292. doi:10.1061/(ASCE)1084-0699(2002)7:4(270).

Smerdon, B.D., Devito, K.J., and Mendoza, C.A. 2005. Interaction of groundwater and shallow lakes on outwash sediments in the sub-humid Boreal Plains of Canada. Journal of Hydrology, **314**(1–4): 246–262. doi:10.1016/j.jhydrol.2005.04.001.

Smerdon, B.D., Mendoza, C.A., and Devito, K.J. 2007. Simulations of fully coupled lake-groundwater exchange in a subhumid climate with an integrated hydrologic model. Water Resources Research, **43**(1): 1–13. doi:10.1029/2006WR005137.

Smerdon, B.D., Mendoza, C.A., and Devito, K.J. 2008. Influence of subhumid climate and water table depth on groundwater recharge in shallow outwash aquifers. Water Resources Research, **44**(8): 1–15. doi:10.1029/2007WR005950.

Spence, C. 2010. A paradigm shift in hydrology: storage thresholds across scales influence catchment runoff generation. Geography Compass, **4**(7): 819–833. doi:10.1111/j.1749-8198.2010.00341.x.

Spence, C., Guan, X.J., Phillips, R., Hedstrom, N., Granger, R., and Reid, B. 2009. Storage dynamics and streamflow in a catchment with a variable contributing area. Hydrological Processes, **24**(16): 2209–2221. doi:10.1002/hyp.7492.

Spence, C., and Phillips, R.W. 2015. Refining understanding of hydrological connectivity in a boreal catchment. Hydrological Processes, **29**(16): 3491–3503. doi:10.1002/hyp.10270.

Spence, C., and Woo, M. 2002. Hydrology of subarctic Canadian shield: bedrock upland. Journal of Hydrology, **262**(1–4): 111–127. doi:10.1016/S0022-1694(02)00010-0.

Spence, C., and Woo, M. 2003. Hydrology of subarctic Canadian shield: soil-filled valleys. Journal of Hydrology, **279**(1–4): 151–166. doi:10.1016/S0022-1694(03)00175-6.

Spence, C., and Woo, M. 2006. Hydrology of subarctic Canadian Shield: heterogeneous headwater basins. Journal of Hydrology, **317**(1–2): 138–154. doi:10.1016/j.jhydrol.2005.05.014.

Spencer, S.A., Anderson, A., and Bladon, K.D. 2016. Long-term watershed research in Alberta. The Forestry Chronicle, **92**(1): 3–5.

Thompson, C., Mendoza, C.A., Devito, K.J., and Petrone, R.M. 2015. Climatic controls on groundwater–surface water interactions within the Boreal Plains of Alberta: Field observations

and numerical simulations. Journal of Hydrology, **527**: 734–746. Elsevier B.V. doi:10.1016/j.jhydrol.2015.05.027.

Tolson, B.A., and Shoemaker, C.A. 2007. Dynamically dimensioned search algorithm for computationally efficient watershed model calibration. Water Resources Research, **43**(1): 1–16. doi:10.1029/2005WR004723.

Toth, B., Pietroniro, A., Conly, F.M., and Kouwen, N. 2006. Modelling climate change impacts in the Peace and Athabasca catchment and delta: I—hydrological model application. Hydrological Processes, **20**(19): 4197–4214. doi:10.1002/hyp.6426.

Vereecken, H., Huisman, J.A., Hendricks Franssen, H.J., Brüggemann, N., Bogena, H.R., Kollet, S., Javaux, M., van der Kruk, J., and Vanderborght, J. 2015. Soil hydrology: Recent methodological advances, challenges, and perspectives. Water Resources Research, **51**(4): 2616–2633. doi:10.1002/2014WR016852.

Wang, X., Yang, W., and Melesse, A.M. 2008. Using Hydrologic Equivlent Wetland concept within SWAT to estimate streamflow in watersheds with numerous wetlands. American Society of Agricultural and Biological Engineers, **51**(1): 55–72. Available from http://jamsb.austms.org.au/courses/CSC2408/semester3/resources/ldp/abs-guide.pdf.

Watson, B.M., McKeown, R.A., Putz, G., and MacDonald, J.D. 2008. Modification of SWAT for modelling streamflow from forested watersheds on the Canadian Boreal Plain. Journal of Environmental Engineering and Science, **7**(Supplement 1): 145–159. doi:10.1139/S09-003.

Westerberg, I.K., and McMillan, H.K. 2015. Uncertainty in hydrological signatures. Hydrology and Earth System Sciences, **19**(9): 3951–3968. doi:10.5194/hess-19-3951-2015.

Whitson, I.R., Chanasyk, D.S., and Prepas, E.E. 2004. Patterns of water movement on a logged Gray Luvisolic hillslope during the snowmelt period. Canadian Journal of Soil Science, **84**(1): 71–82. doi:10.4141/S02-081.

Winter, T.C., Rosenberry, D.O., and LaBaugh, J.W. 2003. Where Does the Ground Water in Small Watersheds Come From? Ground Water, **41**(7): 989–1000.

Zha, T., Barr, A.G., van der Kamp, G., Black, T.A., McCaughey, J.H., and Flanagan, L.B. 2010. Interannual variation of evapotranspiration from forest and grassland ecosystems in western canada in relation to drought. Agricultural and Forest Meteorology, **150**(11): 1476–1484. Elsevier B.V. doi:10.1016/j.agrformet.2010.08.003.

Zhang, K., Kimball, J.S., Mu, Q., Jones, L.A., Goetz, S.J., and Running, S.W. 2009. Satellite based analysis of northern ET trends and associated changes in the regional water balance from 1983 to 2005. Journal of Hydrology, **379**(1–2): 92–110. Elsevier B.V. doi:10.1016/j.jhydrol.2009.09.047.

Zhang, Y., Miao, Z., Bognar, J., and Lathrop, R.G. 2011. Landscape scale modeling of the potential effect of groundwater-level declines on forested wetlands in the New Jersey Pinelands. Wetlands, **31**(6): 1131–1142. doi:10.1007/s13157-011-0223-2.

Zheng, F., Maier, H.R., Wu, W., Dandy, G.C., Gupta, H. V., and Zhang, T. 2018. On lack of robustness in hydrological model development due to absence of guidelines for selecting calibration and evaluation data: Demonstration for data-driven models. Water Resources Research, **54**(2): 1013–1030. doi:10.1002/2017WR021470.

Appendix A
Model 1 Input Files

The Raven input files for the Model 1 structure as summarized here for the House River basin. Note that other than parameterization and discretization the model input files are identical between study basins. The .rvt (time series) files have not been included here since they just call to the time series data and do not inform about model structure. The .rvi (input file) is summarized in **Table A.1** without the custom output commands.

Table A.1: Model 1 .rvi File

Simulation Parameters

Start Date	1982-05-24
Duration	10722
TimeStep	24:00:00

Model Options

Method	ORDERED_SERIES
Interpolated	INTERP_INVERSE_DISTANCE
Catchment Route	TRIANGULAR_UH
Routing	ROUTE_DIFFUSIVE_WAVE
SWRadiationMethod	SW_RAD_DEFAULT
LWRadiationMethod	LW_RAD_DEFAULT
SWCloudCorrect	SW_CLOUD_CORR_DINGMAN
Evaporation	PET_TURC_1961
OW_Evaporation	PET_HARGREAVES_1985
RelativeHumidityMethod	RELHUM_MINDEWPT
PotentialMeltMethod	POTMELT_HBV
RainSnowFraction	RAINSNOW_HBV
OroTempCorrect	OROCORR_HBV
OroPrecipCorrect	OROCORR_SIMPLELAPSE
PrecipIceptFract	PRECIP_ICEPT_USER
Soil Model	SOIL_MULTILAYER 3

Hydrologic Processes

Process	Algorithm	From Compartment	To Compartment	Conditional Statements
Precipitation	PRECIP RAVEN	ATMOS_PRECIP	MULTIPLE	
Canopy Evaporation	CANEVP MAXIMUM	CANOPY	ATMOSPHERE	
Canopy Snow Evaporation	CANEVP MAXIMUM	CANOPY_SNOW	ATMOSPHERE	
Open Water Evaporation	OPEN WATER EVAP	DEPRESSION	ATMOSPHERE	
Lake Evaporation	LAKE EVAP BASIC	SURFACE_WATER	ATMOSPHERE	
Snow Balance	SNOBAL TWO LAYER	SNOW	PONDED_WATER	
Snow Balance -->Overflow	RAVEN DEFAULT	SNOW_LIQ	PONDED_WATER	
Flush	RAVEN DEFAULT	PONDED_WATER	DEPRESSION	HRU_TYPE IS WETLAND
Seepage	SEEP LINEAR	DEPRESSION	SOIL[1]	
Infiltration	INF HBV	PONDED_WATER	SOIL[0]	
Flush	RAVEN DEFAULT	SURFACE_WATER	PONDED_WATER	HRU_GROUP IS DrainToWetlands
Soil Evaporation	SOILEVAP HBV	SOIL[0]	ATMOSPHERE	
Depression Overflow	DFLOW THRESHPOW	DEPRESSION	SURFACE_WATER	
Baseflow	BASE POWER LAW	SOIL[1]	SURFACE_WATER	
Baseflow	BASE_VIC	SOIL[2]	SURFACE_WATER	
Percolation	PERC CONSTANT	SOIL[0]	SOIL[1]	
Percolation	PERC CONSTANT	SOIL[1]	SOIL[2]	
Lateral Flush	RAVEN DEFAULT	DrainToWetlands PONDED_WATER	WETLANDS DEPRESSION	

Table A.2 summarizes the .rvh (model discretization file) for Model 1.

Table A.2: Model 1 .rvh file

Subbasins

SUB ID	NAME	DOWNSTREAM ID	PROFILE	REACH LENGTH (km)	Gauged	TIME CONC (Days)
1	Sub4	2	07CB002	40	0	0.149
2	Sub3	4	07CB002	50	0	0.176
3	Sub2	4	07CB002	22	0	0.150
4	House River	-1	07CB002	30	1	0.151

HRUs

ID	AREA (km2)	ELEV (m)	LAT	LONG	BASIN ID	LAND USE CLASS	VEG CLASS	SOIL PROFILE	SLOPE (deg)	ASPECT (deg)
101	6.744	687.773	55.94	-111.95	1	LAKE	LAKE	LAKE	0.238	319.601
102	0.755	694.514	55.94	-111.95	1	GRASSLAND	GRASSLAND_VEG	GRASSLAND_SOIL	0.244	306.427
103	94.058	697.01	55.94	-111.95	1	WETLAND	WETLAND_VEG	WETLAND_SOIL	0.454	275.295
104	65.449	698.063	55.94	-111.95	1	CONIFEROUS	CONIFEROUS_VEG	CONIFEROUS_SOIL	0.504	267.461
105	0.539	690.485	55.94	-111.95	1	DECIDUOUS	DECIDUOUS_VEG	DECIDUOUS_SOIL	0.353	272.481
201	11.062	675.664	55.80	-111.93	2	LAKE	LAKE	LAKE	0.314	310.933
202	0.114	668.097	55.80	-111.93	2	BARE	BARE_VEG	BARE_SOIL	0.838	245.455
203	0.293	678.734	55.80	-111.93	2	GRASSLAND	GRASSLAND_VEG	GRASSLAND_SOIL	0.25	132.795
204	106.168	678.85	55.80	-111.93	2	WETLAND	WETLAND_VEG	WETLAND_SOIL	0.348	290.5
205	134.585	681.099	55.80	-111.93	2	CONIFEROUS	CONIFEROUS_VEG	CONIFEROUS_SOIL	0.485	271.991
206	9.838	682.131	55.80	-111.93	2	DECIDUOUS	DECIDUOUS_VEG	DECIDUOUS_SOIL	0.594	264.801

HRUs

ID	AREA (km2)	ELEV (m)	LAT	LONG	BASIN ID	LAND USE CLASS	VEG CLASS	SOIL PROFILE	SLOPE (deg)	ASPECT (deg)
301	1.64	678.542	55.54	-111.73	3	LAKE	LAKE	LAKE	1.232	277.661
302	2.33	707.268	55.54	-111.73	3	BARE	BARE_VEG	BARE_SOIL	1.362	258.961
303	16.862	715.912	55.54	-111.73	3	GRASSLAND	GRASSLAND_VEG	GRASSLAND_SOIL	1.684	247.556
304	30.128	715.39	55.54	-111.73	3	WETLAND	WETLAND_VEG	WETLAND_SOIL	1.276	223.55
305	114.188	711.639	55.54	-111.73	3	CONIFEROUS	CONIFEROUS_VEG	CONIFEROUS_SOIL	2.173	240.528
306	5.433	725.926	55.54	-111.73	3	DECIDUOUS	DECIDUOUS_VEG	DECIDUOUS_SOIL	2.121	191.413
401	1.507	677.701	55.66	-112.04	4	LAKE	LAKE	LAKE	0.3	299.47
402	0.208	677.648	55.66	-112.04	4	BARE	BARE_VEG	BARE_SOIL	0.219	324.332
403	0.266	679.074	55.66	-112.04	4	GRASSLAND	GRASSLAND_VEG	GRASSLAND_SOIL	0.28	315.41
404	18.886	677.48	55.66	-112.04	4	WETLAND	WETLAND_VEG	WETLAND_SOIL	0.946	229.549
405	147.676	685.062	55.66	-112.04	4	CONIFEROUS	CONIFEROUS_VEG	CONIFEROUS_SOIL	1.172	228.577
406	5.757	685.631	55.66	-112.04	4	DECIDUOUS	DECIDUOUS_VEG	DECIDUOUS_SOIL	1.118	253.955

HRU Groups

DrainToWetlands	104,105,205,206,305,306,405,406
WETLANDS	103,204,304,404
FORESTLANDS	104,105,205,206,305,306,405,406
GRASSLANDS	102,203,303,403
LAKES	101,201,301,401
DECID_FORR	105,206,306,406
CONIF_FORR	104,205,305,405

Table A.3 summarizes the Model 1 .rvc (initial conditions) file in the House River basin.

Table A. 3: Model 1 .rvc file.

Basin Initial Conditions

ID	Q (m3/s)
1	1
2	1
3	1
4	2.8

Table A.4 summarizes the Model 2 .rvp (parameter file) in the House River basin.

Table A.4: Model 1 .rvp file.

Global Parameters

AdiabaticLapseRate	6.5
PrecipitationLapseRate	0.5
RainSnowTransition	0.27, 2
IrreducibleSnowSaturation	0.05
AvgAnnualRunoff	106
GlobalParameter MAX_SWE_SURFACE	49.97

Soil Properties

SoilClasses

Attributes	%SAND	%CLAY	%SILT	%ORGANIC
Units	none	none	none	none
TOP_WETLAND	0.25	0.08	0.67	0.7
INT_WETLAND	0.25	0.08	0.67	0.2
DEEP_WETLAND	0.25	0.08	0.67	0.2
TOP_FOREST	0.6	0.2	0.2	0.25
INT_FOREST	0.6	0.2	0.2	0.15
DEEP_FOREST	0.6	0.2	0.2	0.15

SoilParameterList

Parameters	Porosity	HBV Beta	Max Perc Rate	Baseflow Coeff	Baseflow N	Max Baseflow Coeff	Field Capacity
Units	none	none	mm/d	1/d	none	mm	none
TOP WETLAND	0.4	1	0.0287	NA	NA	NA	0.17
INT WETLAND	0.3	NA	0.015	0.102	1.22	NA	0.188
DEEP WETLAND	0.3	NA	NA	NA	1.94	0.124	0.188
TOP FOREST	0.4	0.503	0.08	NA	NA	NA	0.33
INT FOREST	0.3	NA	1.75	0.87	1	NA	0.172
DEEP FOREST	0.3	NA	NA	NA	0.534	6.49	0.172

SoilProfiles

	# of Layers	Soil 0		Soil 1		Soil 2	
LAKE	0						
BARE SOIL	3	TOP_FOREST	0.4	INT_FOREST	0.5	DEEP_FOREST	8
DECIDUOUS SOIL	3	TOP_FOREST	0.4	INT_FOREST	0.5	DEEP_FOREST	8
WETLAND SOIL	3	TOP_WETLAND	0.73	INT_WETLAND	1.3	DEEP_WETLAND	8
GRASSLAND SOIL	3	TOP_WETLAND	0.73	INT_WETLAND	1.3	DEEP_WETLAND	8
CONIFEROUS SOIL	3	TOP_FOREST	0.4	INT_FOREST	0.5	DEEP_FOREST	8

Vegetation Properties

VegetationClasses

Attributes	MAX_LAI
Units	none
LAKE	0
BARE_VEG	0
DECIDUOUS_VEG	6
WETLAND_VEG	5.2
GRASSLAND_VEG	4.5
CONIFEROUS_VEG	6.2

VegetationParameterList

Parameters	RAIN_ICEPT_PCT	SNOW_ICEPT_PCT
Units	-	-
LAKE	0	0
BARE_VEG	0	0
DECIDUOUS_VEG	0.12	0.05
WETLAND_VEG	0	0
GRASSLAND_VEG	0	0
CONIFEROUS_VEG	0.1	0.2

Landuse Properties

LandUseClasses

Attributes	IMPERM	FOREST_COV
Units	frac	frac
LAKE	1	0
BARE	0.6	0.05
DECIDUOUS	0	1
WETLAND	0	0.05
GRASSLAND	0	0
CONIFEROUS	0	1

LandUseParameterList

Parameters	MELT FACTOR	MIN MELT FACTOR	HBV MELT FOR CORR	REFREEZE FACTOR	HBV MELT ASP CORR	DEP SEEP K	DEP THRESHHOLD	DEP K	DEP MAX	DEP MAX FLOW	DEP N
Units	mm/d/K	mm/d/K	none	mm/d/K	none	1/d	mm	none	mm	mm/d	none
[DEFAULT]	19.99	1	1	1.49	0.25	0.102	92.26	1	915	31.53	1.01
LAKE	_DEFAULT	_DEFAULT	_DEFAULT	_DEFAULT	_DEFAULT	NA	NA	NA	NA	NA	NA
BARE	_DEFAULT	_DEFAULT	0.95	_DEFAULT	_DEFAULT	NA	NA	NA	NA	NA	NA
DECIDUOUS	_DEFAULT	_DEFAULT	0.89	_DEFAULT	_DEFAULT	NA	NA	NA	NA	NA	NA
WETLAND	_DEFAULT	_DEFAULT	0.89	_DEFAULT	_DEFAULT	_DEFAULT	_DEFAULT	_DEFAULT	_DEFAULT	_DEFAULT	_DEFAULT
GRASSLAND	_DEFAULT	_DEFAULT	0.89	_DEFAULT	_DEFAULT	NA	NA	NA	NA	NA	NA
CONIFEROUS	_DEFAULT	_DEFAULT	0.9	_DEFAULT	_DEFAULT	NA	NA	NA	NA	NA	NA

Appendix B
Model 2 Input Files

The Raven input files for the Model 2 structure as summarized here for the House River basin. Note that other than parameterization and discretization the model input files are identical between study basins. The .rvt (time series) files have not been included here since they just call to the time series data and do not inform about model structure. Some portions of the input file have not been included since it is structurally identical to Model 1. The .rvi (input file) is summarized in **Table B.1** without the custom output commands.

Table B.1: Model 2 .rvi file.

Hydrologic Processes

Process	Algorithm	From Compartment	To Compartment	Conditional Statements
Precipitation	PRECIP RAVEN	ATMOS_PRECIP	MULTIPLE	
Canopy Evaporation	CANEVP MAXIMUM	CANOPY	ATMOSPHERE	
Canopy Snow Evap	CANEVP MAXIMUM	CANOPY_SNOW	ATMOSPHERE	
Open Water Evaporation	OPEN WATER EVAP	DEPRESSION	ATMOSPHERE	
Lake Evaporation	LAKE EVAP BASIC	SURFACE_WATER	ATMOSPHERE	
Snow Balance	SNOBAL TWO LAYER	SNOW	PONDED_WATER	
Snow Balance -->Overflow	RAVEN DEFAULT	SNOW_LIQ	PONDED_WATER	
Flush	RAVEN DEFAULT	PONDED_WATER	DEPRESSION	HRU_TYPE IS WETLAND
Seepage	SEEP LINEAR	DEPRESSION	SOIL[1]	
Infiltration	INF HBV	PONDED_WATER	SOIL[0]	
Flush	RAVEN DEFAULT	SURFACE_WATER	PONDED_WATER	HRU_GROUP IS DrainToWetlands
Percolation	PERC ASPEN	SOIL[1]	SOIL[3]	HRU_TYPE IS WETLAND
Soil Evaporation	SOILEVAP HBV	SOIL[0]	ATMOSPHERE	HRU_GROUP IS NO_DECID
Soil Evaporation	SOILEVAP ASPEN	SOIL[0]	ATMOSPHERE	LAND_CALL IS DECIDUOUS
Depression Overflow	DFLOW THRESHPOW	DEPRESSION	SURFACE_WATER	
Baseflow	BASE POWER LAW	SOIL[1]	SURFACE_WATER	

Hydrologic Processes

Process	Algorithm	From Compartment	To Compartment	Conditional Statements
Baseflow	BASE VIC	SOIL[2]	SURFACE_WATER	HRY_GROUP IS NOT FORESTLANDS
Baseflow	BASE THRESH POWER	SOIL[2]	SURFACE_WATER	HRY_GROUP IS FORESTLANDS
Percolation	PERC CONSTANT	SOIL[0]	SOIL[1]	
Percolation	PERC CONSTANT	SOIL[1]	SOIL[2]	
Latera lFlush	RAVEN DEFAULT	DrainToWetlands PONDED_WATER	WETLANDS DEPRESSION	
Lateral Flush	RAVEN DEFAULT	WETLANDS SOIL[3]	DECID_FORR SOIL[0]	

Table B.2 summarizes the .rvh file. Note only the portion that is different from the Model 1 structure is included here.

Table B. 2: Model 2 .rvh file

HRU Groups

DrainToWetlands	104,105,205,206,305,306,405,406
WETLANDS	103,204,304,404
FORESTLANDS	104,105,205,206,305,306,405,406
GRASSLANDS	102,203,303,403
LAKES	101,201,301,401
DECID_FORR	105,206,306,406
CONIF_FORR	104,205,305,405
NO_DECID	102,103,104,202,203,204,205,302,303,304,305,402,403,404,405

The .rvc file is not included here as it is identical to the .rvc file in Appendix A with the addition of an initial condition for soil layer 2 where the forest HRUs are initialized to 2700 mm. Table B.3 summarizes the .rvp file for the Model 2 structure in the House River basin, note that only the sections with differences from Model 1 have been included.

Table B. 3: Model 2 .rvp file

Soil Properties

SoilClasses				
Attributes	%SAND	%CLAY	%SILT	%ORGANIC
Units	none	none	none	none
TOP_WETLAND	0.25	0.08	0.67	0.7
INT_WETLAND	0.25	0.08	0.67	0.2
DEEP_WETLAND	0.25	0.08	0.67	0.2
STOR_WETLAND	0.6	0.2	0.2	0.25
TOP_C_FOREST	0.6	0.2	0.2	0.25
INT_C_FOREST	0.6	0.2	0.2	0.15
DEEP_C_FOREST	0.6	0.2	0.2	0.15
TOP_D_FOREST	0.6	0.2	0.2	0.25
INT_D_FOREST	0.6	0.2	0.2	0.15
DEEP_D_FOREST	0.6	0.2	0.2	0.15

SoilParameterList

Parameters	POROSITY	HBV_BETA	MAX_CAP_RISE_RATE	MAX_PERC_RATE	BASEFLOW_COEFF	BASEFLOW_N	MAX_BASEFLOW_RATE	PET_CORRECTION	PERC_ASPEN	FIELD_CAPACITY	BASEFLOW_THRESH
Units	none	none	mm/d	mm/d	1/d	none	mm	none	mm/d	none	none
TOP WETLAND	0.4	1.85	0.1	2.5	NA	NA	NA	1	NA	0.33	NA
INT WETLAND	0.3	NA	NA	0.054	0.766	0.39	NA	NA	0.607	0.188	NA
DEEP WETLAND	0.3	NA	NA	NA	NA	0.149	0.4	NA	NA	0.188	NA
TOP C FOREST	0.4	0.503	0.1	0.06	NA	NA	NA	1	NA	0.33	NA
INT C FOREST	0.3	NA	NA	0.521	0.05	2.7	NA	NA	NA	0.172	NA
DEEP C FOREST	0.3	NA	NA	NA	NA	0.449	3.89	NA	NA	0.172	0.88
TOP D FOREST	0.4	0.503	0.1	0.09	NA	NA	NA	1	NA	0.17	NA
INT D FOREST	0.3	NA	NA	1.04	0.05	1.83	NA	NA	NA	0.172	NA
DEEP D FOREST	0.3	NA	NA	NA	NA	0.728	1.51	NA	NA	0.172	0.88
STOR WETLAND	0.4	NA	NA	NA	NA	NA	NA	NA	NA	0.172	NA

SoilProfiles

	# of Layers	Soil 0		Soil 1		Soil 2		Soil 3	
LAKE	0								
BARE_SOIL	4	TOP_C_FOREST	0.498	INT_C_FOREST	1.92	DEEP_C_FOREST	10	STOR_WETLAND	0.01
DECIDUOUS_SOIL	4	TOP_D_FOREST	0.3	INT_D_FOREST	1.03	DEEP_D_FOREST	10	STOR_WETLAND	0.01
WETLAND_SOIL	4	TOP_WETLAND	0.1	INT_WETLAND	0.5	DEEP_WETLAND	4	STOR_WETLAND	1
GRASSLAND_SOIL	4	TOP_WETLAND	0.1	INT_WETLAND	0.5	DEEP_WETLAND	4	STOR_WETLAND	0.01
CONIFEROUS_SOIL	4	TOP_C_FOREST	0.498	INT_C_FOREST	1.92	DEEP_C_FOREST	10	STOR_WETLAND	0.01

Vegetation Properties

VegetationClasses

Attributes	MAX_LAI
Units	none
LAKE	0
BARE_VEG	0
DECIDUOUS_VEG	6
WETLAND_VEG	5.2
GRASSLAND_VEG	4.5
CONIFEROUS_VEG	6.2

VegetationParameterList

Parameters	RAIN_ICEPT_PCT	SNOW_ICEPT_PCT
Units	-	-
LAKE	0	0
BARE_VEG	0	0
DECIDUOUS_VEG	0.12	0.05
WETLAND_VEG	0	0
GRASSLAND_VEG	0	0
CONIFEROUS_VEG	0.1	0.2

Landuse Properties

LandUseClasses

Attributes	IMPERM	FOREST_COV
Units	frac	frac
LAKE	1	0
BARE	0.6	0.05
DECIDUOUS	0	1
WETLAND	0	0.05
GRASSLAND	0	0
CONIFEROUS	0	1

Words

LandUseParameterList

Parameters	MELT_FACTOR	MIN_MELT_FACTOR	HBV_MELT_FOR_CORR	REFREEZE_FACTOR	HBV_MELT_ASP_CORR	DEP_SEEP_K	DEP_THRESHHOLD	DEP_K	DEP_MAX	DEP_MAX_FLOW	DEP_N	OW_PET_CORR
Units	Units	mm/d/K	mm/d/K	none	mm/d/K	none	1/d	mm	none	mm	mm/d	none
[DEFAULT]	22	1.74	1	1.49	0.25	0.102	90.3	1	1127	40.34	0.981	1
LAKE	_DEFAULT	_DEFAULT	_DEFAULT	_DEFAULT	_DEFAULT	NA	NA	NA	NA	NA	NA	1
BARE	_DEFAULT	_DEFAULT	0.95	_DEFAULT	_DEFAULT	NA	NA	NA	NA	NA	NA	NA
DECIDUOUS	_DEFAULT	_DEFAULT	0.89	_DEFAULT	_DEFAULT	NA	NA	NA	NA	NA	NA	NA
WETLAND	_DEFAULT	_DEFAULT	0.89	_DEFAULT	_DEFAULT	_DEFAULT	_DEFAULT	_DEFAULT	_DEFAULT	_DEFAULT	_DEFAULT	0.625
GRASSLAND	_DEFAULT	_DEFAULT	_DEFAULT	_DEFAULT	_DEFAULT	NA	NA	NA	NA	NA	NA	NA
CONIFEROUS	_DEFAULT	_DEFAULT	0.9	_DEFAULT	_DEFAULT	NA	NA	NA	NA	NA	NA	NA

Appendix C
Model 3 Input Files

The Raven input files for the Model 3 structure as summarized here for the House River basin. Note that other than parameterization and discretization the model input files are identical between study basins. The .rvt (time series) files have not been included here since they just call to the time series data and do not inform about model structure. Some portions of the input file have not been included since it is structurally identical to Model 2. The .rvi (input file) is summarized in **Table C.1** without the custom output commands or the portions which are identical to Model 1.

Table C. 1: Model 3 .rvi file.

Hydrologic Processes				
Process	**Algorithm**	**From Compartment**	**To Campartment**	**Conditional Statements**
Precipitation	PRECIP RAVEN	ATMOS_PRECIP	MULTIPLE	
Canopy Evaporation	CANEVP MAXIMUM	CANOPY	ATMOSPHERE	
Canopy Snow Evap	CANEVP MAXIMUM	CANOPY_SNOW	ATMOSPHERE	
Open Water Evaporation	OPEN WATER EVAP	DEPRESSION	ATMOSPHERE	
Lake Evaporation	LAKE EVAP BASIC	SURFACE_WATER	ATMOSPHERE	
Snow Balance	SNOBAL TWO LAYER	SNOW	PONDED_WATER	
Snow Balance -->Overflow	RAVEN DEFAULT	SNOW_LIQ	PONDED_WATER	
Flush	RAVEN DEFAULT	PONDED_WATER	DEPRESSION	HRU_TYPE IS WETLAND
Seepage	SEEP LINEAR	DEPRESSION	SOIL[1]	
Infiltration	INF HBV	PONDED_WATER	SOIL[0]	
Flush	RAVEN DEFAULT	SURFACE_WATER	PONDED_WATER	HRU_GROUP IS DrainToWetlands
Percolation	PERC ASPEN	SOIL[1]	SOIL[3]	HRU_TYPE IS WETLAND
Soil Evaporation	SOILEVAP HBV	SOIL[0]	ATMOSPHERE	HRU_GROUP IS NO_DECID

Hydrologic Processes

Process	Algorithm	From Compartment	To Campartment	Conditional Statements
Soil Evaporation	SOILEVAP ASPEN	SOIL[0]	ATMOSPHERE	LAND_CALL IS DECIDUOUS
Depression Overflow	DFLOW THRESHPOW	DEPRESSION	SURFACE_WATER	
Baseflow	BASE POWER LAW	SOIL[1]	SURFACE_WATER	
Baseflow	BASE VIC	SOIL[2]	SURFACE_WATER	HRY_GROUP IS NOT FORESTLANDS
Baseflow	BASE THRESH POWER	SOIL[2]	SURFACE_WATER	HRY_GROUP IS FORESTLANDS
Percolation	PERC CONSTANT	SOIL[0]	SOIL[1]	
Percolation	PERC CONSTANT	SOIL[1]	SOIL[2]	
Lateral Flush	RAVEN DEFAULT	DrainToWetlands PONDED_WATER	WETLANDS DEPRESSION	
Lateral Flush	RAVEN DEFAULT	WETLANDS SOIL[3]	DECID_FORR SOIL[0]	

Table C.2 summarizes the portions of the .rvh file that is different from Model 1 and Model 2.

Table C.2: Model 3 .rvh file

HRU Groups

DrainToWetlands	104,105,205,206
ALLWETLANDS	103,204,304,404
FORESTLANDS	104,105,205,206,305,306,405,406
GRASSLANDS	102,203,303,403
LAKES	101,201,301,401
DECID_FORR	105,206,306,406
CONIF_FORR	104,205,305,405
NO_DECID	102,103,104,202,203,204,205,302,303,304,305,402,403,404,405
WETLANDS1	103,204
WETLANDS2	304,404

HRUs

ID	Area (km2)	Elev (m)	Lat	Long	Basin ID	Land Use Class	Veg Class	Soil Profile	Slope (deg)	Aspect (deg)
101	6.744	687.773	55.54	-111.73	1	LAKE	LAKE	LAKE	0.238	319.601
102	0.755	694.514	55.54	-111.73	1	GRASSLAND	GRASSLAND_VEG	GRASSLAND_SOIL	0.244	306.427
103	94.058	697.01	55.54	-111.73	1	WETLAND1	WETLAND_VEG	WETLAND_SOIL	0.454	275.295
104	65.449	698.063	55.54	-111.73	1	CONIFEROUS	CONIFEROUS_VEG	CONIFEROUS_SOIL	0.504	267.461
105	0.539	690.485	55.54	-111.73	1	DECIDUOUS	DECIDUOUS_VEG	DECIDUOUS_SOIL	0.353	272.481
201	11.062	675.664	55.54	-111.73	2	LAKE	LAKE	LAKE	0.314	310.933
202	0.114	668.097	55.66	-112.04	2	BARE	BARE_VEG	BARE_SOIL	0.838	245.455
203	0.293	678.734	55.66	-112.04	2	GRASSLAND	GRASSLAND_VEG	GRASSLAND_SOIL	0.25	132.795
204	106.168	678.85	55.66	-112.04	2	WETLAND1	WETLAND_VEG	WETLAND_SOIL	0.348	290.5
205	134.585	681.099	55.66	-112.04	2	CONIFEROUS	CONIFEROUS_VEG	CONIFEROUS_SOIL	0.485	271.991
206	9.838	682.131	55.66	-112.04	2	DECIDUOUS	DECIDUOUS_VEG	DECIDUOUS_SOIL	0.594	264.801
301	1.64	678.542	55.66	-112.04	3	LAKE	LAKE	LAKE	1.232	277.661
302	2.33	707.268	55.54	-111.73	3	BARE	BARE_VEG	BARE_SOIL	1.362	258.961
303	16.862	715.912	55.54	-111.73	3	GRASSLAND	GRASSLAND_VEG	GRASSLAND_SOIL	1.684	247.556
304	30.128	715.39	55.54	-111.73	3	WETLAND2	WETLAND_VEG	WETLAND_SOIL	1.276	223.55
305	114.188	711.639	55.54	-111.73	3	CONIFEROUS	CONIFEROUS_VEG	CONIFEROUS_SOIL	2.173	240.528
306	5.433	725.926	55.54	-111.73	3	DECIDUOUS	DECIDUOUS_VEG	DECIDUOUS_SOIL	2.121	191.413
401	1.507	677.701	55.54	-111.73	4	LAKE	LAKE	LAKE	0.3	299.47
402	0.208	677.648	55.66	-112.04	4	BARE	BARE_VEG	BARE_SOIL	0.219	324.332
403	0.266	679.074	55.66	-112.04	4	GRASSLAND	GRASSLAND_VEG	GRASSLAND_SOIL	0.28	315.41
404	18.886	677.48	55.66	-112.04	4	WETLAND2	WETLAND_VEG	WETLAND_SOIL	0.946	229.549
405	147.676	685.062	55.66	-112.04	4	CONIFEROUS	CONIFEROUS_VEG	CONIFEROUS_SOIL	1.172	228.577
406	5.757	685.631	55.66	-112.04	4	DECIDUOUS	DECIDUOUS_VEG	DECIDUOUS_SOIL	1.118	253.955

Table C.3 summarizes the portion of the .rvp that is different from Model 2.

Table C.3: Model 3 .rvp file.

Landuse Properties

LandUseClasses

Attributes	IMPERM	FOREST_COV
Units	frac	frac
LAKE	1	0
BARE	0.6	0.05
DECIDUOUS	0	1
WETLAND1	0	0.05
WETLAND2	0	0.05
GRASSLAND	0	0
CONIFEROUS	0	1

LandUseParameterList

Parameters	MELT_FACTOR	MIN_MELT_FACTOR	HBV_MELT_FOR_CORR	REFREEZE_FACTOR	HBV_MELT_ASP_CORR	DEP_SEEP_K	DEP_THRESHHOLD	DEP_K	DEP_MAX	DEP_MAX_FLOW	DEP_N	OW_PET_CORR
Units	Units	mm/d/K	mm/d/K	none	mm/d/K	none	1/d	mm	none	mm	mm/d	none
[DEFAULT]	2.37E+01	1.48	1	1.49	0.25	0.102	132.97	1	915	34.9	1.04	1
LAKE	_DEFAULT	_DEFAULT	_DEFAULT	_DEFAULT	_DEFAULT	NA	NA	NA	NA	NA	NA	1
BARE	_DEFAULT	_DEFAULT	0.95	_DEFAULT	_DEFAULT	NA	NA	NA	NA	NA	NA	NA
DECIDUOUS	_DEFAULT	_DEFAULT	0.89	_DEFAULT	_DEFAULT	NA	NA	NA	NA	NA	NA	NA
WETLAND1	_DEFAULT	_DEFAULT	0.89	_DEFAULT	_DEFAULT	0.102	7.74E+01	1	1.23E+03	3.79E+01	8.99E-01	6.01E-01
WETLAND2	_DEFAULT	_DEFAULT	0.89	_DEFAULT	_DEFAULT	0.102	1.23E+02	1	1.01E+03	4.71E+01	1.12E+00	6.01E-01
GRASSLAND	_DEFAULT	_DEFAULT	_DEFAULT	_DEFAULT	_DEFAULT	NA	NA	NA	NA	NA	NA	NA
CONIFEROUS	_DEFAULT	_DEFAULT	0.9	_DEFAULT	_DEFAULT	NA	NA	NA	NA	NA	NA	NA

Appendix D
Calibration Parameters

Table D.1 summarizes the calibration parameters for each model structure including the name used in Chapter 4, which equation it pertains to (if applicable), parameter type, and a description of the parameter.

Table D.1: Summary of odel calibration parameters.

Parameter Name	Model Structure	Equation Number	Parameter Type	Parameter Description
BETA_S	Model 1	20	Soil	Infiltration parameter beta for the summer in the forest soil class
BETA_W	Model 1	20	Soil	Infiltration parameter beta for the winter in the forest soil class
BETA_CS	Model 2, Model 3	20	Soil	Infiltration parameter beta for the summer in the coniferous forest soil class
BETA_CW	Model 2, Model 3	20	Soil	Infiltration parameter beta for the winter in the coniferous forest soil class
BETA_DS	Model 2, Model 3	20	Soil	Infiltration parameter beta for the summer in the deciduous forest soil class
BETA_DW	Model 2, Model 3	20	Soil	Infiltration parameter beta for the winter in the deciduous forest soil class
BETA_G	Model 1, Model 2, Model 3	20	Soil	Infiltration parameter beat in the wetland soil class, only applicable in grassland HRUs
PERCW0	Model 1, Model 2, Model 3	N/A	Soil	Constant percolation rate from soil layer 0 in the wetland soil class
PERCW1	Model 1, Model 2, Model 3	N/A	Soil	Constant percolation rate from soil layer 1 in the wetland soil class
PERCF0	Model 1	N/A	Soil	Constant percolation rate from soil layer 0 in the forest soil class
PERCF1	Model 1	N/A	Soil	Constant percolation rate from soil layer 1 in the forest soil class
PERCCF0	Model 2, Model 3	N/A	Soil	Constant percolation rate from soil layer 0 in the coniferous forest soil class
PERCCF1	Model 2, Model 3	N/A	Soil	Constant percolation rate from soil layer 1 in the coniferous forest soil class
PERCDF0	Model 2, Model 3	N/A	Soil	Constant percolation rate from soil layer 0 in the deciduous forest soil class
PERCDF1	Model 2, Model 3	N/A	Soil	Constant percolation rate from soil layer 1 in the deciduous forest soil class

Parameter Name	Model Structure	Equation Number	Parameter Type	Parameter Description
BASEW1	Model 1, Model 2, Model 3	25	Soil	Baseflow coefficient for quickflow in soil layer 1 in the wetland soil class
WN1	Model 1, Model 2, Model 3	25	Soil	Baseflow exponent for quickflow in soil layer 1 in the wetland soil class
BASEW2	Model 1, Model 2, Model 3	26	Soil	Max baseflow rate for deepflow in soil layer 2 in the wetland soil class
WN2	Model 1, Model 2, Model 3	26	Soil	Baseflow exponent for deepflow in soil layer 2 in the wetland soil class
BASEF1	Model 1	25	Soil	Baseflow coefficient for quickflow in soil layer 1 in the forest soil class
FN1	Model 1	25	Soil	Baseflow exponent for quickflow in soil layer 1 in the forest soil class
BASECF1	Model 2, Model 3	25	Soil	Baseflow coefficient for quickflow in soil layer 1 in the coniferous forest soil class
CFN1	Model 2, Model 3	25	Soil	Baseflow exponent for quickflow in soil layer 1 in the coniferous forest soil class
BASEDF1	Model 2, Model 3	25	Soil	Baseflow coefficient for quickflow in soil layer 1 in the deciduous forest soil class
DFN1	Model 2, Model 3	25	Soil	Baseflow exponent for quickflow in soil layer 1 in the deciduous forest soil class
BASEF2	Model 1	26	Soil	Max baseflow rate for deepflow in soil layer 2 in the forest soil class
FN2	Model 1	26	Soil	Baseflow exponent for deepflow in soil layer 2 in the forest soil class
BASECF2	Model 2, Model 3	27	Soil	Max baseflow rate for deepflow in soil layer 2 in the coniferous forest soil class
CFN2	Model 2, Model 3	27	Soil	Baseflow exponent for deepflow in soil layer 2 in the coniferous forest soil class
BASEDF2	Model 2, Model 3	27	Soil	Max baseflow rate for deepflow in soil layer 2 in the deciduous forest soil class
DFN2	Model 2, Model 3	27	Soil	Baseflow exponent for deepflow in soil layer 2 in the deciduous forest soil class
BASETCF1	Model 2, Model 3	27	Soil	Baseflow saturation threshold for deepflow in soil layer 2 in the coniferous forest soil class
BASETDF1	Model 2, Model 3	27	Soil	Baseflow saturation threshold for deepflow in soil layer 2 in the deciduous forest soil class

Parameter Name	Model Structure	Equation Number	Parameter Type	Parameter Description
FC_W0	Model 1, Model 2, Model 3	N/A	Soil	Field capacity in soil layer 0 in the wetland soil class
FC_F0	Model 1	N/A	Soil	Field capacity in soil layer 0 in the forest soil class
FC_CF0	Model 2, Model 3	N/A	Soil	Field capacity in soil layer 0 in the coniferous forest soil class
FC_DF0	Model 2, Model 3	N/A	Soil	Field capacity in soil layer 0 in the deciduous forest soil class
FC_DF2	Model 2, Model 3	N/A	Soil	Field capacity in soil layer 1 in the deciduous forest soil class
ASPENP1	Model 2, Model 3	N/A	Soil	Constant Aspen transfer rate from wetland soil layer 1 to deciduous forest soil layer 0
DEPTHW0	Model 1, Model 2, Model 3	N/A	Soil	Depth of soil layer 0 in the wetland soil class
DEPTHW1	Model 1, Model 2, Model 3	N/A	Soil	Depth of soil layer 1 in the wetland soil class
DEPTHW2	Model 1, Model 2, Model 3	N/A	Soil	Depth of soil layer 2 in the wetland soil class
DEPTHF0	Model 1	N/A	Soil	Depth of soil layer 0 in the forest soil class
DEPTHF1	Model 1	N/A	Soil	Depth of soil layer 1 in the forest soil class
DEPTHF2	Model 1	N/A	Soil	Depth of soil layer 2 in the forest soil class
DEPTHCF0	Model 2, Model 3	N/A	Soil	Depth of soil layer 0 in the coniferous forest soil class
DEPTHCF1	Model 2, Model 3	N/A	Soil	Depth of soil layer 1 in the coniferous forest soil class
DEPTHCF2	Model 2, Model 3	N/A	Soil	Depth of soil layer 2 in the coniferous forest soil class
DEPTHDF0	Model 2, Model 3	N/A	Soil	Depth of soil layer 0 in the deciduous forest soil class
DEPTHDF1	Model 2, Model 3	N/A	Soil	Depth of soil layer 1 in the deciduous forest soil class
DEPTHDF2	Model 2, Model 3	N/A	Soil	Depth of soil layer 2 in the deciduous forest soil class
SEEP_S1	Model 1, Model 2, Model 3	19	Landclass	Seepage linear storage coeifficient in the summer, in Model 3 this is in the wetland heavy subbasins
SEEP_W1	Model 1, Model 2, Model 3	19	Landclass	Seepage linear storage coeifficient in the winter, in Model 3 this is in the wetland heavy subbasins

Parameter Name	Model Structure	Equation Number	Parameter Type	Parameter Description
SEEP_S2	Model 3	19	Landclass	Seepage linear storage coeifficient in the summer, in Model 3 this is in the non-wetland heavy subbasins
SEEP_W2	Model 3	19	Landclass	Seepage linear storage coeifficient in the winter, in Model 3 this is in the non-wetland heavy subbasins
MELT1	Model 1, Model 2, Model 3	14	Landclass	Maximum potential melt rate
MELT2	Model 1, Model 2, Model 3	14	Landclass	Minimum potential melt rate
SWE1	Model 1, Model 2, Model 3	N/A	Landclass	Maximum snow water equivalent of the surface snow layer
DEPT1	Model 1, Model 2, Model 3	24	Landclass	Threshold of water content for overflow in wetlands, in Model 3 this is in the wetland heavy subbasins
DEPT2	Model 3	24	Landclass	Threshold of water content for overflow in wetlands, in Model 3 this is in the non-wetland heavy subbasins
DEPMF1	Model 1, Model 2, Model 3	24	Landclass	Maximum flow rate from depressions during overflow event, in Model 3 this is in the wetland heavy subbasins
DEPMF2	Model 3	24	Landclass	Maximum flow rate from depressions during overflow event, in Model 3 this is in the non-wetland heavy subbasins
DEPM1	Model 1, Model 2, Model 3	24	Landclass	Maximum wetland depth of the HEW, in Model 3 this is in the wetland heavy subbasins
DEPM2	Model 3	24	Landclass	Maximum wetland depth of the HEW, in Model 3 this is in the non-wetland heavy subbasins
DEPN1	Model 1, Model 2, Model 3	24	Landclass	Overflow exponent, in Model 3 this is in the wetland heavy subbasins
DEPN2	Model 3	24	Landclass	Overflow exponent, in Model 3 this is in the non-wetland heavy subbasins
OW1	Model 1, Model 2, Model 3	N/A	Landclass	Open water PET correction factor applied to wetland HRU classes

Appendix E

Sensitivity Analysis

Table E.1 summarizes the sensitivity analysis for Model 1 as described in Chapter 4. Model 1 parameters were considered sensitive if the NSE changed by more than 10% or if the percent bias changed by more than 600%. Parameters with a sensitivity level of 5 were insensitive to parameter changes of 99%, level 4 parameters were insensitive to changes of 75%, level 3 parameters were insensitive to changes of 50%, level 2 parameters were insensitive to changes of 25% and level 1 parameters were still sensitive to changes of 25%. The only level 1 parameter is the OW AET correction factor applied to the wetlands.

Table E.1: Model 1 parameters and their sensitivities.

Parameter Name	Sensitivity Level
adiabatic lapse rate	5
precipitation lapse rate	5
rainsnow transition temp	5
rainsnow transition range	5
irreducible snow saturation	5
average annual runoff	5
max swe surface	3
soil 0 porosity wetland	4
soil 1 porosity wetland	4
soil 2 porosity wetland	4
soil 0 porosity forest	3
soil 1 porosity forest	5
soil 2 porosity forest	5
BETA Grassland	5
BETA Forest	2
Perc0 Wetland	5
Perc1 Wetland	4
Perc0 Forest	3
Perc1 Forest	5
Base1 Wetland	3
Base1 Forest	5
N1 Wetland	2
N1 Forest	5
N2 Wetland	5

Parameter Name	Sensitivity Level
N2 Forest	5
Base2 Wetland	5
Base2 Forest	5
Wetland FC 0	3
Wetland FC 1	5
Wetland FC 2	5
Forest FC 0	3
Forest FC 1	5
Forest FC 2	5
Soil Depth 0 Bare	5
Soil Depth 1 Bare	5
Soil Depth 2 Bare	5
Soil Depth 0 Deciduous	5
Soil Depth 1 Deciduous	5
Soil Depth 2 Deciduous	5
Soil Depth 1 Wetland	4
Soil Depth 2 Wetland	4
Soil Depth 0 Grassland	2
Soil Depth 1 Grassland	5
Soil Depth 2 Grassland	5
Soil Depth 0 Coniferous	3
Soil Depth 1 Coniferous	5
Soil Depth 2 Coniferous	5
Max Ht Deciduous	5
Max Ht Wetland	5
Max HT Grassland	5
Max HT Coniferous	5
Max LAI Deciduous	5
Max LAI Wetland	5
Max LAI Grassland	5
Max LAI Coniferous	5
Max Leaf Cond Deciduous	5
Max Leaf Cond Wetland	5
Max Leaf Cond Grassland	5
Max Leaf Cond Coniferous	5

Parameter Name	Sensitivity Level
Rain Incept Decid	5
Rain Incept Conif	5
Snow Incep Decid	5
Snow Incep Conif	5
Imperm Frac Bare	5
Imperm Frac Deciduous	5
Imperm Frac Grassland	5
Imperm Frac Coniferous	5
Forest Cov Bare	5
Forest Cov Deciduous	5
Forest Cov Wetland	5
Forest Cov Coniferous	5
melt factor	3
min melt factor	5
hbv melt for corr Lake	5
hbv melt for corr Bare	5
hbv melt for corr Decid	5
hbv melt for corr Wetland	5
hbv melt for corr Grassland	5
hbv melt for corr Coniferous	5
refreeze factor	5
hbv melt asp corr	5
Seep_S	3
Seep_W	4
Threshold_S	3
Dep_K	5
Dep_Max	2
Dep_Max_Flow	3
Dep_N	2
OWPET Wetland	1
alpha	5

Table E.2 summarizes the sensitivity analysis for Model 2. Model 2 parameters were considered sensitive if the NSE changed by more than 2.5% or if the percent bias changed by more than 75%. Parameters with a sensitivity level of 6 were insensitive to parameter changes of 99%, level 5 parameters were insensitive to changes of 75%, level 4 parameters were insensitive to changes of 50%, level 3 parameters were insensitive to changes of 25% and level 2 parameters insensitive to changes of 10% and level 1 parameters were still sensitive to changes of 10%. The only level 1 parameter is the OW AET correction factor applied to the wetlands.

Table E.2: Model 2 parameters and their sensitivities.

Parameter Name	Sensitivity Level
adiabatic lapse rate	3
precipitation lapse rate	6
rainsnow transition temp	6
rainsnow transition range	6
irreducible snow saturation	6
average annual runoff	6
max swe surface	4
soil 0 porosity wetland	5
soil 1 porosity wetland	6
soil 2 porosity wetland	6
soil 0 porosity forest C	5
soil 1 porosity forest C	6
soil 2 porosity forest C	6
soil 0 porosity forest D	5
soil 1 porosity forest D	6
soil 2 porosity forest D	6
BETA Grassland	6
BETA Forest CS	2
BETA Forest CW	3
BETA Forest DS	6
BETA Forest DW	6
Perc0 Wetland	6
Perc1 Wetland	6
Perc0 Forest C	6
Perc1 Forest C	6
Perc0 Forest D	4

Parameter Name	Sensitivity Level
Perc1 Forest D	6
Base1 Wetland	5
Base1 Forest C	6
Base1 Forest D	6
N1 Wetland	2
N1 Forest C	6
N1 Forest D	6
N2 Wetland	6
N2 Forest C	6
N2 Forest D	6
Base2 Wetland	6
Base2 Forest C	6
Base2 Forest D	6
Aspen Perc	3
Base threshold CF	4
Base Threshold DF	6
Wetland FC 0	5
Wetland FC 1	6
Wetland FC 2	6
Forest FC CF 0	2
Forest FC CF 1	6
Forest FC CF 2	6
Forest FC DF 0	4
Forest FC DF 1	6
Forest FC DF 2	3
Soil Depth 0 Deciduous	5
Soil Depth 1 Deciduous	6
Soil Depth 2 Deciduous	6
Soil Depth 0 Wetland	5
Soil Depth 1 Wetland	6
Soil Depth 2 Wetland	6
Soil Depth 0 Coniferous	5
Soil Depth 1 Coniferous	6
Soil Depth 2 Coniferous	6
Max LAI Deciduous	6
Max LAI Wetland	6

Parameter Name	Sensitivity Level
Max LAI Grassland	6
Max LAI Coniferous	6
Rain Incept Decid	6
Rain Incept Conif	6
Snow Incep Decid	6
Snow Incep Conif	6
Imperm Frac Bare	6
Imperm Frac Deciduous	6
Imperm Frac Grassland	6
Imperm Frac Coniferous	5
Forest Cov Deciduous	6
Forest Cov Wetland	6
Forest Cov Coniferous	6
melt factor	3
min melt factor	6
Seep_S	2
Seep_W	6
Threshold_S	2
Dep_K	6
Dep_Max	2
Dep_Max_Flow	2
Dep_N	2
OWPET Wetland	1
Alpha; time of concentration coreection factor	6

Table E.3 summarizes the sensitivity analysis for Model 3. Model 3 parameters were considered sensitive if the NSE changed by more than 2.7% or if the percent bias changed by more than 30%. Parameters with a sensitivity level of 7 were insensitive to parameter changes of 200%, level 6 parameters were insensitive to changes of 99%, level 5 parameters were insensitive to changes of 75%, level 4 parameters were insensitive to changes of 50%, level 3 parameters were insensitive to changes of 25% and level 2 parameters insensitive to changes of 10% and level 1 parameters were still sensitive to changes of 10%. The level 1 parameter consisted of the wetland soil 1 layer baseflow exponent, both wetland overflow exponents, and the wetland open water PET corrections factor.

Table E.3: Model 3 parameters and their sensitivities.

Parameter Name	Sensitivity Level
adiabatic lapse rate	4
precipitation lapse rate	6
rainsnow transition temp	7
rainsnow transition range	7
irreducible snow saturation	7
average annual runoff	7
max swe surface	4
soil 0 porosity wetland	5
soil 1 porosity wetland	5
soil 2 porosity wetland	7
soil 0 porosity forest C	5
soil 1 porosity forest C	7
soil 2 porosity forest C	7
soil 0 porosity forest D	6
soil 1 porosity forest D	6
soil 2 porosity forest D	7
BETA Grassland	7
BETA Forest CS	3
BETA Forest CW	4
BETA Forest DS	7
BETA Forest DW	7
Perc0 Wetland	6
Perc1 Wetland	6
Perc0 Forest C	7
Perc1 Forest C	7
Perc0 Forest D	7
Perc1 Forest D	6
Base1 Wetland	4
Base1 Forest C	7
Base1 Forest D	6
N1 Wetland	1
N1 Forest C	7
N1 Forest D	7
N2 Wetland	7
N2 Forest C	6

Parameter Name	Sensitivity Level
N2 Forest D	7
Base2 Wetland	7
Base2 Forest C	7
Base2 Forest D	7
Aspen Perc	4
Base threshold CF	4
Base Threshold DF	7
Wetland FC 0	4
Wetland FC 1	7
Wetland FC 2	7
Forest FC CF 0	4
Forest FC CF 1	7
Forest FC CF 2	7
Forest FC DF 0	3
Forest FC DF 1	7
Forest FC DF 2	7
Soil Depth 0 Deciduous	6
Soil Depth 1 Deciduous	6
Soil Depth 2 Deciduous	7
Soil Depth 0 Wetland	4
Soil Depth 1 Wetland	4
Soil Depth 2 Wetland	7
Soil Depth 0 Coniferous	3
Soil Depth 1 Coniferous	7
Soil Depth 2 Coniferous	7
Max LAI Deciduous	7
Max LAI Wetland	7
Max LAI Grassland	7
Max LAI Coniferous	7
Rain Incept Decid	7
Rain Incept Conif	7
Snow Incep Decid	7
Snow Incep Conif	7
Imperm Frac Bare	7
Imperm Frac Deciduous	7
Imperm Frac Grassland	7

Parameter Name	Sensitivity Level
Imperm Frac Coniferous	7
Forest Cov Deciduous	7
Forest Cov Wetland1	7
Forest Cov Wetland2	7
Forest Cov Coniferous	7
melt factor	4
min melt factor	7
Seep_S1	2
Seep_S2	2
Seep_W1	7
Seep_W2	7
Threshold_S1	2
Threshold_S2	4
Dep_K1	7
Dep_K2	7
Dep_Max1	5
Dep_Max2	5
Dep_Max_Flow1	4
Dep_Max_Flow2	4
Dep_N1	1
Dep_N2	1
OWPET Wetland	1
Alpha; time of concentration coreection factor	7